SELF-ASSEMBLED MULTIPLE MOLECULAR LAYERS OF COBALT PHTHALOCYANINES.

by

Charles C. Van Kirk

Submitted in Partial Fulfillment of the Requirements

for the Degree of

Master of Science

in the

Chemistry

Program

SCHOOL OF GRADUATE STUDIES

YOUNGSTOWN STATE UNIVERSITY

JUNE 1999

Self-Assembled Multiple Molecular Layers of Cobalt Phthalocyanines.

Charles C. Van Kirk

I hereby release this dissertation to the public. I understand that this dissertation will be housed at the Circulation Desk of the university library and will be available for public access. I also authorize the University or other individuals to make copies of this dissertation as needed for scholarly research.

Signature: Charles C. Van Kirk 6/7/99

Charles C. Van Kirk, Student — Date

Approvals:

Larry S. Curtin 6/7/99

Larry S. Curtin, Ph.D., Thesis Advisor — Date

S.M. Schildcrout 6/7/99

Steven M. Schildcrout, Ph.D., Committee Member — Date

James H. Mike 6/7/99

James H. Mike, Ph.D., Committee Member — Date

Peter J. Kasvinsky 6/7/99

Peter J. Kasvinsky, Ph.D., Dean of Graduate Studies — Date

ABSTRACT

The chemical and electrochemical properties of self-assembled monolayers on gold electrodes constructed from pyridine tagged alkanethiols were explored by cyclic voltammetry. A pyridine tagged alkanethiol chain was used as an anchoring group in the construction of the self assembled monolayer. The monolayer was subsequently extended into multi-layer films using cobalt phthalocyanine with pyrazine spacer groups.

1-(10-mercaptodecyl)isonicotinate was synthesized in a four step process prior to the formation of the monolayers. Cleaned and polished gold electrodes were allowed to soak in a stirred 1 mM aqueous solution of 1-(10-mercaptodecyl)isonicotinate for 24 hours to promote self assembly onto the gold surface. Subsequent attachment of cobalt phthalocyanine moieties to the pyridine was accomplished via axial ligation from a 1.0 mM solution of cobalt phthalocyanine in methylene chloride. The resulting layers were further extended using a pyrazine spacer, followed by attachment of cobalt phthalocyanine or cobalt octafluorophthalocyanine to yield homogeneous and/or heterogeneous multi-layer films.

Multi-layer films were constructed in this manner in hopes of creating molecular electronic and optical devices. Films were characterized via cyclic voltammetry after the addition of each new layer. This system was found to be air, water and thermodynamically stable for several weeks.

Acknowledgements

In the beginning, God created fire and it was good. Then God created the chemist to perpetuate the fire and so, the field of chemistry was born.

I would like to thank my family for giving me the support that I have needed through the years. My Mom and Dad, my sisters (Debbie, Tina, and Joanne), my brother-in-laws (Jim and Eddie) and all my nieces and nephews. I want to thank my Aunt Flossy for allowing me to live with her during my last few weeks in Youngstown and for providing me with warm meals and encouraging words when needed. May you never act your age. I wish to thank my mother-in-law for her love and support. I especially would like to thank my wife for her support and for sharing in this special time of my life. I was able to draw the strength I needed from all of you to complete this thesis, a voyage I could not have traveled without all of your love and the grace of God.

I extend my gratitude to Youngstown State University, the Ohio Board of Regents, the National Science Foundation, and the graduate school for the funding for most of the major instrumentation that is at YSU. I would also like to thank YSU for the opportunity to participate in many fire drills, evacuation procedures and hazardous material clean-ups. Because of these experiences, I feel prepared to deal with almost any bureaucratic disaster.

I would like to thank my committee, Dr. Schildcrout and Dr. Mike for their suggestions and the time spent in reviewing this thesis. Dr. Schildcrout has also been a source of guidance to me and it has been a great benefit to me to be able to have open-minded discussions with him on a regular basis.

The Curtin research group (Bill Filler, Francesca Filler, Steve Kotowich, Jeff Satterwaithe, Katy Landis (a Van Kirk now), Mike Lufaso, Colleen Bodner and Jeff Meyers) has also played an important role in my life and in my research. I will always be thankful for having the opportunity to work with them. I would like to thank my friends at YSU, particularly Carrie Curtin and Ronnie Hefley, for the fun and support. Keep my seat warm at BW-3's. I would like to send a special thank you to the big chief- Dr. Daryl Mincey for his wit and charm. I'll miss his tailgating parties and YSU football. A thank you should also go to Sue Viglione and Ray Hoff, for their help in keeping this department operational. Ray has especially been helpful to the Curtin group.

I would like to thank my academic "father" Dr. Larry 'Bone' Curtin for allowing me to continue this project even when it seemed destined to fail. I still had faith in it and Larry gave me the freedom to support this faith. While we may have differing views on certain issues, I am thankful for having the opportunity to work for an advisor that encourages individuality and creativity. It has been great teaching him how to drink and make a really hot barbecue. I'll miss abusing him on a routine basis, but make sure you keep my desk in order. I have benefited greatly from my experiences, both good and bad and I will carry these lessons with me while I work on my Ph.D. I wish to thank Larry on a personal note for his friendship and for the entertainment that he has provided. He has been my partner in pyro since our days at Temple and I will miss that most when I leave.

Most importantly, I would again like to thank my wife, Katy. Her love and devotion have been an essential source of my sanity and have enabled me to complete this thesis. Katy has been a terrific wife, with a comical sense of being that keeps me constantly entertained. I love her dearly.

Table of Contents

List of Tables

List of Figures

This thesis is dedicated to my Mother and Father

for their guidance and support and

to my wife, Katy, for her love, strength and shu-fly pie.

CHAPTER 1 : INTRODUCTION

1.1 CHEMICALLY MODIFIED ELECTRODES

The chemistry of modified electrodes is quickly becoming an area of increased interest. Formed from adsorbed species, which are either electroactive or electroinactive, the modified electrode is fabricated to obtain a specific localized chemistry at the electrode surface.[1] Therefore, interactions caused by the bulk solution can be minimized and the response of a desired species can be obtained. This greatly improves the sensitivity and selectivity of the modified electrode for analytes and allows the surface to be chemically "customized" to achieve desired characteristics. The resulting customized surface enables the exploitation and exploration of a tailored system's characteristics. This technique is similar to having a unique control variable rarely found in any other scientific area of study.

When a new species is created, every effort is made to fully identify both its physical and chemical properties. Few areas of science are able to obtain the large amount of information on a particular system as in the realm of electrochemistry. By utilizing electrochemical techniques, information about a species' electronic structure, charge, bond strengths, and degrees of interaction with the surrounding system can be readily determined.[2] These techniques enable the study of molecules forced to undergo both favorable and unfavorable chemical and electrochemical processes. In this particular investigation, the species studied will be a pyridine tagged alkanethiol chain covalently bonded to a gold electrode. A cobalt phthalocyanine molecule will be bound to the pyridine in successive steps in order to create molecular multi-layers for potential

use in molecular electronic devices. This technique of binding species to an electrode surface is known as chemically modifying the electrode.

Electroactive monolayers formed by self-assembly are of great interest because they inherently possess a high degree of order, orientation, and reproducibility and have potential applications in molecular electronics, electrocatalysis, non-linear optics, and biological and chemical sensors.[3] Electroactive species act as electron shuttles. These electroactive molecules can also serve as a mechanistic tags and are used to follow a reaction indirectly on an atomic/electronic level. Since the molecules in the monolayer are readily observed during an electrochemical experiment, changing the experimental conditions usually alters their electrochemical profiles. Observed differences are then used to relate structure/property correlations to environmental changes, e.g. the electrochemical response of the molecules can be correlated to significant changes in pH, temperature, electrolyte (ion-pairing effects), and initial potential.[2-12] It is this measurable change which makes such analysis so valuable.

Electroinactive species (typically insulators) adsorbed onto an electrode surface will diminish the amount of electrochemical contact the electrode has with the surrounding environment.[2] They are commonly used as protective coatings, lubricants, or casings to preserve the metal underneath.[13,14] These insulators prevent or slow down solution redox processes by increasing the distance of the electron transfer. Electroinactive monolayers have been shown to slow down a kinetically fast electrochemical process into the measurable range. This allows the determination of the chemical and electrochemical characteristics of many systems and processes previously believed to occur too rapidly to be observed on the voltammetric time scale. With a well-

designed modified electrode, the chemical and electrochemical properties of such systems can be quantified.

When an electrode is modified via self-assembly, the species on the surface tend to spontaneously organize into closely-packed thermodynamically and kinetically stable configurations (see Figure 1.1). Monolayers are formed when this naturally occurring phenomenon results in modified electrodes having a one-molecule thickness.[5,9] Monolayers often behave like mediators, separating the solution from the electrode surface and creating an insulating interfacial region.

1.2 SELF-ASSEMBLED MONOLAYERS (SAM's)

Self-assembled monolayers are used to look into the heart of electron transfers and to follow such processes from to the end of the chain to the electrode. The monolayer typically consists of an electroactive head group that is separated from the electrode by an ordered, insulating (electroinactive) alkane chain.[16] The chain is adsorbed onto the electrode through chemical covalent bonds, thereby anchoring the chain to the electrode. The alkyl chains interact with each other to further increase the stability of the monolayer. Typically, self-assembled monolayers are used to gather information on isolated redox active molecules, without the degree of interaction observed in macroscopic systems.

The main advantage of using self-assembled monolayers (SAM's) is that the responses of the system generated under different influences (i.e., a potential gradient) are magnified.[2-5,11,12,17] This increase in sensitivity is a result of the monolayer inhibiting certain processes, e.g. solvent interactions, and promoting others, e.g. the oxidation of a

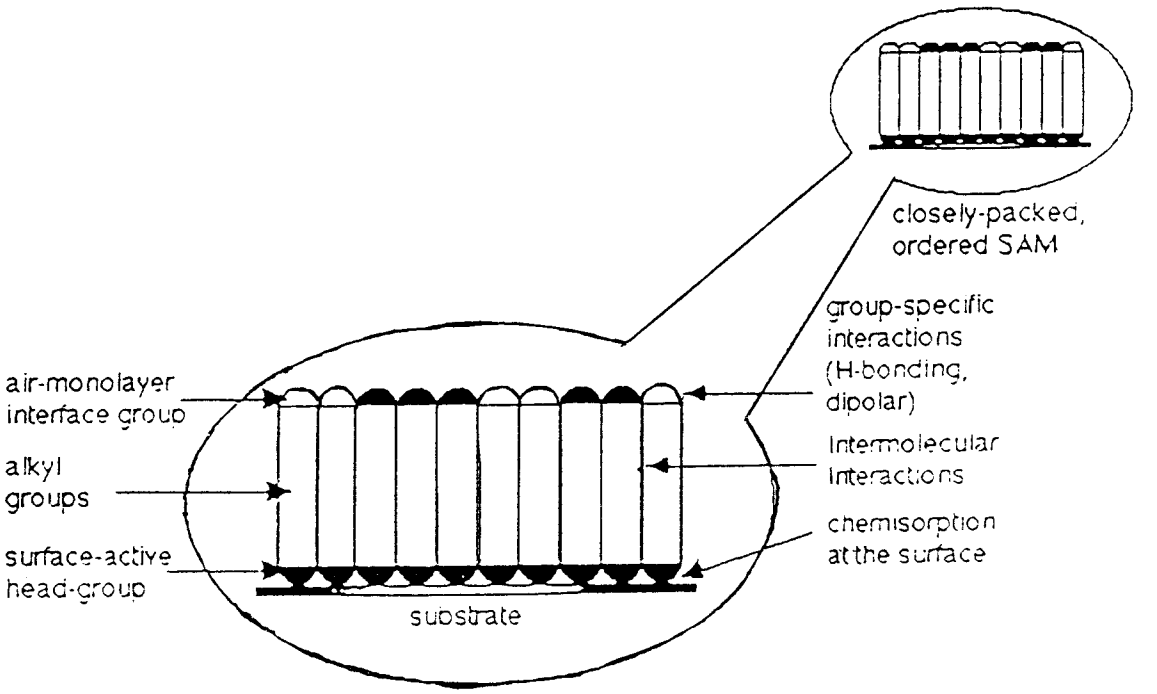

Figure 1.1 : Self-assembled monolayer.

(Reprinted from ref. 5)

surface confined species. In addition, SAM's possess an inherent degree of order and stability, allowing electrochemical investigations in essentially crystalline media.[18,20] Electron hopping and electron transfer rates, surface coverage, formal potential, and ordering parameters can be quantified via cyclic voltammetry.

Several synthetic schemes are available for the creation of modified electrodes. Langmuir-Blodgett techniques are dependent upon compression of amphiphilic molecules onto the electrode surface from a solution.[21] Although this process is not considered to involve self-assembly, it is a common method for producing mono- and multi-molecular films on surfaces. Another common method to produce SAM's is the use of triethoxy or trichlorosilanes attached to hydroxylated surfaces, as is commonly seen in the preparation of reverse phase chromatography columns. The final method employs the self-assembly of alkanethiols onto metal surfaces. All of these types of monolayers are commonly used to study structure/property relationships, interfacial phenomena, and competing electrode-substrate interactions.[2,3]

1.2.1 LANGMUIR-BLODGETT FILMS

Perhaps the best known modification process involves Langmuir-Blodgett techniques, which date back to the 18th century, and have been alluded to in earlier texts.[11,12,19,21] Langmuir-Blodgett techniques enable the construction of ordered molecular assemblies through hydrophobic interactions of a species within an interfacial region. Typically this region is a solution-air interface, however, studies between solution-solution interfaces also exist.[21]

To create a Langmuir-Blodgett film,[5] a glass slide is drawn through a solution

(usually water or oil) containing a bipolar species (see Figure 1.2). The bipolar molecules adsorb onto the glass and then are mechanically compressed into a tightly packed layer using a hydraulic press. When removed from solution this condensed layer is relatively unstable and can be easily removed. The instability of these films arises because the bipolar species are not chemically bonded to the surface and possess more degrees of freedom than found in the self-assembled examples. This increased mobility makes the films less reproducible and therefore not as reliable as SAM's. Langmuir-Blodgett films are also thermodynamically unstable, when compared to SAM's, as the adsorbed layer can easily collapse and fold on the slide. The properties of the layer are greatly influenced by the surrounding environment, particularly with conventional atmosphere,[21] and such studies are usually conducted in a temperature/humidity controlled inert atmosphere. To achieve this, sophisticated and costly equipment is generally needed.

A widely used application of Langmuir-Blodgett films is the study of the electrical and optical properties of customized electrodes containing specific molecular species.[2,3,11,12,19,21,22] Construction of these films most likely initiated the study of molecular electronic and optical devices. Langmuir-Blodgett films of organic materials have been used in studies of non-linear optics, piezoelectricity, chemical sensors, and dielectric devices. The list of potential experiments involving Langmuir-Blodgett films is essentially endless. However, such films are plagued by stability complications and therefore with reproducibility.

Multi-layer films of bipolar species have been constructed using Langmuir-Blodgett techniques by sequential deposition of a species onto a previously existing

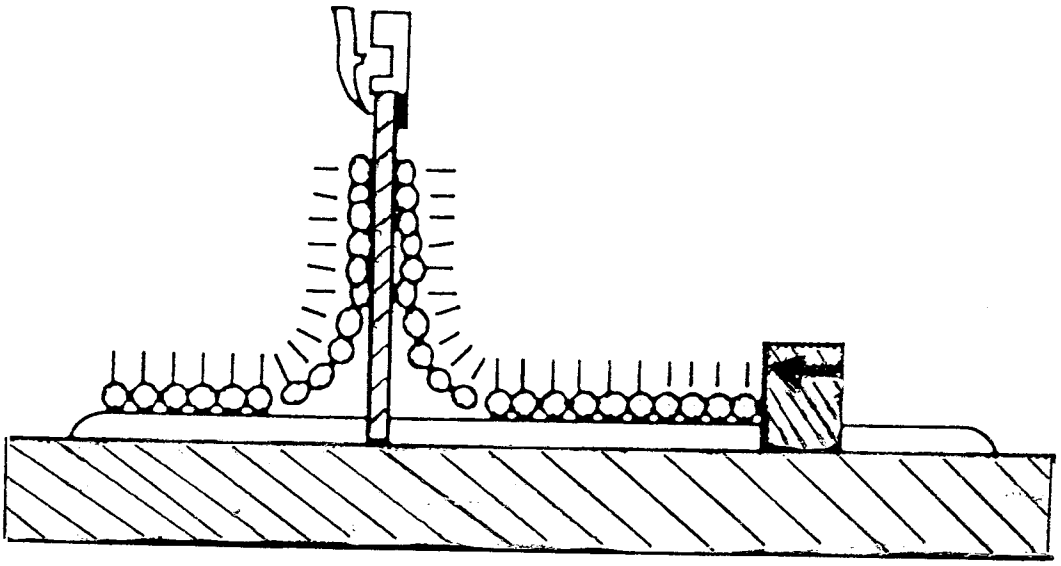

Figure 1.2 : Langmuir-Blodgett film construction.

(Reprinted from ref. 21)

monolayer. However, the instability of Langmuir-Blodgett films are manifested in decreased current responses with increasing number of voltammetric scans.[19] This decrease indicates the loss of sensitivity of the technique to monitor changes in the potential of the monolayer and also how the adsorbed species are still mobile on the surface. The mobility observed in Langmuir-Blodgett films is a manifestation of their thermodynamic instability. These multi-layer films are polymeric in nature and can be used to increase the stability of the system.[21] The use of Langmuir-Blodgett films for such studies has resulted in increased understanding of the adsorption process of bipolar species to an electrode's surface and an increased understanding of surface interactions in the microscopic world.

1.2.2 SILANIZATION - ORGANOSILANES

Another common method used to form chemically modified surfaces involves reaction of trichloro- or triethoxysilane derivatives with hydroxylated surfaces. Typically, the silanes are used to create a surface with a specific hydrophobicity, and are formed via chemisorption of the species to a hydroxylated surface.[21] A silane derivative monolayer is constructed by immersing a hydroxylated electrode into a coating solution of analyte in an organic solvent. The silanes form a three-dimensional array, with interactions with the surface as well as neighboring molecules (see Figure 1.3). The head group/surface interactions create an extended network, and while they tend to be more stable than Langmuir-Blodgett films, the organosilane monolayers tend to be bulky, relatively disordered, and sometimes environmentally toxic.

Silane monolayers possess a degree of order above Langmuir-Blodgett

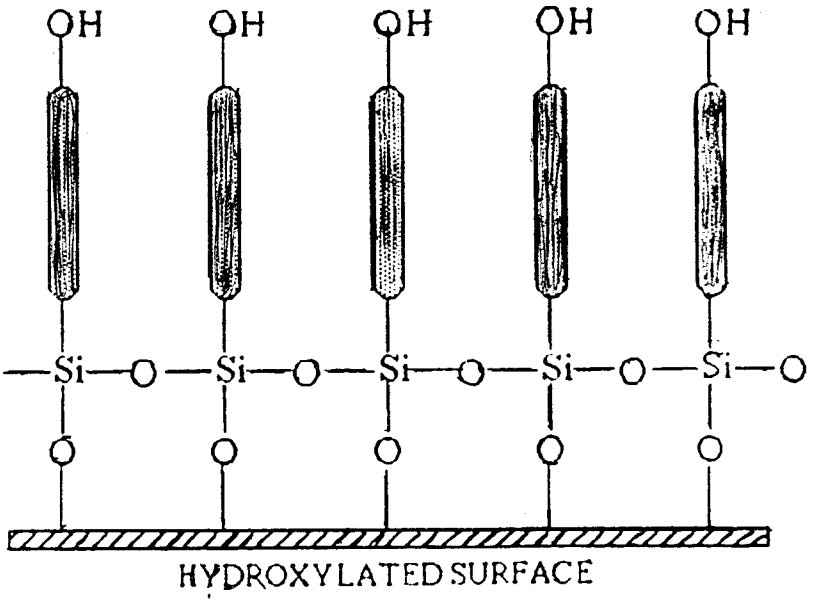

Figure 1.3 : Silane monolayers on a hydroxylated surface.

(Reprinted from ref. 21)

films since the monolayer is formed from chemically bound species. While this increases the stability of the monolayer, monolayer disorder is observed when siloxanes cross-link with other species or bind at different points to the electrode surface.[11,21] This method creates an ill-defined surface that will complicate observed responses in electrochemical studies. These monolayers are considered more reproducible than the Langmuir-Blodgett films since monolayer formation can be controlled under specific synthetic conditions. Another advantage of the siloxane monolayer formation is that it does not require the costly sophisticated equipment of the Langmuir-Blodgett techniques.

Siloxane SAM's are not without disadvantages. These monolayers are extremely sensitive to water and to the pH of the environment because the hydroxyl end group is highly reactive. This also further complicates the disorder of the monolayer and makes analysis of isolated redox sites an arduous task to perform. In these systems the formation of peroxides and the release of hydrogen is a common occurrence, which limits the stability of the monolayer. Also, the determination of electrochemical reversibility is difficult as the electron transfer kinetics have been found to be independent of monolayer chain length.[5] This indicates that the monolayer is not highly ordered and several pathways exist for charge transfer, i.e. the response signal is not be from an isolated electroactive species.

The formation of multi-layers of well-ordered silane monolayers has been shown to exist despite the above problems.[21] Multi-layers are formed by deprotonating the hydroxyl end group and covalently attaching another siloxane group to the readily accessible oxygen. The multi-layers are made more stable by the formation of an extended siloxane network. However, such monolayer and multi-layers are not typically

air or water stable and were investigated in an inert atmosphere. These monolayers are not as reproducible as SAM's and are plagued by problems with humidity, temperature, and pressure.[21]

1.2.3 ALKANETHIOL SELF-ASSEMBLED MONOLAYERS (SAM's)

A widely used method for attaching a redox active species to an electrode is through covalent bond formation between an alkanethiol and a metal surface, e.g. gold, silver, copper, and mercury.[5,9,18,20,23] The alkanethiol is the anchoring group that connects the electron donor/acceptor to the electrode surface via covalent bonding.[6] Alkanethiols display significant advantages over other types of modified electrodes (e.g. Langmuir-Blodgett or siloxane based films), which are manifested in the stability and ordering of alkanethiol SAM's, resulting in refined information about the system being studied. Other advantages include the ease of electrode preparation, reproducibility, air/water stability, and the use of relatively inexpensive equipment.

The primary driving force for alkanethiol monolayer formation is a strong gold-sulfur covalent bond, calculated to be 35-40 kcal/mol,[23] which firmly anchors the chain to the electrode surface. The secondary driving force for ordering is the ability of the alkanethiol chains to orient in a stable configuration due to an increase in van der Waals forces between neighboring alkane chains.[2,3] The monolayer will tend to organize itself into a stable configuration, i.e. an extended all *trans* configuration, with the alkane chains ideally tilting from the surface normal in order to maximize the van der Waals interactions (see Figure 1.4). Typically this tilting is 20-35° from the surface normal on gold electrodes.[5,9] An anchored alkane chain will exhibit chemical, physical, and

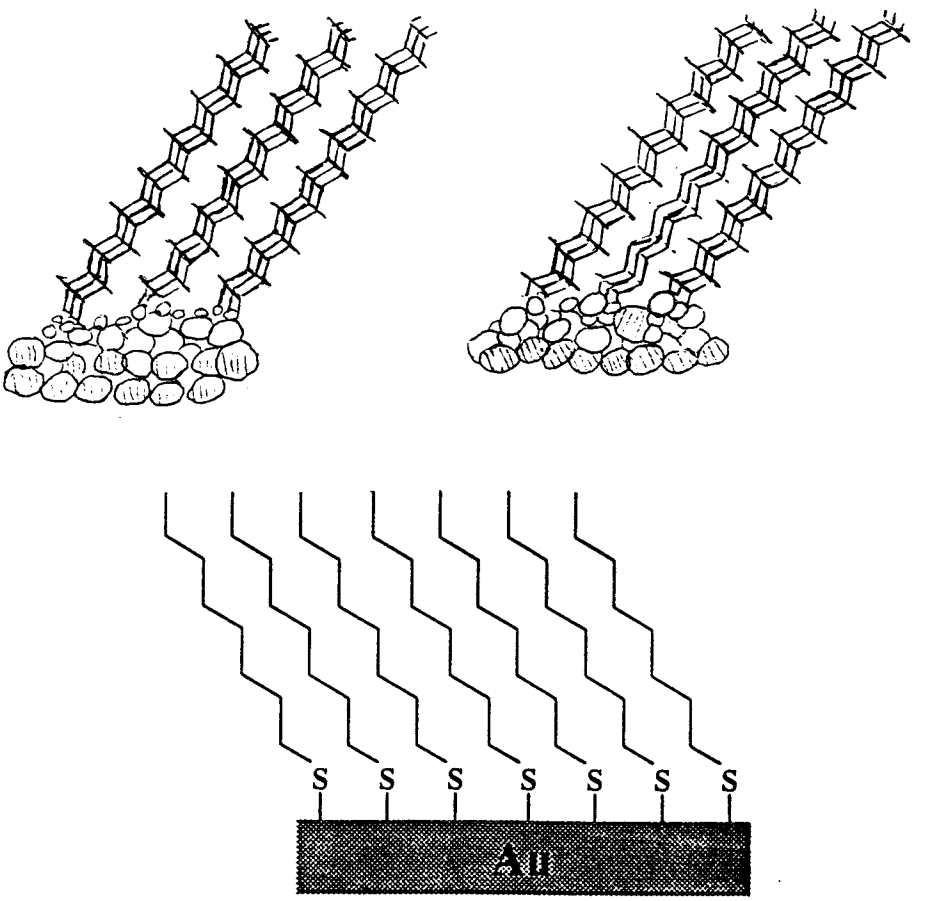

Figure 1.4 : SAM tilting and orientation.

(Reprinted from ref. 5)

electrochemical properties that are characteristic of its structure, composition, and interactions with the neighboring environment.[9]

The self-assembly process establishes a monolayer order, with the alkane chains pointing away from the electrode surface and arranging in what can be considered a crystalline configuration.[5] This arrangement makes the monolayer stable and resistant to interferences from air or water. The order of a SAM can be determined through electrochemical analysis and contact angle measurements.[2,21,22] Contact angle measurements correlate the difference in hydrophobicity of the monolayer and the electrode to monolayer order and uniformity. The monolayer's order will be greatly affected by chain length, the structure and order of surface defects, electrode-substrate interactions, and the electroactive terminal group's chemistry.[21]

When the SAM's begin to form, the molecules are not initially confined to the surface and are highly mobile, as observed via high-vacuum STM and quartz-crystal microbalance experiments.[9,22] After this initial period of mobility, some thiol chains begin to attach to the electrode and aggregate near one another. The collected chains form into small "islands" on the electrode surface and other chains begin to nucleate around these islands until surface saturation is achieved (see Figure 1.5).

Monolayer order is also dependent on the chain length of the alkanethiol. Shorter alkane chains typically have less ordering than long alkane chains.[11,21,22] Chains having less than six carbons have been found to posses the highest degree of disorder, while chains having greater than ten carbons form monolayers which are truly crystalline. Chains of six to ten carbons form somewhat disordered monolayers. Many have attributed this phenomenon to the increase of van der Waals interactions in the long

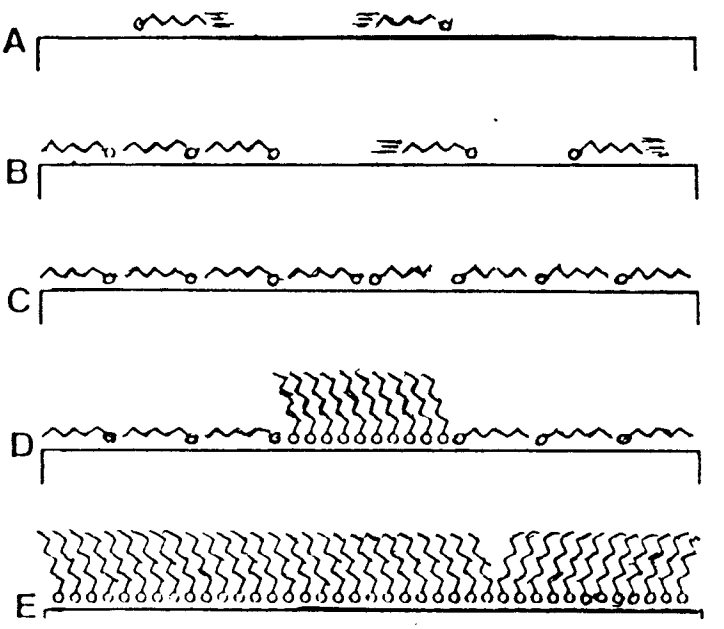

Figure 1.5 : Schematic of self-assembly mechanism for alkanethiols on a gold electrode. (A) Thiols adopt the highly mobile lattice-gas phase at very low coverages. (B) Above a critical value of surface coverage, striped-phase islands, characterized by surface-aligned molecular axes, nucleate heterogeneously and grow in equilibrium with a constant-pressure lattice gas. (C) Surface reaches saturation coverage of striped phase. (D) Surface undergoes lateral-pressure-induced solid-solid phase transition by nucleation of high-density island at striped-phase domain boundaries. (E) High-density islands grow at the expense of the striped phase until the surface reaches saturation.

(Reprinted from ref. 9)

chains, which also results in the chains aligning (tilting) in an all *trans* configuration.[5] Monolayer order and orientation have been studied by ellipsometry, contact angle goniometry, STM, X-ray and neutron diffraction, and electrochemistry.[2-8]

When polar, electroactive terminal groups are used an increase in monolayer disorder is observed.[5] This is a result of intermolecular interactions, and resolving an electrochemical single is tedious. This is due to the alkanethiol chain having an electroactive terminal group, which may interact with other terminal groups, or directly with the electrode surface. Interactions of this type will result in broad cyclic voltammograms and non-linear Tafel plots, which are used to graphically represent the overpotential (see below).

If the electroactive species are isolated, then the signal obtained is from independent and identical electroactive sites.[2,9,10,13-15] To achieve this separation, an electroinactive diluent material is commonly co-adsorbed with the analyte. Inclusion of diluent will keep the analyte molecules from interacting with each other, and in equilibrium with the electrode. When a high concentration of electroactive species is adsorbed, the electrochemical signal may be saturated and complicated by molecular interactions in the film, making analysis of the electrochemical data difficult.[2] With the addition of diluent, the intensity of the signal will be reduced. If too much diluent is used, however, then the signal will not be detectable. Therefore, an intermediate ratio of electroactive and diluent thiols is commonly chosen to obtain a reasonable signal intensity range. The presence of diluent will also increase monolayer order by keeping the electroactive chains from overly interacting with each other, thereby creating isolated chains. The two species will compete for binding sites, and the mole fraction of each

from the coating solution can be altered until the desired coverage is achieved.[2,9]

Alkanethiol SAM's can also be used to tailor desired reactions since the species adsorbed onto the electrode can act as an insulator. The electroactive monolayer slows the electron charge transfer of all redox processes. This enables the study of kinetically fast processes and of the redox process of the specifically adsorbed analyte. This increases the sensitivity of an already sensitive monitoring system and enables the study of species, both stable and transient, on a molecular level and perhaps at an atomic level. The greatest advantage of SAM's is seen in this degree of experimental control used to study desired species.

A highly packed monolayer of long alkane chains will prevent most solution redox reactions from occurring, thereby limiting electrode processes. This is a result of the alkane chain and the chemistry of terminal groups, as well as the surface configuration of the electrode. The alkane chains keep the terminal group at a fixed distance from the electrode surface, enabling the study of electron transfer kinetics by slowing the kinetics into the measurable range.

To summarize, SAM's are ideally highly ordered and specifically orientated as a result of the length of the alkane chain and the chemistry of the terminal groups. This allows for the study of intra- and intermolecular interactions. Since self-assembled monolayers overcome the stability problems of Langmuir-Blodgett films and the ordering difficulties of monolayers of organosilane derivatives, the use of SAM for the construction of molecular multi-layers is preferred.

1.3 PHTHALOCYANINES

Some types of electroactive species commonly used are metallo-porphyrins and -phthalocyanines,[24-28] where the electroactivity and surface orientation of these species can be readily modified. Cobalt phthalocyanine was chosen for the construction of multi-layers in these studies because they are planar molecules that can arrange to form extended π-systems. These species tend to possess a high degree of order on the electrode or monolayer surface and can be tailored to bind to an electrode in a specific orientation; based on attachment site.[29] Attachment to these large ring systems can be made either longitudinally, through a non-metal substituent or axially, directly to the metal center (see Figure 1.6). The longitudinal attachment usually results in the system adopting a tilted orientation, while the axial attachment is a more head-to-tail arrangement.[24-31] With the ability to arrange in two very different fashions, phthalocyanines can be used to study surface orientation effects on the electrochemistry of a monolayer.

Since most metals can exist in various stable oxidation states, studying the properties of the metal in mixed electronic states is possible.[31] These mixed valence states offer a unique situation because the metal can be forced to exist in a rare or unstable oxidation state, and the chemical properties of these states can be observed, if the potential of each layer can be separated.[24] This is commonly performed in biological studies, where these macrocycles resemble the active sites in enzymes and proteins. They can also form oligomers to study the metals' redox chemistry and long distance electron transfers.[25]

When the macrocycles are arranged parallel to the electrode surface the chains are

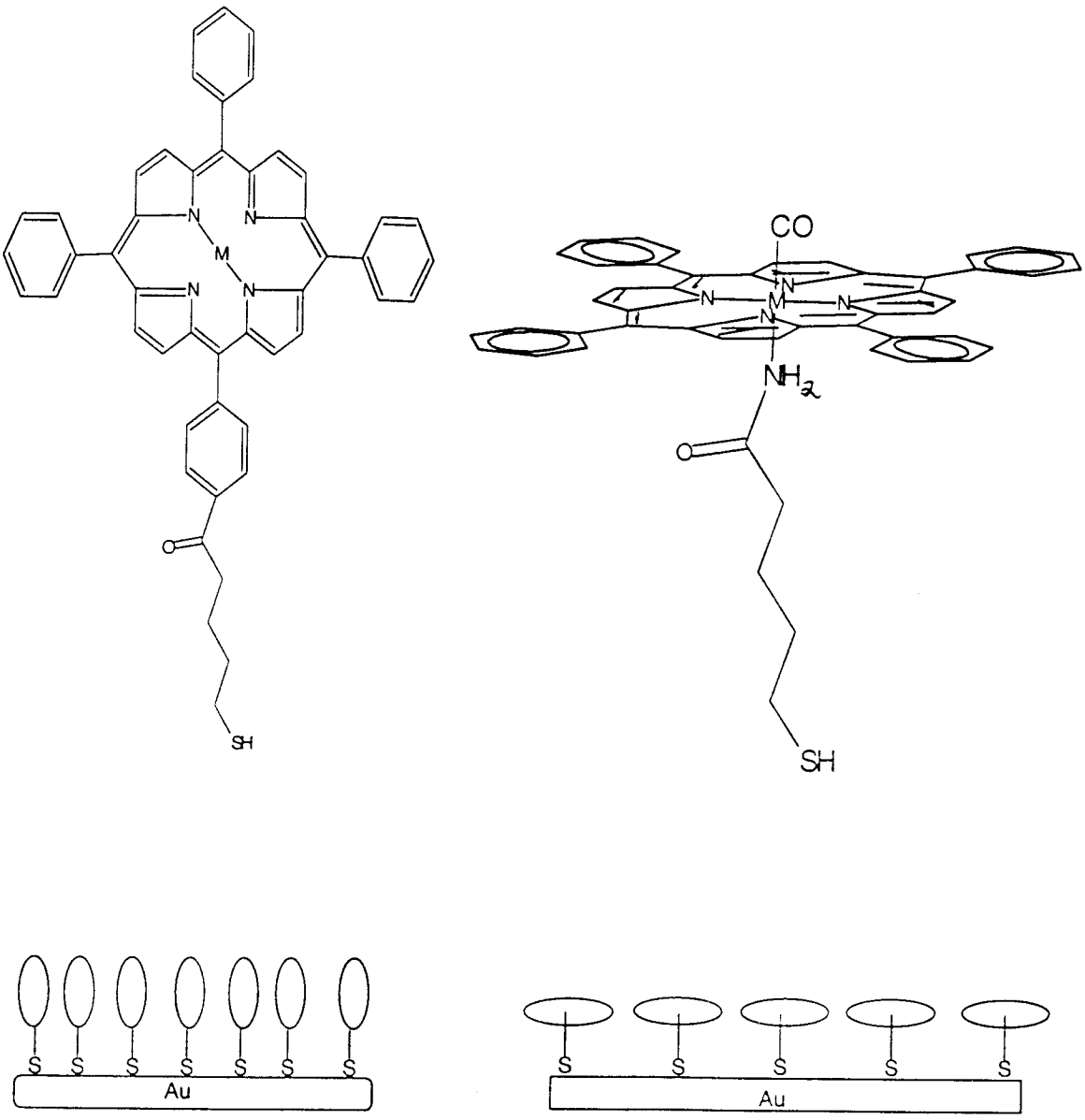

Figure 1.6 : Macrocycle orientation of self-assembled monolayers on a gold electrode showing longitudinal and axial attachment.

attached directly to the metal center.[32-34] This arranges the macrocycles in a parallel fashion allowing extended π- overlap of the electron clouds between the phthalocyanine rings. The use of phthalocyanines should maximize these π-interactions since the rings possess an extended flat π-system and the metal is situated within a square planar array of nitrogens. The electrode's topmost layer would then be viewed as a large π cloud.[33] Neighboring macrocycles will then have electron transfers specific to this orientation, possibly exhibiting a unique electron hopping mechanism. This orientation has been used for protective coatings, where the top layer would be a sacrificial layer inhibiting oxidation processes at the substrate.[32] The alkanethiol chains can also enhance the electrochemical signal at the macrocycle's redox center, particularly in stacked layers were the potentials of the redox couples may overlap, by slowing down the electron transfer kinetics. This can be used to show how the metal's center is affected by different electronic environments.

With the use of very large macrocycles tethered to alkanethiols, the surface coverage of these phthalocyanines should be considerably lower than that observed for simple alkanethiols tagged with end groups smaller than the phthalocyanines.[35] This can be envisioned by comparing the relatively large size of a phthalocyanine to the width of an alkanethiol chain, especially when considering how the large ring is expected to arrange perpendicular to the tightly-packed parallel chains. Therefore, many chains will be covered by, but unattached to, the ring. Intensification of the macrocycles', e.g. metallo-phthalocyanines, current response from the background signal can be either obtained through doping the multi-layers or by substitution on the ring to impart the appropriate functionality to the ring.[32] This can be achieved by incorporating electron-withdrawing

groups, e.g. fluorine on the phthalocyanine, with the desire of creating a molecular rectifier.[29,36,37] The fluorine addition was found to shift the formal potential of the phthalocyanine rings into a measurable range. The phthalocyanine is expected to enhance the current response since it has been shown to exhibit unidirectional molecular conduction behavior.[34,36,37]

The physical properties of these multi-layers can be characterized by such techniques as CV, UV-Vis, spectroscopy, and spectroelectrochemistry. Since the phthalocyanine has a large absorption coefficient in the UV-Vis region, and can be easily capped with an additional chromophore, the system is expected to be a good candidate for IR, UV-Vis, and spectroelectrochemical analysis.

1.4 MULTI-MOLECULAR LAYERS

After the formation of a SAM, the monolayer can be extended by the addition of electroactive macrocycles.[35,38,39] Metallo-porphyrins and -phthalocyanines are the most commonly used types of macrocycles. Many have been found to form air, water, and thermodynamically stable films for electrochemical investigations. Addition of the macrocycle forms a bi-layer of a specific thickness, which can be subsequently extended into the macroscopic range, through repetitive exposure to a coating solution of analyte. The use of spatially defined bi-layer films of redox active polymers and vapor-deposited films of molecular semiconductors has recently been an area of intense interest for applications in electrocatalysis, chemical sensing, and optical and high speed computing applications.[36] Another method to form bi-layer molecular films is through self-assembly, where complete synthetic control is preserved. With this method, the

formation of homogeneous and heterogeneous bi- and multi-molecular layers that are extremely well defined, is possible.

To stabilize and enhance the chemical and electrochemical nature of extended multi-layers, a molecular spacer unit is employed.[23,40] The spacer unit's main objective is to create spatially defined layers, but it can also be used to facilitate, or limit, electron transfers and thus increase the systems' flexibility. Typically, spacers are used to limit (impede) electron transfers, particularly in studying systems with kinetically fast electron transfers, but in this study the spacer was chosen for its ability to facilitate electron transfer.[32] The spacer must also be bidentate in order to bind one layer to another. The use of an aromatic and rigid spacer, e.g. pyrazine, can achieve these desired results. Other types of bidentate ligands, e.g. ethylenediamine, could potentially be used to link multi-layers together, however, such spacers would not be able to maintain rigid, ordered layers because of their flexibility.

As multi-layers of large macrocycles form, they begin to stack according to the nature of the underlying substrate, anchoring groups, and π-π interactions between the rings.[32,33,41] In polymer films this stacking tends to be more tilted, while multi-layers formed on self-assembled monolayers the stacks are more rod-like.[37] The SAM arrangement is analogous to stacked poker chips with the delocalized π-systems of the rings strongly interacting with neighboring rings, creating an extended π-system. This orientation maximizes π-π interaction between neighboring rings. Multi-layers of macrocycles with extended π-systems on SAM's have also been found to form planar layers with rotated macrocycles in alternating layers, as observed in single crystals (see Figure 1.7). The rotation is a result of the macrocycles arranging themselves in a fashion

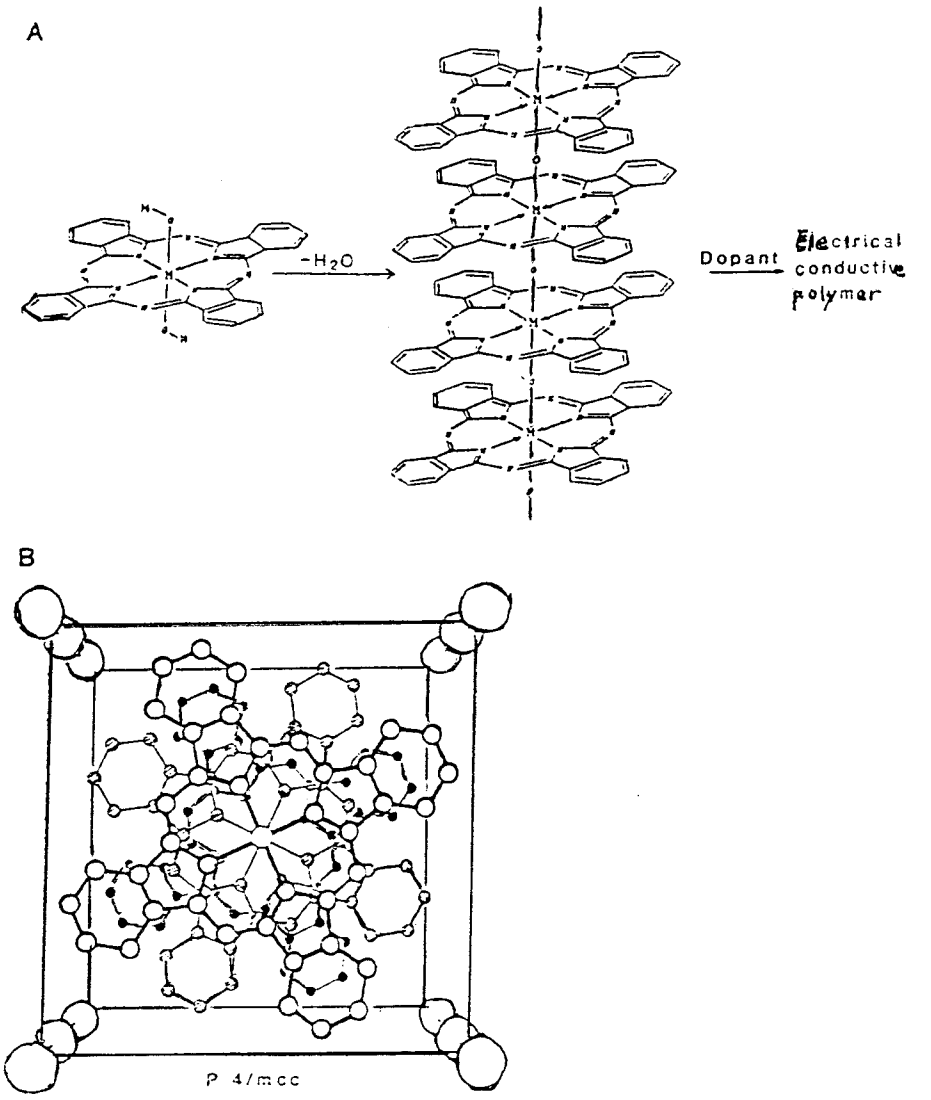

Figure 1.7 : (A) Strategy for the assembly of structure-enforces, electrically conductive arrays of group IV A metallo-phthalocyanines. (B) Schematic depiction of the similar crystal structures of halogen and nitrosyl doped $[Si(Pc^{p+})O]_n$ salts.

(Reprinted from ref. 33)

which maximizes π-π interactions between neighboring rings.

1.4.1 POLYMERIC AND VAPOR DEPOSITED THIN FILMS

Spatially defined bi-layer films are constructed via placement of a film of a given material on an electrode surface followed by deposition of a second layer of a different (or mixed) material(s).[21,22] Vapor deposition and spin coating of cobalt phthalocyanine films onto an electrode surface followed by deposition of a layer of cobalt octafluorophthalocyanine results in a device that displays the properties of molecular rectification.[36] Thin bi-layer films formed from two different semi-conducting phthalocyanines on an electrode surface behave as a diode.[36] Although these films are not polymeric in nature, they are considered thick when compared to multi-molecular layers formed from SAM's. Thin film bi-layer formation can result in uneven and non-uniform layers. This can complicate the analysis of the electron transfer pathway since the subsequent deposition of new layers would be made on high and low areas of the underlying layers and the electron can be envisioned as hopping across the layer, rather than through the film. Thin films bi-layers can also form into different orientations, compared to the normal of the electrode surface, within a layer. This makes calculation of the surface coverage of each layer extremely difficult to determine. However, these layers may also exhibit rectification properties with the correct mix of materials.

Molecular rectification is obtained when an electrochemical potential gradient is established between two different species in different layers.[36] One layer (typically the outer layer) must have a more negative redox potential compared to the other (the inner layer). These layers are arranged so that the inner layer becomes the rate limiting step in

the charge transfer process, i.e. the outer layer is unable to undergo a redox process until the inner layer is oxidized or reduced. When this potential is achieved, charge is able to flow through the layers and the electrochemical response is dramatically increased, i.e. charge transfer is enhanced. This response is comparable to a capacitor building up charge on one side and then discharging across the gap. Therefore, the system with the more negative redox potential is expected to enhance the mobility of the charge transfer between layers. Molecular rectifiers are analogs of p-n junction diodes and the increase in charge transfer is several orders of magnitude greater than the lone redox response (see Figure 1.8).

Thin films of phthalocyanines have been shown to stack in a cofacial arrangement, which is enhanced through the use of appropriate spacer molecules.[5,21,23,32-34,36,42] When a bias is applied across the bi-layer film, current flow was observed to occur in one direction, through the phthalocyanine rings. This is due to the ring's partially filled and spatially delocalized electronic energy levels, which occurs when the rings are partially oxidized. As the layers begin to superimpose over each other, the degree of overlapping energy bands also increase (see Figure 1.9). This in turn enhances charge transfer, particularly in mixed valent systems as the energy required to promote charge transfer is diminished with increasing number of layers.[32] Charge transfer is also facilitated in partially oxidized layers, as this results in unfilled energy levels where electrons can "hop" between the layers. The rectification process is observed in the voltammogram as a dramatic increase in the current response of the heterogeneous bi-layer of the films, when compared to the homogeneous layers (see Figure 1.10). The voltammetry of a molecular rectifier also indicates the dependence of the outer layer to

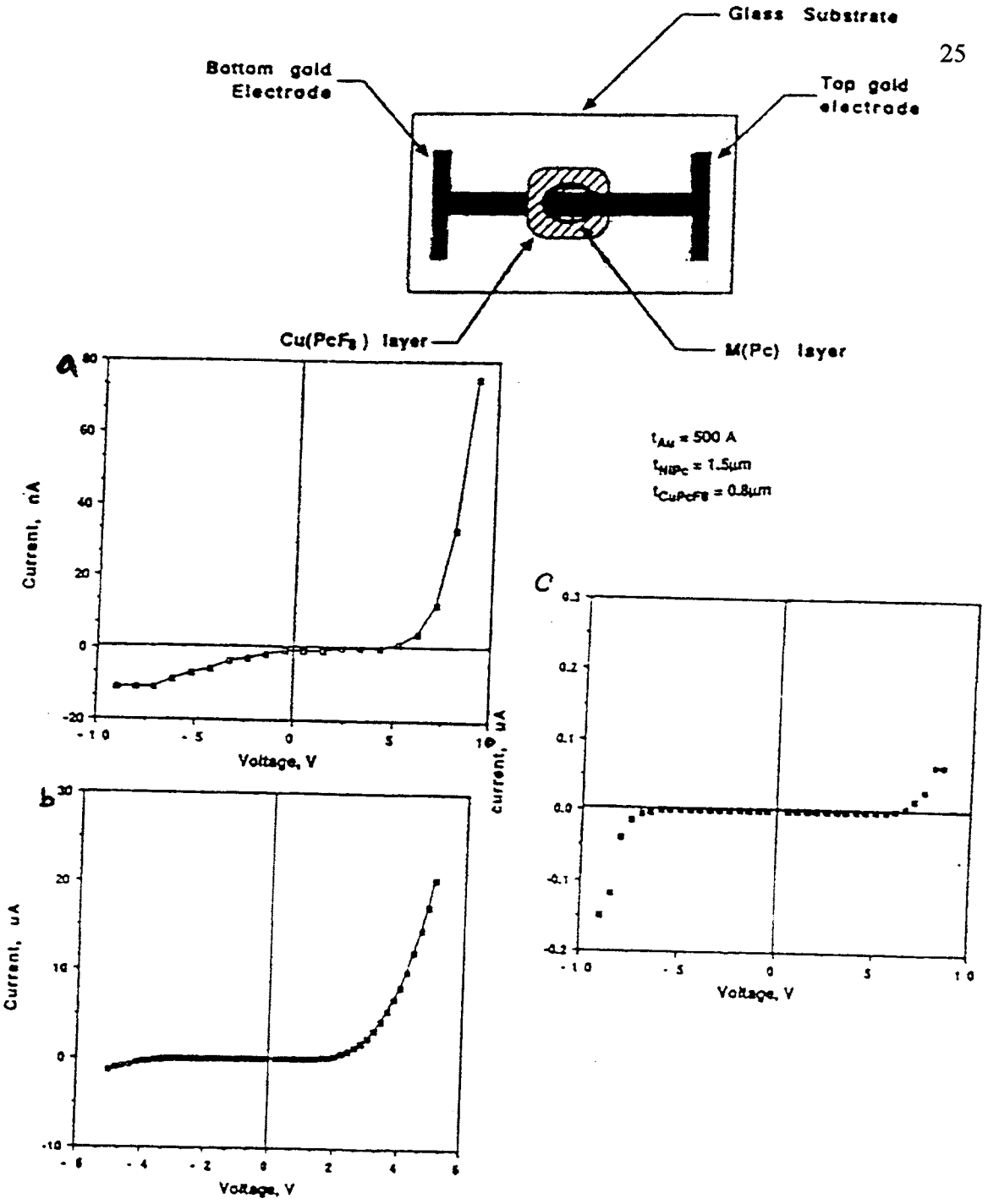

Figure 1.8 : Top: Schematic representation of a metallophthalocyanine bi-layer junction device. Bottom: Current-voltage profile of (a) Cu(Pc)F8/Cu(Pc), (b) Cu(Pc)F8/Ni(Pc), and Cu(Pc)/Ni(Pc) bi-layer films under dry, deoxygenated argon.

(Reprinted from ref. 36)

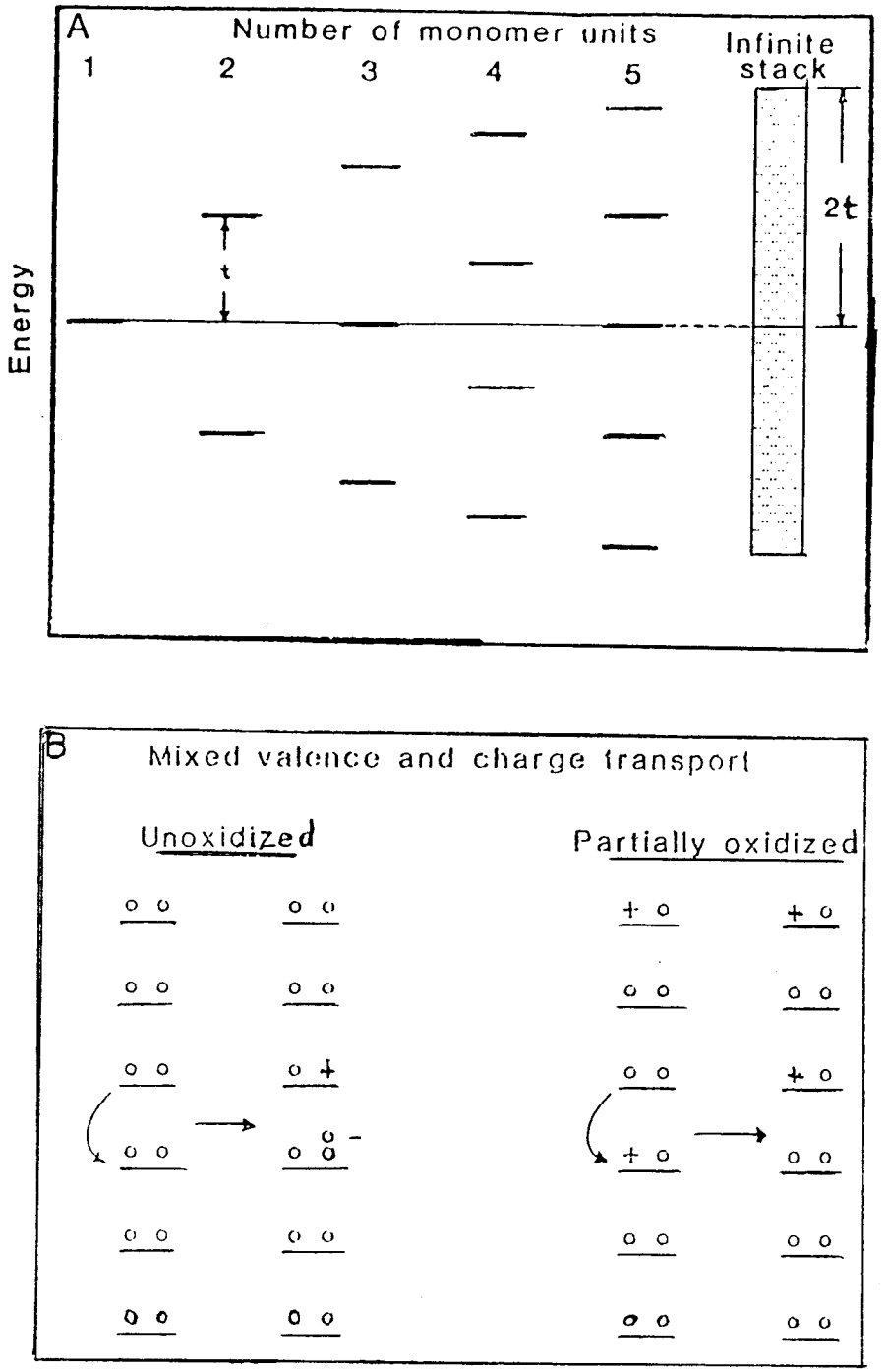

Figure 1.9 : (A) Schematic illustration of the energies of arraying increasing numbers of molecular subunit HOMO's, resulting finally in band formation. The parameter *t* is the tight-binding transfer integral, analogous to the Hückel β integral. (B) Schematic depiction of how partial oxidation enhances charge mobility in a simple molecular stack.

(Reprinted from ref. 32)

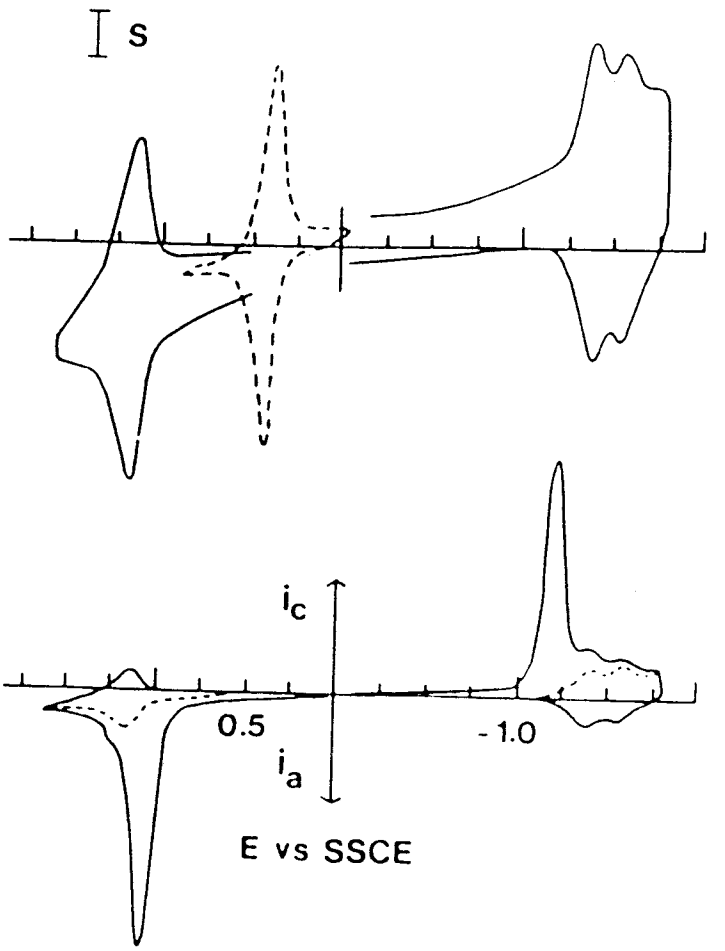

Figure 1.10 : Top: cyclic voltammetry of two independent polymer coated platinum electrodes poly-$[Ru(vbpy)_3]^{2+}$ and poly(vinylferrocene) films. S = 91 $\mu A/cm^2$. Bottom: cyclic voltammetry of bi-layer on a platinum electrode consisting of an outer layer of poly(vinylferrocene) and an inner layer of poly-$[Ru(vbpy)_3]^{2+}$. S = 227 $\mu A/cm^2$. Illustration of molecular rectification.

(Reprinted from ref. 22)

the inner layer oxidation. Therefore, an outer layer which is easier to oxidize than the inner layer on separate studies, will not be oxidized until the inner layers have underwent oxidation. Although easy to manufacture, polymer film thickness is difficult to reproduce and to form an electrically conductive array the molecules in the film must be arranged and stacked in as highly ordered array as possible. Also, in polymer films the counter ions from the electrolyte solution must diffuse through the outer layer towards the electrode in order to enable the redox process to occur.

1.4.2 FORMATION WITH SAM's

Another way to form a bi-layer is by soaking a pyridine modified electrode in a solution of cobalt phthalocyanine.[33,34] This forms a physically bound bi-layer that should be much more stable than the polymer film example. One noticeable advantage is that the phthalocyanine molecules are expected to form strong covalent bonds to active functional end groups. Perhaps a greater advantage inherent in this system is that the bi-layer is expected to form a uniform and densely covered film.[42] This is because excessive deposition should be eliminated as self-assembly will cease when surface functionality is depleted. Some other advantages include the ability to form mixed multi-layers of a specific thickness and the ability to monitor site specific interactions, through synthetic manipulations.

It has been demonstrated that molecular electronic devices (e.g. molecular rectifiers) can be produced from macroscopic films of polymers, thin films of phthalocyanines, and SAM's.[32-36] Studies on molecular rectification have provided important information on electron and ion transport, and have been explored for use in

non-linear optical devices and electrocatalysis.[32] Efficient catalysis is only observed when fast electron transfer dynamics were present.

Spatially defined monolayer structures offer some significant advantages over polymeric or other types of macroscopic electronic devices. The most significant advantage is that counter-ion diffusion upon oxidation or reduction is extremely rapid. When polymers are oxidized or reduced, counter-ions must either enter into or egress from the polymer layer (see Figure 1.11), which has a relatively large thickness.[30] Diffusion of ions throughout the majority of polymer matrices is a relatively slow process that can limit the ability of electronic devices. In monolayer films, however, the counter-ions are already located in close proximity to the redox active sight and therefore do not have to diffuse in order to balance the charge developed upon oxidation or reduction. Thus, monolayer films should have much more rapid response times than macroscopic devices.

Another advantage of monolayer systems over polymeric systems is that many polymers swell when exposed to a solvent, leading to solvent effects on charging and discharging of the film and ion and electron transport.[31] This dramatically complicates interpretation of voltammetric data as the film is no longer uniform or spatially defined.

Adhesion of polymers to electrodes and to other polymers is not well understood. This leads to problems with the reproducibility and mechanical stability of the device. Since monolayers are covalently bound to the electrode surface, they are quite difficult to remove and will have enhanced mechanical stability. Also, the monolayers do not swell when exposed to solvents,[24] yielding simplified data interpretation. Lastly, it is very difficult to reproduce the thickness of polymer films,[25] leading to devices with activities

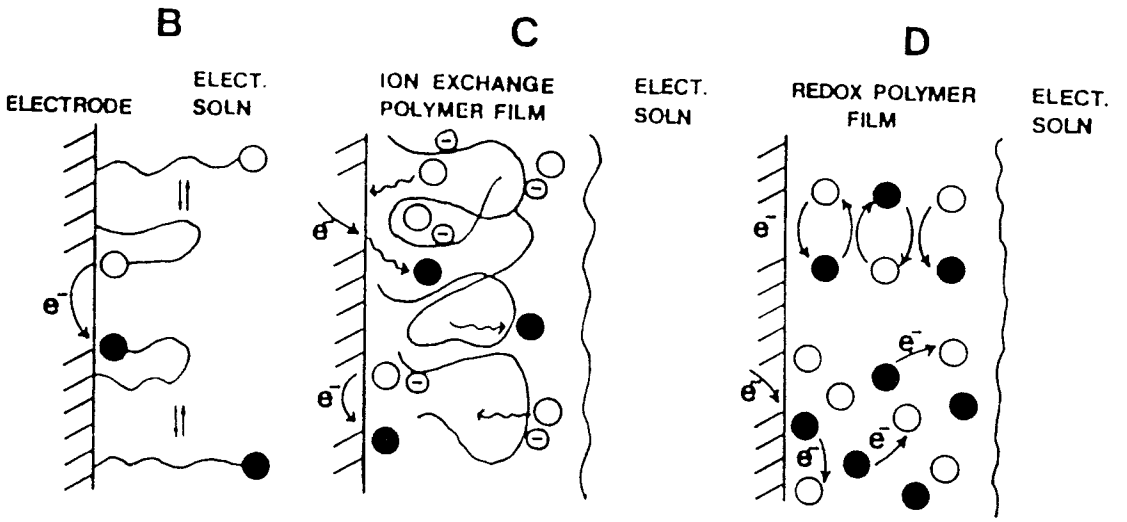

Figure 1.11 : Curve B, schematic reduction of monolayers attached by insulating yet flexible molecular chains; Curves C and D, schematic reduction of multimonolayers of ion exchange and redox polymers.

(Reprinted from ref. 22)

that are widely variant. Whereas SAM formation is highly reproducible, building a multi-layer via sequential deposition should also be highly reproducible. The multi-layer should exhibit rapid responses that are proportional to the number of layers formed, indicating that molecular multi-layer formation was successful.

1.5 ELECTROCHEMICAL BACKGROUND

Electrochemistry deals with the fundamental phenomenon of charge transfer and provides a foundation for the comprehensive study of chemical and electrochemical processes. Such studies investigate the interactions between elements (e.g. metal to metal charge transfers) and try to determine the significance and relationship that these interactions hold in our world. Typically, the focus of the interaction is on electron transfer mechanisms between the electrode and the analyte. Charge transfers are divided into two main categories: homogeneous and heterogeneous.[2,3] Homogeneous transfers occur within a solution in which charge is being moved, i.e. from one species to another. Heterogeneous transfers utilize an electrode, which acts as an electron reservoir, to transport electrons to or from an electroactive species.

In an electrochemical experiment one species is oxidized and another is reduced. Therefore, two electrodes are needed to allow both half reactions to occur. Oxidation takes place at the anode and reduction takes place at the cathode. Generally, only one electrode is of interest and is hence called the working electrode. The most common type of working electrode materials are: platinum, gold, mercury (used as a cathode only), and carbon because these are conductive and inert materials. The second electrode is used to complete the electrical circuit and is known as the counter electrode. Both working and

counter electrodes need to be polarizable so that they can act as either the anode or the cathode, depending on the applied potential.

To help quantify electrode reactions a reference electrode is used.[2,6] This electrode is a non-polarizable electrode and is used to obtain accurate potential values for the electrochemical reactions by maintaining a constant bias with the working electrode. The reference electrode contains a material that has a well-behaved redox profile (i.e. a stable redox process), and so is used as a standard in electrochemistry. Typical reference electrodes include standard hydrogen, saturated calomel, and silver/silver chloride. The potential of the working electrode is controlled relative to the reference electrode.[2,3] An impedance is placed between the working and reference electrodes to prevent current flow between the two. If current did flow, then the potential of the reference electrode would be altered, since it would then be actively involved in the redox process. This would result in a drift in the reference electrode's potential and the measured potential would not accurately reflect that of the analyte. Thus, current flows between the counter and working electrodes and not the working and reference electrodes.

At the electrode-solution interface (i.e. the Nernst layer), a charge separation is established such that the electrostatic potential of species nearest to the electrode is different from that of the bulk solution.[3] The layer closest to the electrode, the inner Helmholtz layer, contains specifically absorbed solvent molecules and partially desolvated ions. Beyond this first layer, another layer (the outer Helmholtz layer) of fully solvated ions collects. These two layers are collectively known as the double layer, or the Helmholtz layers (see Figure 1.12). Thus, the double layer yields a relatively compact region of charge at the surface of the electrode. The interaction of the ions and

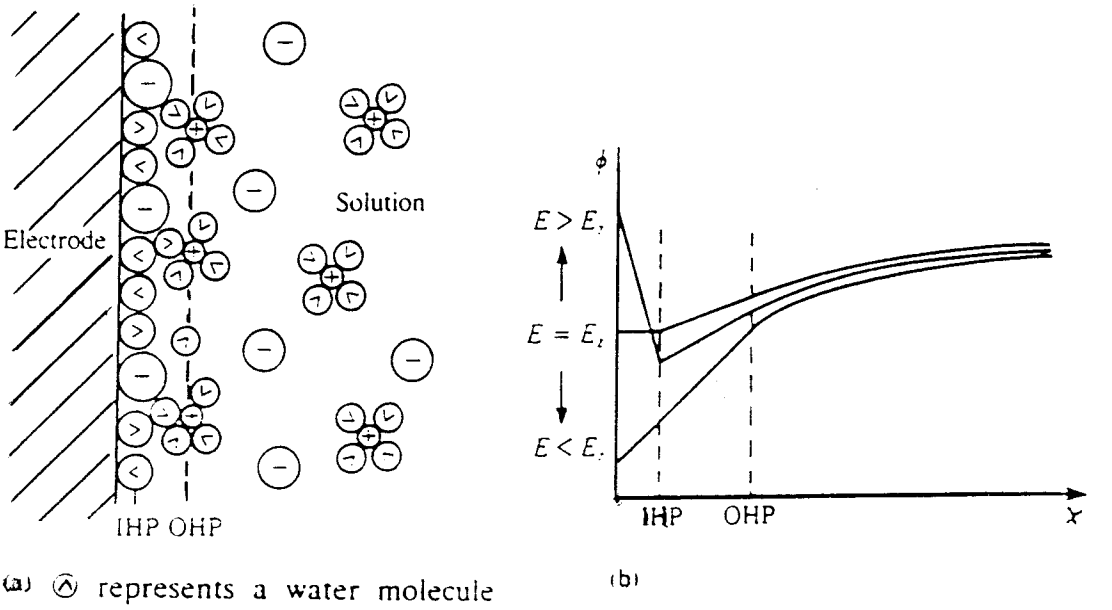

Figure 1.12 : The model of Bockris et al. of the double layer. (A) Arrangement of ions and solvent molecules. (B) Variation of electrostatic potential, ϕ, with distance, x, from the electrode.

(Reprinted from ref. 3)

the charged metal surface can also include the effects of relatively long-range electrostatic forces. This gives rise to a diffuse layer near the electrode surface in which the concentration of anions or cations is higher than that in the bulk of the solution. The size of the diffuse layer is dependent on the total ionic concentration in the solution and the potential of the electrode. Electrode processes can be affected by the structure of this double layer, especially if the electroactive species is not specifically absorbed to the electrode surface. In this case, the total potential that is observed by the redox couple is less than the potential at the electrode/solution interface because the applied potential is somewhat depleted across the double layer. This depletion is intensified when an insulating layer exists near the electrode, or when the resistance of the solution is high.

It is within the double layer region where the electrochemistry of interest occurs. In this area, electroactive species will be oxidized or reduced, depending on the potential applied to the electrode (see Figure 1.13). This is also the case for species from the bulk solution which diffuse or migrate to the electrode. This motion is known as mass transport.

Mass transport consists of three aspects: diffusion, hydrodynamic motion, and ion migration.[2,3] Diffusion is the motion of a species under the influence of a concentration gradient (i.e. from areas of high concentration to areas of low concentration). Diffusion is particularly relevant to solution voltammetry when the solution is not stirred and contains a large excess of supporting electrolyte. When the solution is stirred, hydrodynamic motion takes place, which increases the rate of mass transport to the electrode/solution interface. Hydrodynamic mass transport does not remove the Nernst layer and analytes must still diffuse across it to reach the electrode. However, the

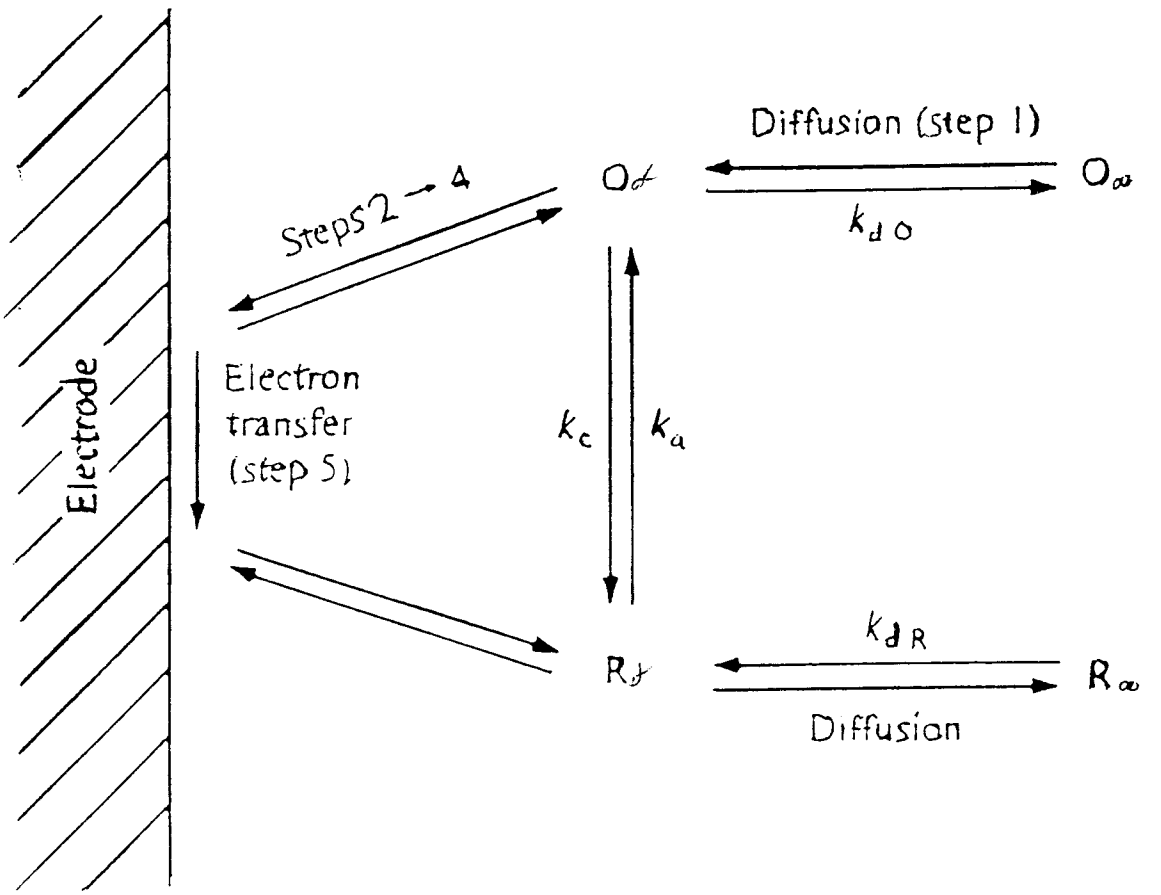

Figure 1.13 : Scheme of electron transfer at an electrode. Step 1: Diffusion of the species from the bulk to the electrode. Step 2: Rearrangement of the ionic atmosphere. Step 3: Reorientation of the solvent dipoles. Step 4: Alterations in the distances between the central ion and the ligands. Step 5: Electron transfer. Step 6: Relaxation in the inverse sense.

(Reprinted from ref. 3)

thickness of the Nernst layer decreases due to the replenishment of analyte near the electrode surface. Ion migration involves the motion of a charged species in response to the potential gradient at the electrode surface. Migration effects may be limited by adding a large excess of a supporting electrolyte, so that most of the electrostatic charge is carried by the electrolyte and not the electroactive species.

When electrochemical experiments are performed in an unstirred environment with a large excess of supporting electrolyte, diffusion becomes the principal means of moving the reactant to the surface of the electrode. Since this is a relatively slow process, it cannot maintain a concentration/distance profile in a steady-state (see Figure 1.14). If this is the case, the depletion zone grows as the analyte is consumed at the electrode surface and the rate of mass transport increases until the surface concentration approaches zero. Therefore, mass transport becomes the rate-limiting step. The thermodynamics and kinetics of mass transport are then determined and used to establish chemical and electrochemical kinetics. Electron transfer kinetics are grouped as chemically and electrochemically reversible, quasi-reversible (a gray area), and irreversible.

A reversible chemical reaction is one in which the species formed can be converted back into the initial species with no loss.[2,3,18] An irreversible chemical reaction occurs when an oxidized or reduced analyte decomposes, or otherwise changes, into a different moiety that can not be converted back into the initial species via chemical means.

A reversible electrochemical reaction is one in which the electron transfer kinetics are considered extremely rapid, i.e. a redox equilibrium is established at the electrode surface that obeys the Nernst equation.[44] This occurrence is usually magnified in most

cases with adsorbed species. The reversible case must follow a Nernstian profile and, therefore, exhibit a linear response with respect to potential and time; which is taken from the log of the increasing current response of the system (see Figure 1.15). The kinetics of such a system are then directly proportional to the concentrations of reduced and oxidized species.

An irreversible electrochemical reaction has slow electron transfer kinetics. The analyte may be converted back into its original form, but an overpotential must be applied to obtain the desired level of current. Quasi-reversible reactions occur when an absolute classification is difficult to make and is dependent on the experimental conditions. The quasi-reversible reaction can be made to become reversible, or irreversible, when certain temperatures and scan rates.

When investigating the kinetics of adsorbed species, as in SAM's, kinetic parameters are reported along with the degree of surface coverage, a thermodynamic controlled parameter.[3] The surface coverage (Γ in mol/cm^2) is represented as:

$$\Gamma = Q/(nFA)$$

Where Q is the current peak area expressed in volts × amperes, n is the number of electrons transferred, F is Faraday's constant (96,485 C/(mol or equiv)), and A is the electrode's area in cm^2. The surface coverage is used to quantify the strength and packing density of the adsorbed species. The ordering phenomena of adsorption, particularly in forming a monolayer, is greatly affected by the energy of the surrounding system and the formation is restrained by the kinetics of the system. Several theories, known as isotherms, exist to explain the observed phenomena to relate surface coverage as a function of concentration at constant temperature .[11] Each isotherm has its own

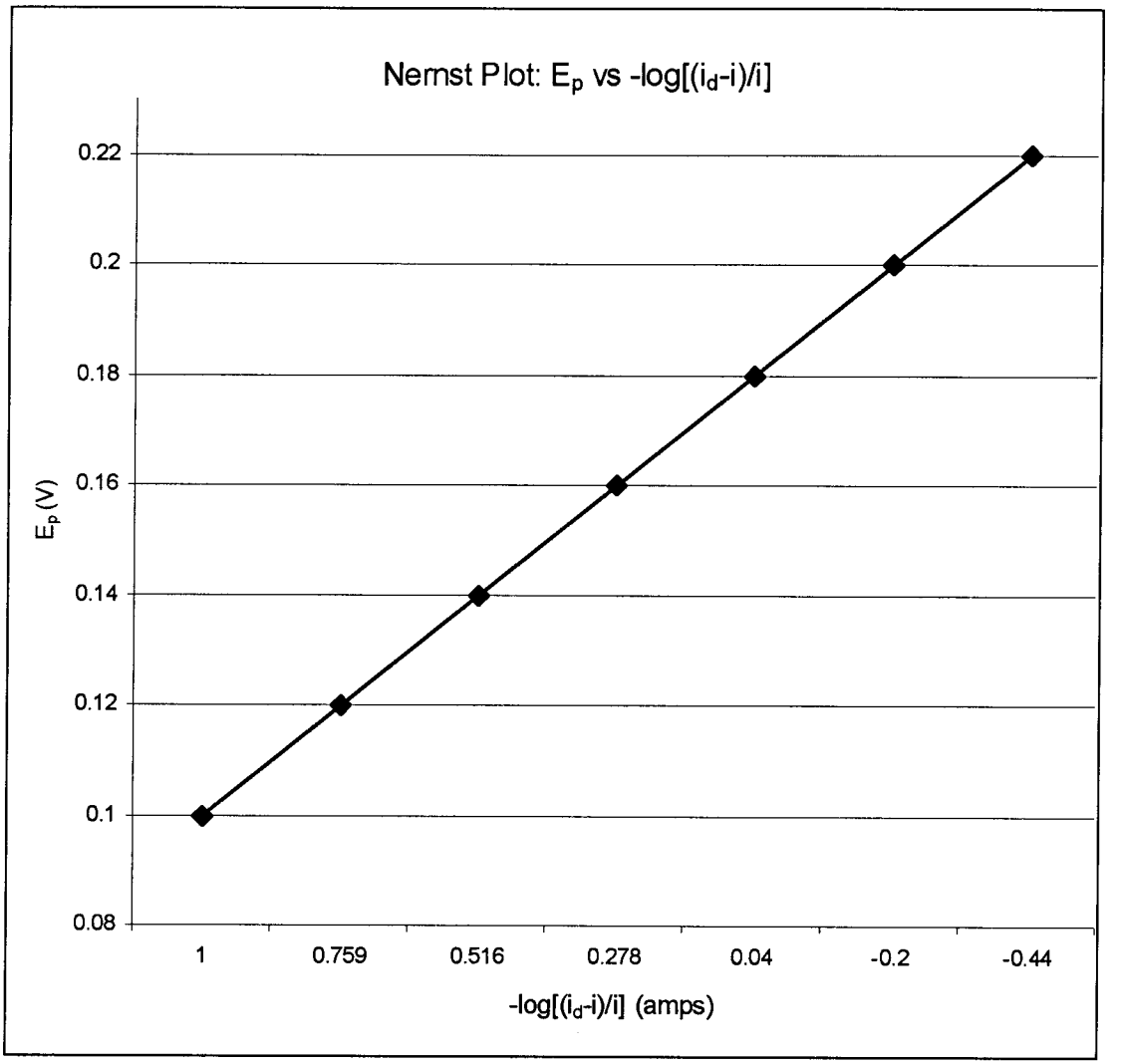

Figure 1.15 : Nernst plot of oxidized species.

approximations and assumptions. The most common is the Langmuir isotherm. In this theory the surface is assumed to be smooth and saturated by non-interacting adsorbed species and is represented as:

$$(\Gamma_i)/(\Gamma_s-\Gamma_i) = \theta = \beta_i a_i \quad \text{and} \quad \beta_i = \exp[(-\Delta G_i)/RT]$$

Where Γ_i is the excess of species "i," Γ_s is the surface coverage of a species on the electrode (the monolayer coverage), θ is known as the fraction of surface coverage, β is the energetic coefficient of proportionality and is used to assess the thermodynamics of the system, and a_i is the activity coefficient of species "i." The terms Γ_s and Γ_i are also commonly designated as Γ_O and Γ_R and represent the coverage of the oxidized and reduced forms of the adsorbed species, respectively. This isotherm also assumes that the heat of adsorption is independent of surface coverage. To correct for this the Temkin isotherm is used and is represented as:

$$\Gamma_i = [(RT)/(2g)] * \ln(\beta_i a_i)$$

Where g, measured in [(J/mol) per mol/cm^2], is used to quantify the energy of interaction between adsorbed species, i.e. the g term is a constant which reflects whether the interactions are attractive or repulsive. This isotherm assumes that the surface and species interactions are heterogeneous and can also be used to relate potential to surface interactions. An expanded form of this isotherm is the Frumkin isotherm, which examines all interactions between adsorbed species and is represented by:

$$\Gamma_i = [(RT)/(2g)] * \ln(\beta_i a_i)*\ln[(\Gamma_s-\Gamma_i)/ \Gamma_i]$$

All isotherms are extrapolated to the potential of zero charge on a plot of θ versus potential to determine the formal potential ($E^{0'}$) of the reaction. At this point the surface coverage is equal to the surface excess ($\Gamma_s = \Gamma_i$) and the energy of adsorbed species'

interactions tends toward zero. The isotherms can be integrated into the Butler-Volmer equation, discussed below, to determine system kinetics and the energy of adsorption.

1.6 CYCLIC VOLTAMMETRY (CV)

In electrochemical experimentation, the most utilized technique for the study of chemical and electrochemical processes is cyclic voltammetry.[2,3] A cyclic voltammogram is generated by applying a linear potential ramp to the working electrode and then scanning from an initial potential to a predetermined switching potential (E_λ); at a given sweep rate (see Figure 1.16). The direction of the scan is then reversed, usually to the initial potential. The current response is plotted as a function of the applied potential. The potential (E_p) at the height of the current response (i_p) is then recorded. This is done for both anodic and cathodic peaks. The potential difference (ΔE_p) and half reaction potential ($E_{1/2}$) between these peaks are determined by:

$$\Delta E_p = |E_{pa} - E_{pc}|$$

$$E_{1/2} = (|E_{pa} + E_{pc}|)/2$$

Such values are then tabulated and used to explain processes occurring at the electrode/solution interface by comparing the experimental values with theoretical values. These tabulated values are then graphically represented and analyzed via statistical analysis, e.g. least squares. Some advantages of cyclic voltammetry are that a small amount of analyte is needed to perform the experiment, the instrument has a high degree of sensitivity, and the experiment is relatively easy to perform.

Cyclic voltammetry is commonly used for determining the formal potential ($E^{0'}$) of a half-reaction.[6,10] The potential that is applied to the working electrode can be

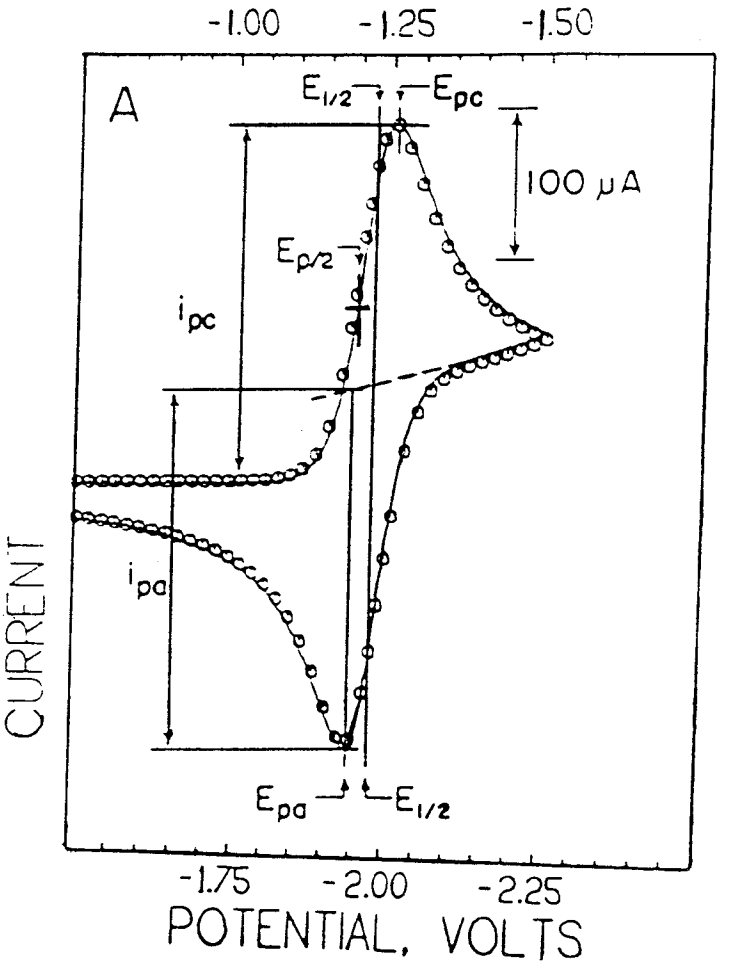

Figure 1.16 : Cyclic voltammogram at a mercury electrode. Scan rate: 100 mV/s. Temperature: 20 °C. Reference electrode: Ag/0.01 M $AgNO_3$/0.10 M $(C_2H_5)_4NClO_4$ in acetonitrile. Curves: experimental. Symbols: theoretical (digital simulation). 1 mM O_2; 0.10 M $(C_2H_5)_4NClO_4$ electrolyte. Electrode area: 0.016 cm^2; simulation parameters: $E_{1/2}$ = -1.221 V; $k_s/(D_o)^{1/2} = 354s^{-1/2}$.

(Reprinted from ref. 6)

considered an excitation signal which results in a current response. The response can then be described by the Nernst equation. The Nernst equation relates the potential of the system to the relative concentrations of the oxidized and reduced forms of the analyte. The Nernst equation is represented as:

$$E = E^{0'} + (RT)/(nF) \ln [O]/[R]$$

Where E is the cell's potential measured in volts, $E^{0'}$ is the formal potential, R is the gas constant (8.3144 J/(mol-K)), T is the temperature in Kelvin, n is the number of electrons transferred, F is Faraday's constant (96,485 C/(mol or equiv)), and [O] and [R] are the concentrations of the oxidized or reduced forms of the analyte, respectively.

The current response due to the applied potential obtained from the voltammogram can be used to describe activity on the molecular level. At this level, chemical and electrochemical reactions occur at the working and counter electrode surfaces. The half-reactions that occur are indicative of the chemical and electrochemical changes that are taking place in the cell. An electrochemical reaction occurs in response to an interfacial potential difference at the corresponding electrodes. An oxidation occurs when the potential of the working electrode is moved from a potential where no electrolysis is occurring, to more positive potentials. In this process, the energy levels of the electrons in the electrode decreases until it is energetically favorable for an electron to be transferred from the analyte to the electrode (see Figure 1.17). When the potential of the working electrode is moved to more negative values, the energy levels of the electrons in the metal increases until it is energetically favorable for an electron to be transferred to the analyte, resulting in reduction of the analyte.

Two forms of current may be observed in a voltammogram; Faradaic and non-

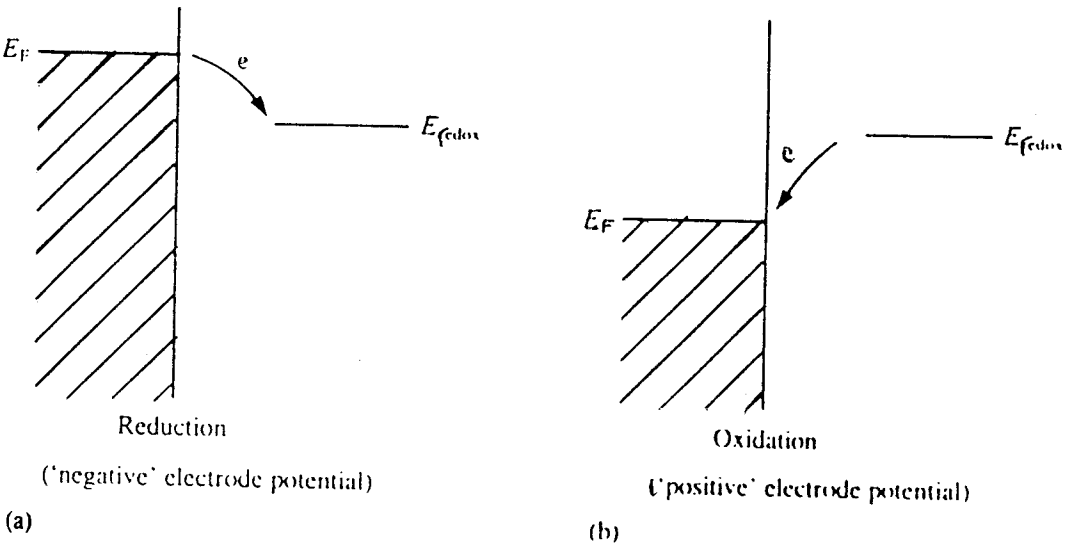

Figure 1.17 : Electron transfer at an inert metal electrode. The potential applied to the electrode alters the highest occupied electronic energy level, E_F, facilitating (a) reduction or (b) oxidation.

(Reprinted from ref. 3)

Faradaic. Non-Faradaic currents are background currents, charging currents, and currents that result from resistive impurities that may be on the surface of the electrode. Non-Faradaic currents arise from the motion of ions in the electrolyte as a result of the potential gradient and will "take up" some of the applied potential so that the potential felt by the analyte will be less than that which is applied, i.e. potential is dropped across the solution resistance. Non-Faradaic currents limit the sensitivity of the experiment by diminishing the signal to noise ratio of the current response (signal) that is observed relative to the charging current. If the non-Faradaic currents are large with respect to the signal, then the analyte's signal currents are hidden within the background response. Thus, it becomes impractical to resolve the signal from the charging currents. Faradaic currents are a result of the charge transfers to and from the analyte that occur within the electrochemical cell. Faradaic currents are the signal of interest, i.e. from the analyte, because it is a manifestation of the thermodynamic and kinetic properties of the electrochemical reaction.

The current associated with the oxidation or reduction reaches a maximum when the surface concentration of the analyte at the electrode/solution interface has been driven to zero. The current then decreases with increasing potential because mass transport of analyte to the electrode surface is slow with respect to the rate of the electron transfer. Fick's first law correlates the flux occurring at the electrode surface to the concentration gradient of the analyte in the solution and is represented as:

$$J_i(x) = -D_i(\delta C_i(x)/\delta x)$$

Where $J_i(x)$ measures the flux of species "i" in mol/(sec-cm^2) at a distance of "x" cm from the electrode, D_i is the diffusion coefficient (cm^2/sec), and $\delta C_i(x)/(\delta x)$ is the

concentration gradient. In a concentration-distance profile, the change in concentration at location 'x' is determined by the change in flux into and out of a system that has a given width of dx. This relationship demonstrates how concentration changes as a function of potential and is also dependent on of the surface area of the electrode itself.

The currents generated in a voltammogram are also a function of scan rate and therefore vary with time.[2] Fick's second law relates the change in analyte concentration with time. The chemical and electrochemical reactions taking place in the cell must also be considered along with mass transport. To accurately describe this system, the Nernst-Planck equation, or Fick's second law is applied:

$$J_i(x) = -D_i\,(\delta C_i(x))/(\delta x) - (z_iF)/(RT)\,D_iC_i\,(\delta\phi(x))/(\delta x) + C_iv(x)$$

Where $(\delta\phi(x))/(\delta x)$ is the potential gradient at a distance "x", z_i is the charge of species "i", C_i is the concentration of species "i", and v(x) is the velocity that a species is moving along the "x" direction in (cm/sec). Several restraining boundary conditions, including initial conditions, semi-infinite diffusion, and electrode surface, also need to be considered. These constraints must be taken into consideration when studying mass-transfer in an electrochemical system. The initial conditions include the bulk concentration of analyte in the solution and the rest potential of the analyte. The semi-infinite boundary conditions are determined by the length of the diffusion pathway, i.e. the thickness of the inner Helmholtz layer. If the distance to the sides of the cell is large with respect to the size of the electrode then the difference in the concentration of the species at the electrode surface compared to the concentration of species approaching the electrode becomes negligible.[2,3] Therefore, the concentration of the bulk solution reaches a constant value and a steady state of diffusion is obtained. The electrode surface

boundary conditions state that the surface area of the electrode is directly proportional to the concentration gradient at the electrode surface. When the solution is well stirred, or if the currents are kept low so that the concentration is uniform throughout the solution, the surface concentration should not differ greatly from the bulk value.

The Butler-Volmer equation, derived from Fick's laws, may be used to approximate the relationship between current and overpotential.[2] The overpotential is defined as an excess of potential beyond $E^{0'}$ for a given system; it is the extra-potential needed to cause a slow electrochemical reaction to take place. When mass-transfer effects are neglected, overpotential can be related to any given current response as the activation energy, by the equations:

$$\eta = E - E^{0'}$$

$$\eta = (RT)/(\alpha nF) \ln i_o - (RT)/(\alpha nF) \ln i$$

Where η is the overpotential measured in volts, α is the transfer coefficient (usually assigned as 0.5), i_o is the exchange current measured in amperes (i.e. the Faradaic activity between oxidized and reduced species), and i is the current of interest (either the anodic or cathodic current) measured in amperes. The overpotential also reflects the kinetics of the electron transfer, whereas a low exchange current will result in a larger activation overpotential for any given current. The overpotential can be represented graphically (see Figure 1.18), and a linear response is expected between natural log of the flux and the overpotential, for a reversible process. This plot is useful to determine the values of i_o (or j_o, the exchange current density), α, and $E^{0'}$.

The Butler-Volmer equation is applicable to voltammetric experiments only when the applied overpotential is small with respect to the reorganization energy.

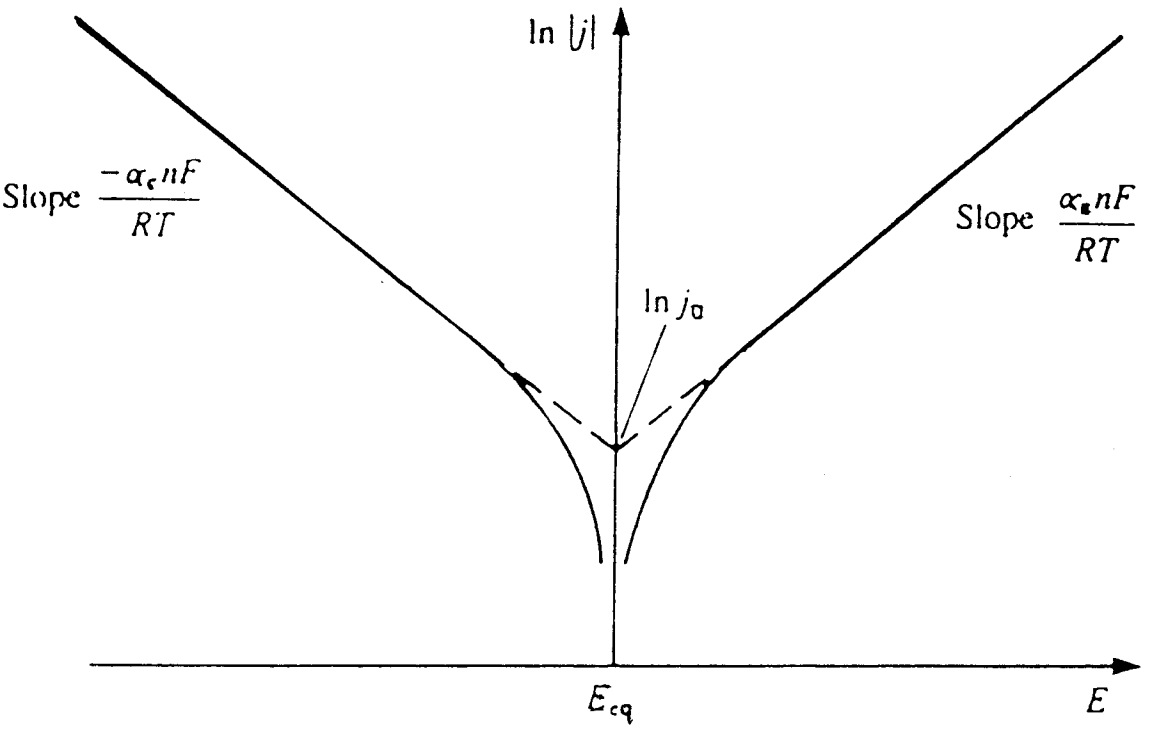

Figure 1.18 : Tafel plot of ln |j| vs. E showing how to measure j_o and α from the slopes of the lines.

(Reprinted from ref. 3)

These conditions are met in most electrochemical experiments and so Butler-Volmer is widely applied in analyzing voltammetric data. This equation is represented as:

$$i = i_0 [([O]_{(o,t)})/([O]^*) e^{(-\alpha n f \eta)} - ([R]_{(o,t)})/([R]^*) e^{(1-\alpha) n f \eta}]$$

Where [O or R]* are the bulk concentrations of oxidized and reduced species, respectively, and f = F/(RT). When mass transfer effects can be neglected, as is the case with monolayer studies, the Butler-Volmer equation can be simplified to:

$$i = i_0 [e^{(-\alpha n f \eta)} - e^{(1-\alpha) n f \eta}]$$

Information obtained from the voltammograms can be used to describe activity on the molecular level; based on Faradaic and non-Faradaic currents.[6,40] Once the voltammogram has been generated, the redox waves are then examined for reversibility.[44]

Reversibility may be chemical or electrochemical, as stated above. Electrochemical reversibility is determined by the rate of the electron transfer.[2,3] If it is rapid enough to maintain an equilibrium of reduced and oxidized forms of the analyte at the electrode surface, then the reaction is considered to be electrochemically reversible. The proper equilibrium ratio is determined by the Nernst equation such that ΔE_p should be 0 mV for surface confined species (e.g. SAM's) at all scan rates for the electron transfer to be considered reversible (see Figure 1.19). That is, a symmetric oxidation peak should be the mirror image of the symmetric reduction peak in a truly reversible case. A truly reversible wave with non-interacting surface species, i.e. a system which follows a Langmuir isotherm, will also demonstrate a full width at half maximum of 90.6/n mV at all scan rates.[22]

In the electrochemically irreversible case, as the scan rate is increased the oxidation and reduction peaks begin to separate (see Figure 1.20). The electron transfer

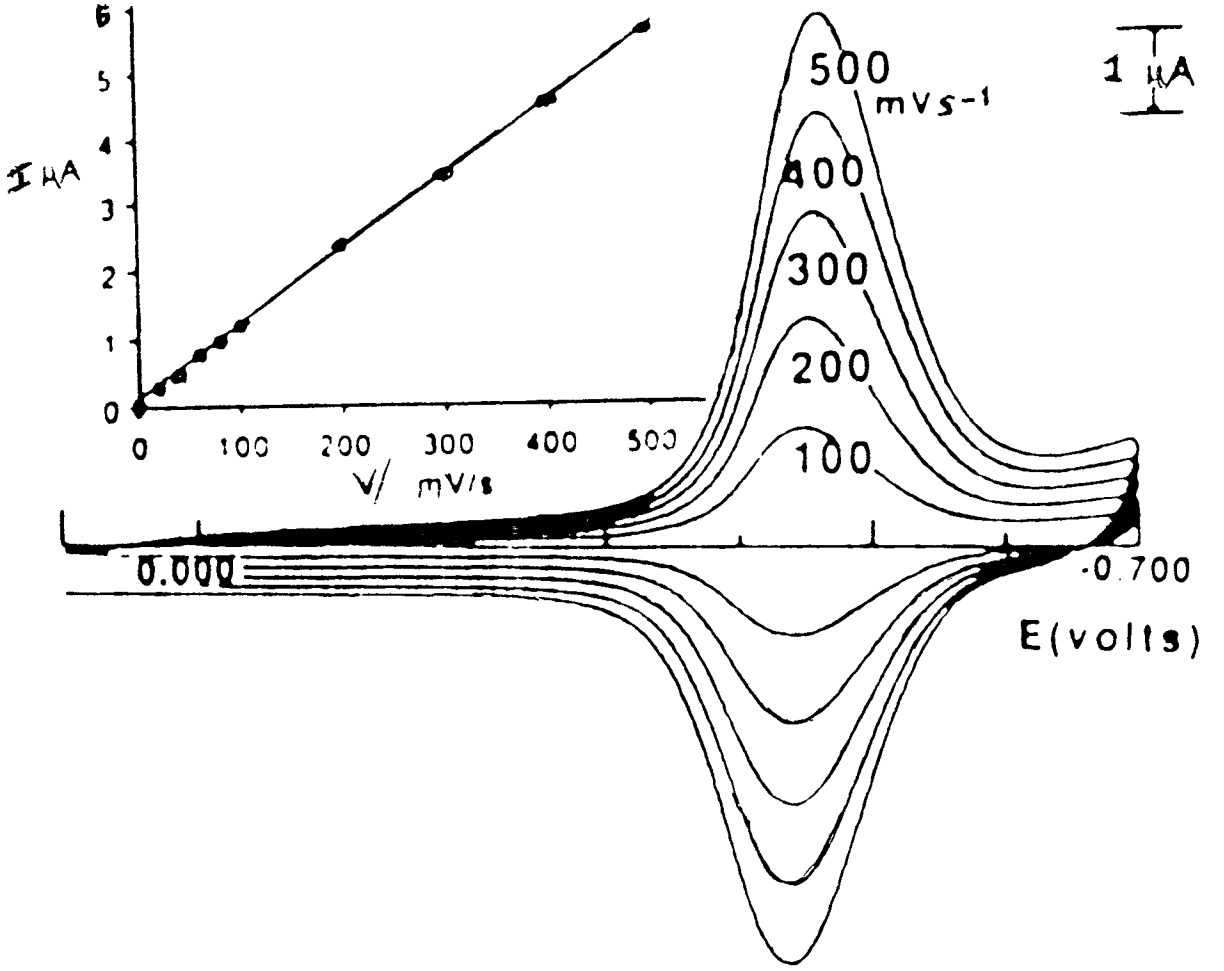

Figure 1.19 : Cyclic voltammograms of Au/OM/1 ($\Gamma = 0.45 \times 10^{14}$ mol/cm^2), area = 0.20 cm^2 in 0.1 KC, showing reversibility at increasing scan rate. Insert: plot of peak current vs. scan rate.

(Reprinted from ref. 18)

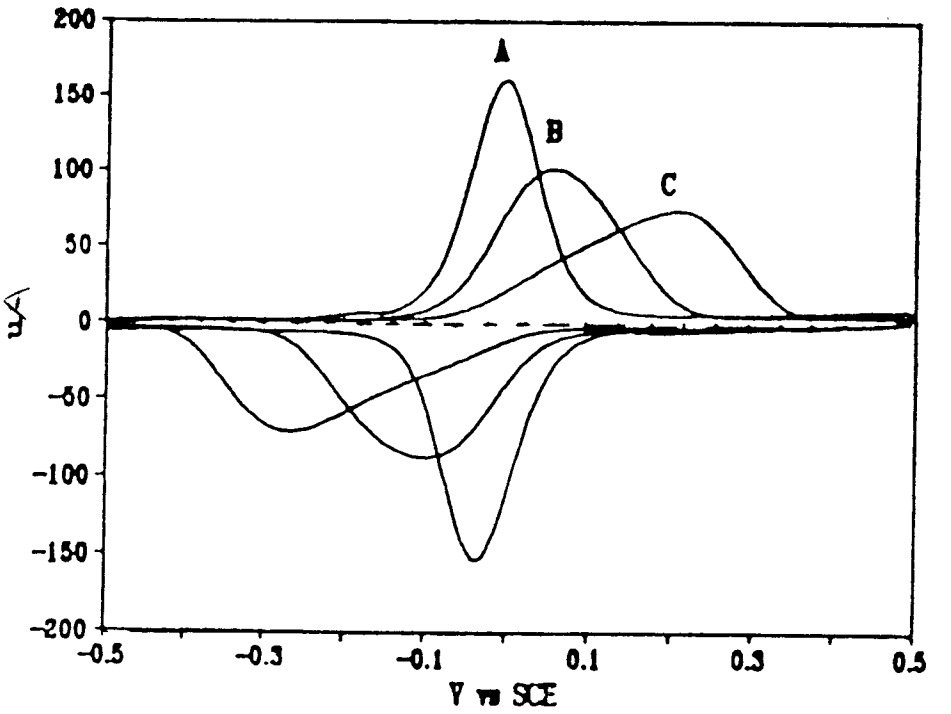

Figure 1.20 : Irreversible CV's of a 100% HS-C_{15}-Ru monolayer. The CV's are acquired in 0.2 M Na_2SO_4 with an immersed area of 1.0 cm^2. Curves A-C are for scan rates of 0.10, 1.0, and 5.0 V/s. The currents have been normalized to a scan rate of 1.0 V/s.

(Reprinted from ref. 43)

rate constant can then be determined by how the peaks separate with increasing scan rate.[46] If the peaks show no overlap on the potential axis and are greater than 150 mV apart, then the electron transfer is considered irreversible. Quasi-reversible electrochemical systems, those with somewhat faster electron transfer kinetics, manifest in ΔE_p's that increase with increasing scan rate but still overlap on the potential axis and are less than 150 mV apart.

A chemically reversible redox wave is one in which the net cell reaction is driven either forward or backward by changing the potential and every species that is oxidized can be subsequently re-reduced. This is mathematically quantified as:

$$i_{pa}/i_{pc} = 1$$

Variation from unity may express a chemically irreversible process and would be manifested in the voltammogram as a loss in the relative magnitude of the return wave, compared to its forward wave. Chemically irreversible processes involve more than the simple electron transfer from the electrode and are usually the result of a coupled chemical reaction. These reactions can cause the monolayer to undergo structural rearrangements, without the breaking covalent bonds, and are observed in the voltammograms as the sudden appearance or disappearance of a voltammetric wave (see Figure 1.21). These mechanisms are irreversible on a finite, yet sometimes infinitesimal, time scale and can be made to appear reversible; provided the instrumental ability to measure currents on this time scale is available. For a diffusionless system, e.g. monolayers, the peak current will demonstrate a linear dependence on the scan rate and is a manifestation of a completely oxidized/reduced monolayer.

A modified version of the Butler-Volmer equation, using formal potential is:

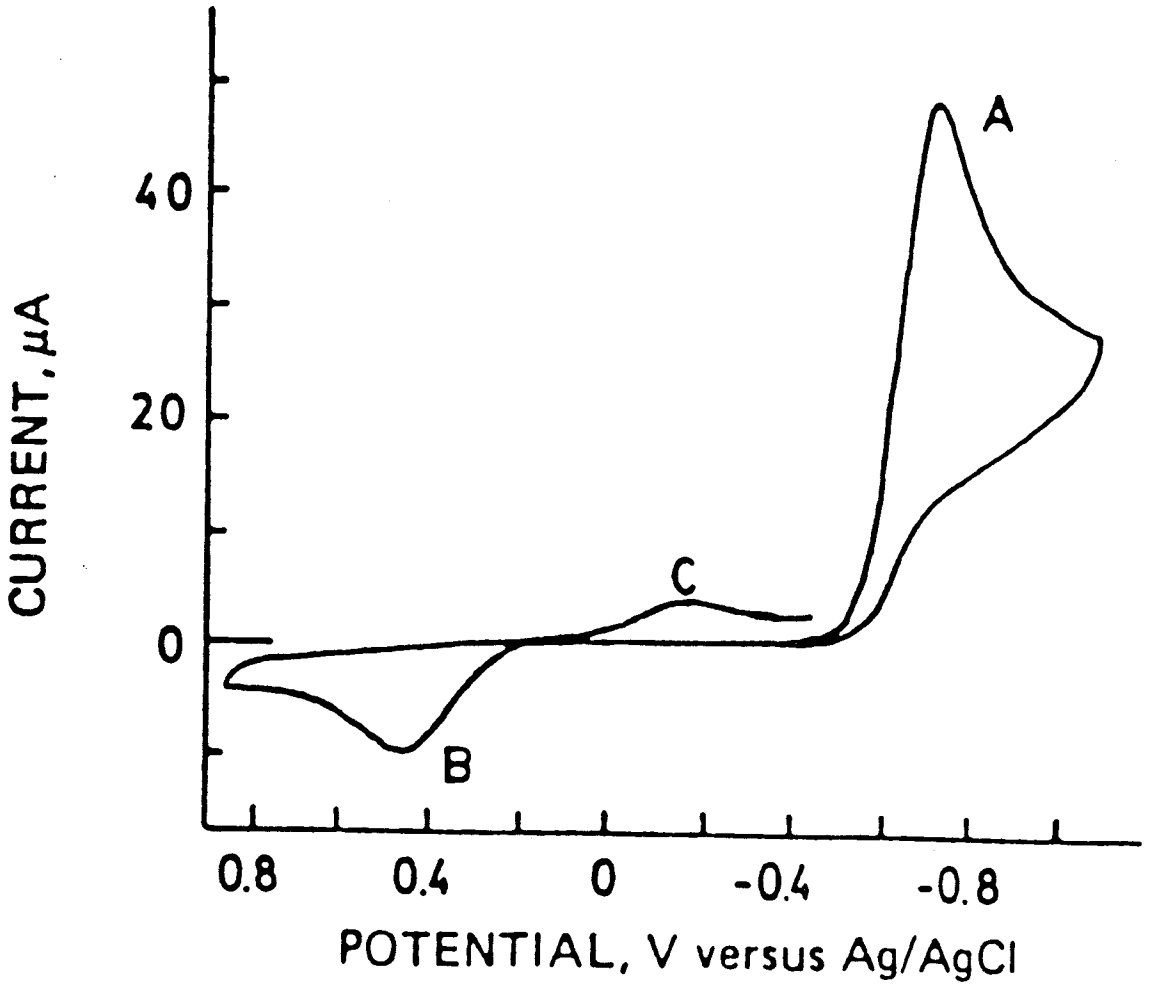

Figure 1.21 : Chemically irreversible CV of chloramphenicol in 0.1 M acetate Buffer, pH = 4.62. Working electrode: carbon paste. Reference electrode: Ag/Ag^{+}. Scan rate = 350 mV/s. Scan was initiated in the negative direction. Peak A is the initial reduction, peak B is the oxidation of A, and peak C is the reduction of the chemical coupled product formed from peak B.

(Reprinted from ref. 44)

$$E^{0'} = E^0 - (RT/nF)\ \ln(b_O/b_R) \quad \text{and} \quad b_{O\ or\ R} = \exp(-\Delta G_{O\ or\ R}/RT)$$

Where E^0 is the surface standard potential and b_O and b_R are the adsorption coefficients of the oxidized and reduced species, respectively.[45,46] This can then be combined with the ratio of surface coverages:

$$\Gamma_O/\Gamma_R = \exp\,[(nF/RT)\eta]$$

To create an expression, which expresses the energy of interactions between adsorbed species, based on potential as:

$$nF(E^{0'} - E^0) = \Delta G_O - \Delta G_R$$

This equation then relates the thermodynamics of the system to the potential and can be used to quantify how strongly a species in the oxidized or reduced form is adsorbed onto the electrode surface.[45]

An important piece of information that can be obtained from cyclic voltammetry is the charge transfer kinetics of an electrochemical reaction. In a kinetically slow charge transfer, ΔE_p increases with increasing scan rate. Rate constants may be determined using the Butler-Volmer relation, assuming a homogeneous surface with non-interacting adsorbed species. This method, developed by Laviron,[45,46] is represented as:

$$i = -nFAk_s(\Gamma_O\eta^{-\alpha} - \Gamma_R\eta^{(1-\alpha)})$$

Where k_s is the heterogeneous electron transfer rate constant of the observed surface reaction measured in Hertz (sec^{-1}). This kinetic parameter, also known as the standard kinetic rate constant (k^0), can be derived from a plot of ΔE_p versus scan rate. The rate constant will be inversely proportional to the slope of this line; i.e. k_s is proportional to (1/m). These ΔE_p plots have been tabulated by Laviron based on the 1/m values for any scan rate (see Figure 1.22).

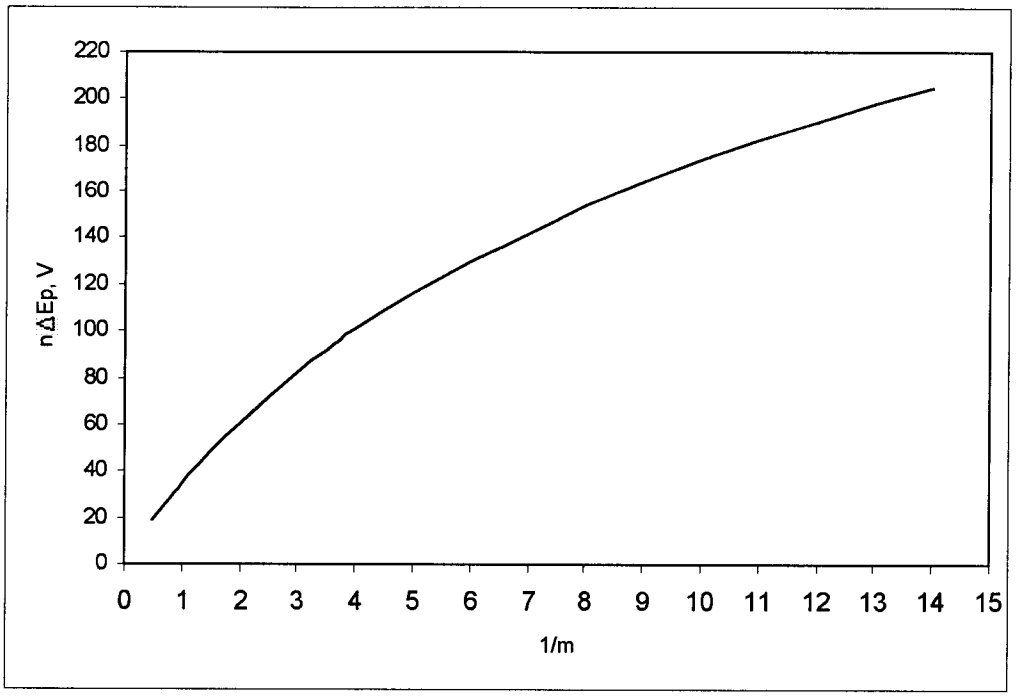

1/m	0.5	0.8	1	1.5	2	2.5	3	3.5	4	5
$n\Delta E_p$ (mV)	19	27	35	48.8	61.2	72.2	82.4	91.8	101	116

1/m	6	7	8	9	10	11	12	13	14
$n\Delta E_p$ (mV)	130	142	154	164	173	182	190	198	205

Figure 1.22 : Plot of $n\Delta E_p$ versus 1/m based on Laviron's tabulated values to determine the rate constant of a redox couple.

(Reprinted from ref. 46)

The rate constant (k_s) can then be related to the slope by:

$$k_s = (mFn\upsilon)/RT$$

Where m is obtained from the Laviron table, n is the number of electrons transferred, and υ is the scan rate measured in mV/s; all other variables have their usual meaning. The energization and activation rates of the adsorbed species are also dependent upon $E^{0'}$ and will effect all measurable and composite values.

Heterogeneous electron transfer rate constants may also be calculated using a modeling program. Experimental values, however, are difficult to match with the theoretical values obtained from a modeling program when studying monolayer systems. This is because commercially available software is designed for systems which include analyte diffusion and do not apply to studies involving monolayers. In addition, electron transfers in monolayer systems do not follow a classical charge transfer pathway. The path that an electron transfer in a monolayer follows may be viewed in a non-classical scenario. The electron must first overcome a potential barrier to initiate oxidation or reduction in an electroactive species, i.e. the applied potential must be great enough to initiate a redox process. The greater the amount of states for each level, the probability for the electron to populate these states increases; relative to the Boltzman distribution.

Currently available software programs are based on the standard Butler-Volmer equations, and the assumptions contained within. Such programs examine a system for diffusional components that are found in studies involving solution voltammetry but are not found in surface confined systems. These components give rise to the characteristic "duck" shaped peaks in solution experiments and the "bell" shaped peaks found in SAM's. Another complication is the inability of modeling programs to recognize that in

many SAM's the reorganization energy is not small with respect to the overpotential, or the density of states in the metal electrode. These complications can, generally, be overcome through the use of Marcus-Hush theory, which is an expanded version of Butler-Volmer theory and involves extensive mathematical manipulations. However, there are no commercially available programs employing Marcus-Hush theory that can be used to evaluate a system without diffusional components.

In spite of the analysis lost by not using a modeling program, the standard rate constant (k^0) can be determined using the Laviron method, if the kinetics are slow, but not too slow.[3] Thus, the rate of the electron transfer associated with the cobalt $2^+/3^+$ couple in the cobalt phthalocyanine containing monolayers can be obtained as a function of the number of cobalt phthalocyanine layers attached to the pyridine tagged self-assembled monolayer, using the Laviron method.[46]

Cyclic voltammetry provides information on surface coverage (Γ), standard potential (E^0), peak potential (E_p), peak current (i_p), differences in peak potentials (ΔE_p), the ratio of anodic to cathodic peak currents (i_{pa}/i_{pc}), standard kinetic rate constant (k^0), thermodynamic stability, and electron transfer pathways. These values can also be validated through other electrochemical techniques, such as chronocoulometry, chronoamperometry, and AC impedance.

1.6.1 TYPICAL DATA ANALYSIS

To ascertain if a system being studied behaves as an ideal, surface confined, reversible system, the peak currents and peak potentials observed in the cyclic voltammograms are plotted versus the scan rate or the square root of the scan rate, and

statistical analyses are performed. In a diffusionless system, e.g. SAM's, the anodic and cathodic peak currents are linearly related to the scan rate plot (see Figure 1.23). If these peak currents were linear with respect to the square root of the scan rate, then the system is diffusion controlled and other forms of mass transport are actively present.

Chemical reversibility is determined by the ratio of anodic to cathodic peak currents; which should equal one at all scan rates for a truly chemically reversible process.[18] Deviations from a ratio of one indicate processes which are not specifically reversible and may illustrate a coupled chemical reaction or a chemical (structural) rearrangement on the electrode's surface.[10,43]

Electrochemical reversibility is determined by a plot of ΔE_p versus the scan rate, and is expected to show ΔE_p increases exponentially with increasing scan rate (see Figure 1.24). From this plot k^0 can be derived.

Surface coverage is commonly used to determine if the electrode is partially or totally covered with the monolayer. Typical literature values, for species similar to those investigated herein, are reported at $1\text{-}9 \times 10^{-10}$ mol/cm^2.[16,20,35]

1.7 RESEARCH PROPOSAL

This is a proposal to study the extent of communication between a gold electrode and monolayers containing cobalt phthalocyanines, through a pyridine tagged alkanethiol chain. This project was expanded to study the construction of multi-layer films from the monolayer to produce molecular electronic devices. SAM's have become increasingly popular in the field of electrochemistry, and while binding a straight chain alkane to a surface may be interesting, applications are greatly increased through the use of

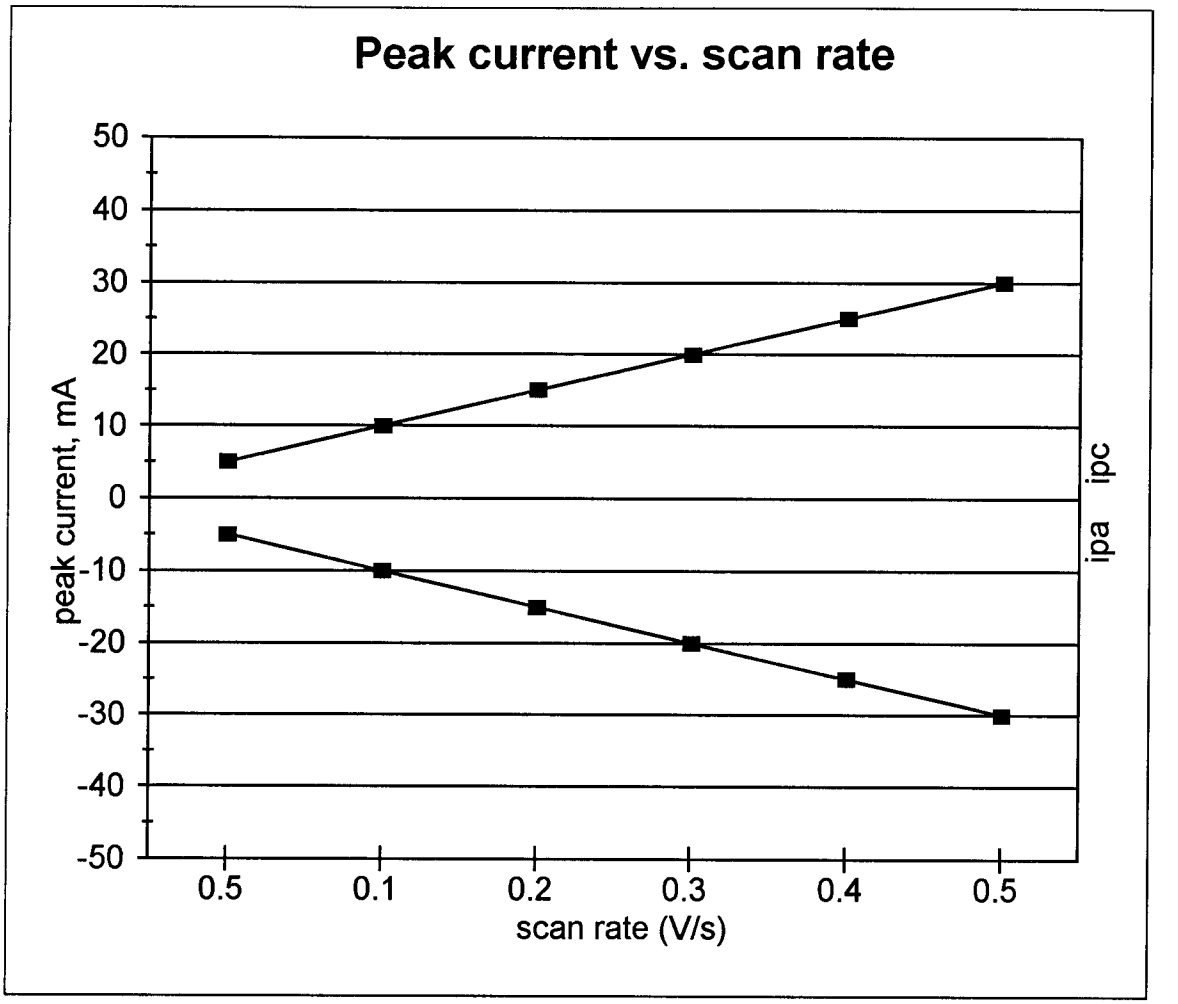

Figure 1.23 : Plot of i_{pc}, i_{pa} versus scan rate for a surface confined species, graphically representing the absence of diffusion in adsorbed species.

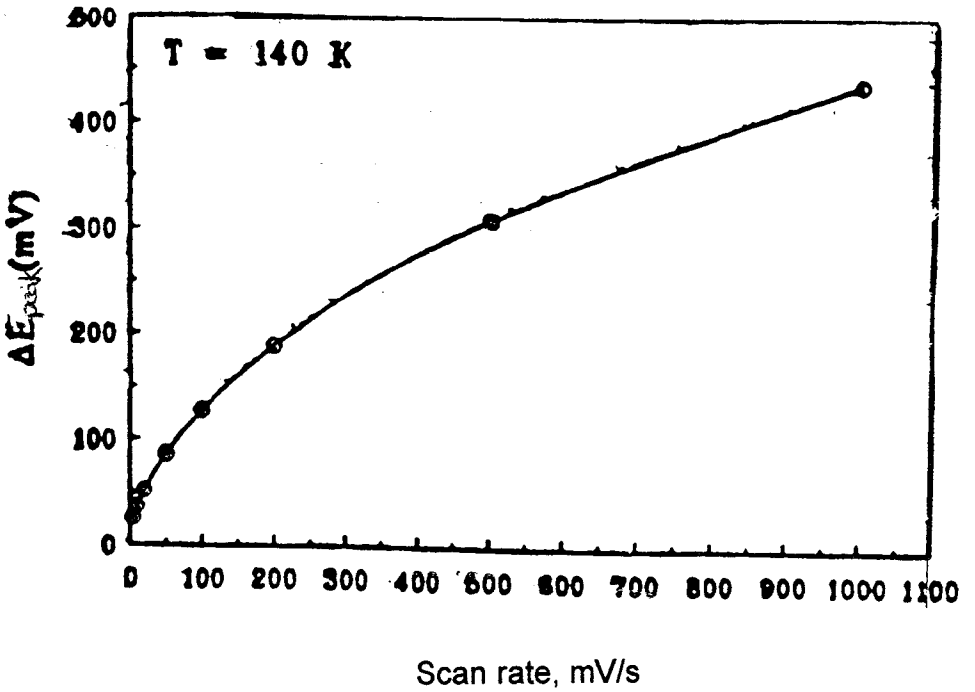

Figure 1.24 : ΔE_p as a function of potential scan rate for a silver electrode coated with a mixed monolayer of $CpFeCp(CH_2)_8SH$ and $CH_3(CH_2)_7SH$ (prepared from a 0.1 mM $CpFeCp(CH_2)_8SH$/0.83 mM $CH_3(CH_2)_7SH$ ethanolic solution). Reference electrode = Ag wire and electrolyte solution = 0.075 Bu_4NPF_6 in 2:1 EtCl/PrCN.

(Reprinted from ref. 47)

electroactive terminal groups. The properties of the electrode solution interface are determined by the number and nature of these terminal groups, e.g. polarizability, hydrophobicity, and chemical reactivity.

After a stable monolayer was formed, further layers can be added to extend the SAM. Typically, an electroactive group is attached to the terminus of the alkanethiol chain, and further attachments are made to this species.[26] The terminal group can be easily altered to adjust the chemical and physical characteristics of the monolayer through synthetic chemistry. In this study, a pyridine terminal group will be used because cobalt phthalocyanine has been shown to bind strongly to amines. Other layers can then be formed from this bi-layer and will consist of various combinations of layers of cobalt phthalocyanine and cobalt octafluorophthalocyanine. Successive layers will be separated by pyrazine spacers. These bidentate aromatic ligands should provide the phthalocyanines with a rigid support, while enhancing electron transfer through the metal-phthalocyanine and pyrazine π-system. As the layers form, they should begin to stack, and the orientation of this stacking is indicative of the degree of molecular interactions. Theoretically, these layers can be made from truly microscopic films to films which are several microns thick. Thus, the properties of films which bridge the macroscopic domain and the microscopic realm can be characterized. The experimental control gained through the use of SAM's should then enable the characterization of the region between truly microscopic and macroscopic systems, a currently obscure area. Multi-layers are characterized by techniques such as CV, STM, AFM, and X-ray diffraction.[30] Multi-layering processes have been used to create modern computer chips and sensing devices.

The proposed research makes use of the distinct advantages presented by monolayers in the production of molecular electronic devices and electrocatalysts. The approach involves the use of cobalt-phthalocyanine and cobalt-octafluorophthalocyanine in multi-layer films, in which the number and type of molecules can be readily controlled in stoichiometric amounts through systematic synthetic chemistry. Thus, structure/property correlations can be studied under highly controlled conditions in which the composition of the monolayer is systematically varied. The significance of this study is that it provides a unique approach, which is completely general for the production of molecular electronic devices. Such devices are currently being developed for application in electrocatalysis, and optical and high speed computing technologies.[2-4]

The major innovation employed by this research is that the devices which will be constructed are truly on the molecular scale. This offers significant advantages over devices constructed from macroscopic bi-layer films. In addition, this approach allows the construction of homogeneous and/or heterogeneous multi-layer films in which the number and type of active sites can be controlled in a fashion which is impossible on the macroscopic scale. Thus, the physical and electrochemical properties of the devices can be easily studied as a function of the number and type of molecular layers. This will allow for the optimization of the rectification properties of the devices for commercial applications. It is anticipated that successful completion of this research will lead to a greater understanding of molecular electronic devices and electrocatalysis.

References

(1) Anson, F. *J. Chem. Educ.* **1959**, *36*, 394-395.

(2) Bard, A.; Faulkner, L. *Electrochemical Methods*; Wiley: New York, **1980**.

(3) Brett, C. *Electrochemistry-Principles, Methods, and Applications*; Oxford University Press: New York, **1993**.

(4) Gale, R. *Spectroelectrochemistry- theory and practice*; Plenum Publishing: New York, **1988**.

(5) Ulman, A. *Chem. Rev.* **1996**, *96*, 1533-1554.

(6) Evans, D. *J. Chem. Educ.* **1983**, *60*, 290-293.

(7) Kuwana, T.; Heineman, W. *Acc. Chem. Res.* **1976**, *9*, 241-248.

(8) Heineman, W. *J. Chem. Educ.* **1983**, *60*, 305-308.

(9) Poirier, G.; Pylant, D. *Science* **1996**, *272*, 1145-1148.

(10) Nicholson, R; Shain, I. *Anal. Chem.* **1964**, *36*, 706-723A.

(11) Bockris, J.; Khan, S. *Surface Electrochemistry*; Plenum Press: New York, **1993**.

(12) Lingane, J. *Electroanalytical Chemistry*; Interscience: New York, 2nd Ed., **1958**.

(13) Anson, F. *Acc. Chem. Res.* **1975**, *8*, 400-407.

(14) Anson, F. *Anal. Chem.* **1966**, *38*, 54-57.

(15) Anson, F.; Osteryoung, J. *J. Chem. Educ.* **1983**, *60*, 293-296.

(16) Willicut, R.; McCarley, R. *J. Am. Chem. Soc.* **1994**, *116*, 10823-824

(17) Tour, J.; Jores, L.; Pearson, D.; Lamba, J.; Burgin, T.; Whitesides, G.; Allara, D.; Parikh, A.; Sundar, A. *J. Am. Chem. Soc.* **1995**, *117*, 9529-9534.

(18) Creager, S.; Collard, D.; Faox, M. *Langmuir* **1990**, *6*, 1617-1620.

(19) Kwan, V.; Cammarata, V.; Miller, L.; Hill, M.; Mann, K. *Langmuir* **1992**, *8*, 3003-3007.

(20) Lee, B. *Langmuir* **1990**, *6*, 709-712.

(21) Ulman, A. *An Introduction to Ultrathin Organic Films*; Academic Press: New York, **1994**.

(22) Murray, R. *Molecular Design of Electrode Surfaces*; Wiley: New York, **1992**.

(23) Bain, C.; Evall, J.; Whitesides, G. *J. Am. Chem. Soc.* **1989**, *111*, 7155.

(24) Bear, J.; Han, B.; Huang, S. *J. Am. Chem. Soc.* **1993**, *115*, 1175-1177.

(25) Kadish, K. M.; Adamian, V.; Van Camelbecke, E.; Tan, Z.; Tagliatesta, P.; Bianco, P.; Boschi, T.; Yi, G.; Khan, M.; Richter-Addo, G. *Inorg. Chem.* **1996**, *35*, 1343-1348.

(26) Han, B.; Kadish, K. M.; Bear, J. *Inorg. Chem.* **1993**, *32*, 4175-4176.

(27) Bear, J.; Han, B.; Huang, S.; Kadish, K. M. *Inorg. Chem.* **1996**, *35*, 3012-3021.

(28) Bear, J.; Li, Y.; Han, B.; Van Camelbecke, E.; Kadish, K. M. *Inorg. Chem.* **1996**, *35*, 3053-3055.

(29) Orihashi, Y.; Ohro, H.; Tsuchida, E. *Molecular Crystals and Liquid Crystals*, **1988**, *160*, 139-149.

(30) Mu, X. H.; Kadish, K. M. *Inorg. Chem.* **1988**, *27*, 4720-4725.

(31) Finkleu, H.; Hanshew, D. *J. Am. Chem. Soc.* **1992**, *114*, 3173-3178.

(32) Marks, T. *Science* **1985**, 227, 881-888.

(33) Zak, J.; Yuan, H.; Ho, M.; Woo, L.; Porter, M. *Langmuir* **1993**, *9*, 2772-2774.

(34) Simpson, T.; Revell, D.; Cook, M.; Russell, D. *Langmuir* **1997**, *13*, 460-64.

(35) Hutchinson, J.; Posthlewaithe, T.; Murray, R. *Langmuir* **1993**, *9*, 3277-3283.

(36) Anderson, T.; Komplin, G.; Pietro, W. *J. Phys. Chem.* **1993**, *97*, 6577-

6578.

(37) Yamakado, H.; Yakushi, K.; Kosugi, N.; Kuroda, H.; Kawamoto, A.; Tanaka, J.; Sugano, T.; Kinoshita, M.; Hino, S. *Bull. Chem. Soc. Jpn.* **1989**, *62*, 2267-2272.

(38) Creuger, S.; Hockett, L.; Rowe, G. *Langmuir* **1992**, *8*, 854-861.

(39) Widrig, C.; Chinkap, C.; Porter, M. *J. Electroanal. Chem.* **1991**, *310*, 335-359.

(40) Evans, D. *Acc. Chem. Res.* **1977**, *10*, 313-319.

(41) Ruhlmann, L.; Nakamura, A.; Vos, J.; Fuhrhop, J. *Inorg. Chem.* **1998**, *37*, 6052-6059.

(42) Li, D.; Swanson, B.; Robinson, J.; Hoffbauer, M. *J. Am. Chem. Soc.* **1993**, *115*, 6975-6980.

(43) Finklea, H.; Hanshew, D. *J. Am. Chem. Soc.* **1992**, *114*, 3173-3181.

(44) Kissinger, P.; Heineman, W. *J. Chem. Educ.* **1983**, *60*, 702-706.

(45) Laviron, E. *J. Electroanal. Chem.* **1979**, *100*, 263-270.

(46) Laviron, E. *J. Electroanal. Chem.* **1979**, *101*, 19-28.

(47) Curtin, L.; Peck, S.; Tender, L.; Murray, R. *Anal. Chem.* **1993**, *65*, 386-392.

CHAPTER 2 :

THE SYNTHESIS AND CHARACTERIZATION OF 1-(10-MERCAPTODECYL)ISONICOTINATE, A PYRIDINE TAGGED ALKANETHIOL DERIVATIVE.

2.1 INTRODUCTION

This chapter is devoted to the discussion of the synthesis, purification, and characterization of 1-(10-mercaptodecyl)isonicotinate. This molecule was chosen for self-assembly because the procedure utilized the thiol component to form a strong, covalent bond with gold and the pyridine end group to form a bond with the cobalt ion in cobalt phthalocyanine.[1-3] The synthetic protocol is outlined in Figure 2.1. The synthesis was performed by first thiolating a bromoalkane using sodium hydrosulfide hydrate. Next, the thiol group was protected by an adamantyl group. A pyridine derivative was then added to the chain via an ester addition. Finally, the thiol was deprotected with mercuric acetate leaving a pyridine tagged alkanethiol chain. A discussion of the self-assembly of this species onto a gold electrode, forming an electroactive monolayer, is then presented. The final synthetic phase involved the formation of multi-layer films of cobalt phthalocyanine built upon the 1-(10-mercaptodecyl)isonicotinate anchoring group. A description of other synthetic pathways which were attempted and the problems encountered with each will also be given.

STEP 1 : THIOLATION OF 10-BROMODECANOL

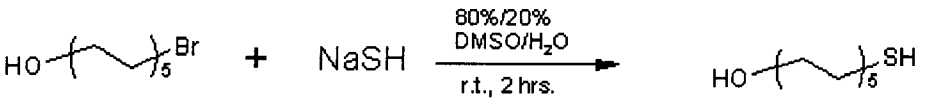

STEP 2 : PROTECTION OF 10-THIODECANOL

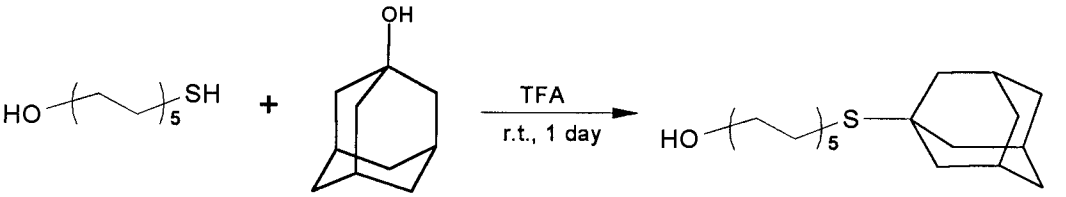

STEP 3 : FORMATION OF PYRIDINE CONTAINING ESTER

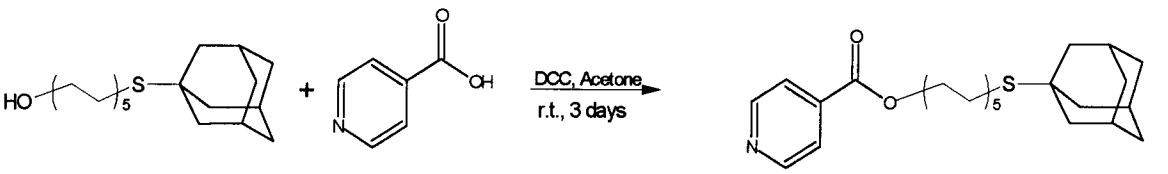

STEP 4 : DEPROTECTION OF THIOL

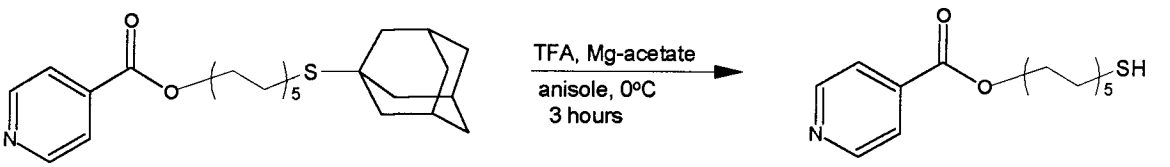

Figure 2.1 : EXPERIMENTAL SYNTHETIC PATHWAYS

2.2 EXPERIMENTAL

2.2.1 CHEMICALS

1-adamantol (adamantyl alcohol) (Aldrich, 99%), acetone (cert. ACS, Fisher, 99.5%), 1.0 μm aluminum oxide (Leco), anisole (Aldrich, 99.7%), argon (Praxair, 99.999%), 10-bromodecanol (Aldrich, 98%), 12-bromodecanol (Aldrich, 98%), chloroform (cert. ACS, Fisher, 99.9%), chlorotrimethylsilane (1.0 M in THF, Aldrich), cobalt(II) phthalocyanine (β-form, Aldrich, 97%), 1,12 dibromododecane (Aldrich, 98%), *N,N'*-dicyclohexylcarbodiimide (DCC) (1.0 M in methylene chloride, Aldrich), *N,N*-dimethylformamide (DMF) (HPLC grade, Aldrich, 99.9%), dimethylsulfoxide (DMSO) (cert. ACS, Aldrich, 99.9%), dinitrogen (Praxair, 99.999%), Epon 825 epoxy resin (Miller-Stephenson), ethyl acetate (cert. ACS, Fisher, 99.8%), hexanes (reag. ACS, Fisher, 98.5%), 1,1,1,3,3,3-hexamethyldisilazane (Aldrich, 97%), mercuric acetate (cert. ACS, Fisher, 99.4%), methylene chloride (cert. ACS, Fisher, 99.9%), 1,3-phenylenediamine (Aldrich, 99+%), phosphorus tribromide (Aldrich, 99.99%), potassium hydroxide (KOH) (pellet, cert. ACS, Aldrich, 85%), potassium chloride (KCl) (cert. ACS, Aldrich, 99%), pyrazine (cert. ACS, Aldrich, 99.9%), 4-pyridylcarbinol (Aldrich, 99%), 4-pyridylcarboxylic acid (isonicotinic acid) (Aldrich, 99%), sea sand (washed, Fisher), silica gel (200-400 mesh, 60Å, Aldrich), sodium bicarbonate (cert. ACS, Fisher, 99.8%), sodium chloride (cert. ACS, Fisher, 99+%), sodium hydride (60% dispersion in mineral oil, Aldrich), sodium hydrosulfide hydrate (Aldrich), sodium sulfate (cert. ACS, Aldrich, 99+%), tetrabutylammonium fluoride (Aldrich, 98%), tetrahydrofuran (THF) (HPLC grade, Fisher, 99.9%), triethylamine (cert. ACS, Fisher, 99.9%), and trifluoroacetic acid (TFA) (spec. grade, Fisher, 99.9%) were used as received. Cobalt

octafluorophthalocyanine was prepared via the method of Pietro.[4] Sodium acetate trihydrate (cert. ACS, Fisher, 99+%) and Tetra-n-butylammonium perchlorate (Fluka, 98%) were recrystallized before use.[5]

The general procedures used have been described in detail previously.[6] Unless otherwise noted, all reactions and any subsequent manipulations were conducted at ambient temperatures using conventional techniques for the manipulation of organic and inorganic compounds.[7-11] Where required, anaerobic and anhydrous conditions were maintained by using a prepurified argon atmosphere administered via a Schlenk line. Where necessary, reagents were purified before use and solvents were dried and deaerated by standard procedures and stored under dinitrogen or argon.[5]

2.2.2 INSTRUMENTATION

Mass spectra were obtained with a Finnigan GCQ ion-trap spectrometer with direct probe inlet using electron ionization (EI) and chemical ionization (CI). ^{1}H NMR and ^{13}C NMR were recorded on a Varian Gemini-2000 400 MHz NMR spectrometer with reference to the deuterium signal of the solvent employed. Chemical shifts are reported in parts per million down field from tetramethylsilane. Cyclic voltammetry was performed with a Bioanalytical Systems (BAS) 100W Potentiostat. Electrodes were polished on a Leco VP-160 polisher running at 110 rpm using "LECLOTH" flocked twill polishing cloths. Electrochemical cleaning of the electrodes was performed with an EG&G Princeton Applied Research Galvanostat model 273. Gold disk (1.6 mm diameter) working electrodes were purchased from Bioanalytical Systems, or were prepared from a 3mm diameter gold rod (Aldrich, 99.99%) via the method of Murray et

al.[12] Platinum counter electrodes, platinum disk (1.6 mm diameter) working electrodes, silver/silver chloride aqueous and silver/silver$^+$ non-aqueous reference electrodes, and single-compartment electrochemical cells were used as received from BioAnalytical Systems.

2.2.3 SYNTHESIS OF 10-THIODECANOL

10-thiodecanol was prepared via nucleophilic displacement of 10-bromodecanol with sodium hydrosulfide under static argon.[11] 885.1 mg (0.001579 mol, 300% excess) sodium hydrosulfide was first pulverized, then dissolved in 150 mL of an 80%/20% mixture of DMSO/H_2O in a 300 mL 3 neck round bottom flask. 1.2518 g (0.005263 mol) 10-bromodecanol was dissolved in 20 mL of methylene chloride and added dropwise via syringe to the thiol solution. The solution was allowed to stir for 2 hours at room temperature. Initially the thiol solution was yellow, but upon addition to the 10-bromodecanol the solution became very dark green. The reaction was monitored via thin layer chromatography using methylene chloride as the eluent. Upon completion of the reaction the thiolated species was extracted into methylene chloride. The organic layer was then washed several times with distilled water and brine and allowed to dry over sodium sulfate for one day. Excess solvent was then removed via rotary evaporation under reduced pressure. The crude product was then purified via column chromatography using methylene chloride as the eluent. The fraction that contained 10-thiodecanol (R_f= 0.5) was collected and the solvent removed, leaving 600.0 mg (0.003159 mol) of 10-thiodecanol (60.0% yield). The resulting white solid was characterized via ^{1}H and ^{13}C NMR yielding the following results (the lettered notation is

to used to relate the signal to the group and can be clearly seen on the appropriate NMR spectra):

^{1}H NMR ($CDCl_3$) : 5.296 ppm(s, 1H, OH, 'f'), 3.623 ppm(t, 2H, HO-C*H*$_2$, 'e'), 2.673 ppm(t, 2H, HS-C*H*$_2$, 'd'), 1.662 ppm(t, 2H, HS-CH_2-C*H*$_2$, 'b'), 1.541 ppm(s, 1H, SH, 'a'), 1.265 ppm(broad s, 12H, HO-CH_2-*(CH$_2$)$_6$*, 'c').

^{13}C NMR ($CDCl_3$) : All peaks represent 1 carbon singlets with peak position based on the carbon at HO-*C*H_2 being C^1: 64.212 ppm(C^1, 'a'), 40.413 ppm(C^9, 'b'), 34.018 ppm(C^2, 'c'), 30.846 ppm(C^4, 'd'), 30.748 ppm(C^5, 'e'), 30.680 ppm(C^6, 'f'), 30.482 ppm(C^7, 'g'), 30.460 ppm(C^8, 'h'), 29.769 ppm(C^3, 'i'), 26.992 ppm(C^{10}, 'j').

2.2.4 SYNTHESIS OF 10-(1-ADAMANTYL)THIODECANOL

The thiol in 10-thiodecanol was protected using 1-adamantyl alcohol in trifluoroacetic acid.[6] Protection of the thiol was necessary to prevent the formation of a thio-ester during the ester coupling reaction in the next step of the reaction sequence. Under static argon, 353.8 mg (0.001862 mol) 10-thiodecanol was placed into a 250 mL 3 neck round bottom flask. 290.8 mg (0.001910 mol) of 1-adamantyl alcohol was dissolved in 100 mL of trifluoroacetic acid. The solution was added slowly via an addition funnel to the 10-thiodecanol. The resulting solution was allowed to stir overnight (~17 hours) at room temperature. The reaction was monitored via thin layer chromatography employing 70%/30% and 30%/70% hexane/ethyl acetate and pure methylene chloride, as the eluents. Methylene chloride provided the best separation with the R_f values obtained being 0.4 for 1-adamantol, 0.5 for the 10-thiodecanol, and 0.9 for the 10-(1-adamantyl) thiodecanol. Upon completion of the reaction, the solution had a

faint yellow color. The excess trifluoroacetic acid was removed via rotary evaporation under reduced pressure. The solution became slightly cloudy during solvent removal, however no precipate was observed. To induce crystallization cold distilled water was added to the solution. The solution was then sonicated to fully dissolve the suspension and then allowed to cool slowly to room temperature; in order to recrystallize the product. This was done to avoid excessive heating, which might have decomposed the product. Sonication immediately caused the formation of a suspension of a white solid. Most of the water was then evaporated from the solution using a hot plate, leaving a thick milk-like suspension (~30 mL). The product was believed to be more stable and resistive to decomposition once it had recrystallized from solution. This suspension was then cooled to –78 °C in a dry ice/acetone bath and a white, flaky solid precipitated out of solution. The precipitate was isolated via vacuum filtration. The crude product was dissolved in methylene chloride and purified via flash column chromatography, using methylene chloride as the eluent. The product was formed in quantitative yields, 604.3 mg being collected, after the solvent was removed from the fraction containing the desired product. The resulting white solid was then characterized via ^{1}H NMR yielding the following results:

^{1}H NMR ($CDCl_3$) : 5.296 ppm(s, 1H, OH, 'a'), 4.339 ppm(t, 2H, HO-CH_2, 'e'), 3.625 ppm(t, 2H, adamantyl-S-CH_2, 'b'), 1.856 & 1.679 ppm(broad s, 6H, adamantyl $(CH_2)_3$, C" and C^x), 2.026 ppm(s, 3H, adamantyl $(CH)_3$, C'), 1.602 & 1.261 ppm(broad s, 16H, HO-CH_2-$(CH_2)_8$, 'f').

2.2.5 SYNTHESIS OF 10-(1-ADAMANTYL)THIODECYL ISONICOTINATE

10-(1-Adamantyl)thiodecyl isonicotinate was prepared via an ester coupling reaction between 4-pyridyl carboxylic acid (isonicotinic acid) and 10-(1-adamantyl)thiodecanol employing dicyclohexylcarbodiimide (DCC) as the coupling reagent.[6-9] 230.7 mg (0.001871 mol) isonicotinic acid was placed in a 2 L erlenmeyer flask and dissolved in ~1500 mL of acetone. The solution was gently heated (~30°C) and stirred for approximately 26 hours to dissolve the slightly soluble isonicotinic acid. After complete dissolution, the solution was transferred to a 2 L 3-neck round bottom flask, with stirring. 500.7 mg (0.002421 mol, 130% excess) DCC was then added. 604.3 mg (0.001864 mol) 10-(1-adamantyl)thiodecanol was dissolved in a minimal amount of acetone (~50 mL) and added dropwise to the stirred solution via syringe. The addition was performed under static argon. Thin layer chromatography was used to monitor the reaction's progress and after 3 days of stirring at room temperature the reaction was deemed to be complete. Heating was not introduced into this reaction to prevent the formation of by-products through unwanted side reactions.[6] The resulting suspension was vacuumed filtered, leaving a powdery white precipate. The precipate was recrystallized in acetone, washed with distilled water, and dried under vacuum. 558.8 mg of product was collected, correlating to a 69.9% yield. Thin layer chromatography, employing methylene chloride as the eluent, revealed that the compound had an R_f value of 0.6 and that the product was pure. This product was then characterized via ^1H and ^{13}C NMR yielding the following results:

^1H NMR ($CDCl_3$) : 8.315 ppm(broad, 4H, N*(CH)*$_4$, 'a' and 'd') [seen as a doublet of doublets in D_2O], 2.165 & 1.515 ppm(broad s, 6H, adamantyl $(CH_2)_3$, C" and C^x), 2.204

ppm(s, 3H, adamantyl CH, C'), the following peak positions are based on the carbon at C(=O)O-CH_2 being C^1: 4.337 ppm(t, 2H, C^1H_2, 'e'), 2.889 ppm(t, 2H, $C^{10}H_2$, 'b'), 1.414 ppm(m, 16H, $C^{2\text{-}9}H_2$, 'f').

^{13}C NMR ($CDCl_3$) : 163.111 ppm(s, 1C, $N(CH_2)_2(CH)$-*C*=O, 'g'), 162.762 ppm(broad s, 1C, $N(CH_2)_2$-*C*H, 'h'), 157.914 ppm(s, 2C, $N(CH)_2$*(CH)*$_2$, 'd'),150.836 ppm(s, 2C, $N(CH)_2$, 'a'), 51.019 ppm(s, 1C, S-C[adamantyl], 'i'), 50.549 & 37.599 ppm(broad s, 3C each, adamantyl's $(CH_2)_3$, C^x and C'), 44.829 ppm(broad s, 3C, adamantyl's $(CH)_3$, C"), (unless otherwise noted the following peaks represent 1C singlets with peak positions based on the carbon at C(=O)O-*C*H_2 being C_1): 54.130 ppm(C^1, 'e'), 35.027-26.795 ppm($C^{2\text{-}9}$, 'f' and 'j-p'), 26.143 ppm(C^{10}, 'b').

2.2.6 SYNTHESIS OF 1-(10-MERCAPTODECYL)ISONICOTINATE

Deprotection of the thiol was initiated using mercuric acetate in trifluoroacetic acid.[6-11] 558.8 mg (0.001331 mol) 10-(1-adamantyl)thiodecyl isonicotinate was placed into a 100 mL 3-neck round bottom flask containing 55 mL trifluoroacetic acid. 479.4 mg (0.001547 mol) mercuric acetate, which was previously dissolved in 20 mL trifluoroacetic acid and 1 mL anisole (used as a scavenger), was added slowly via syringe, under static argon. The solution was then cooled to ~0 °C by placing the flask in an ice/water bath. Initially the solution was white, and upon addition of the mercuric acetate the mixture bubbled vigorously and turned a light yellow color. The reaction was allowed to stir for 2 hours and was monitored via thin layer chromatography. After the reaction was complete, the excess trifluoroacetic acid was removed under reduced pressure via rotary evaporation until only a few milliliters of solution remained. The

resulting suspension contained a white precipitate that was isolated via vacuum filtration on a sintered glass frit and washed with ether. The precipitate was then recrystallized twice from distilled water, filtered, and re-washed with ether. This resulted in a gray-white solid. 135.6 mg (0.0004590 mol) of final product was collected (40.2%). Thin layer chromatography employing methylene chloride as the eluent revealed one product with a R_f value of 0.8. This product was then characterized via ^1H NMR and mass spectrometry yielding the following results:

^1H NMR ($CDCl_3$) : 8.800 ppm(t, 2H, N*(CH)*$_2$, 'a'), 7.875 ppm(t, 2H, N(CH)$_2$*(CH)*$_2$, 'd'), 3.467 ppm(q, 2H, pyridine-(C=O)-O-C*H*$_2$, 'e'), 2.341 ppm(t, 2H, HS-C*H*$_2$, 'b'), 2.168 ppm(broad s, 2H, HS-CH$_2$-*CH*$_2$, 'g'), 1.560 & 1.248 ppm(broad s, 16H, HS-CH$_2$-*(CH*$_2$*)*$_8$, 'f'), 0.875 ppm(s, 1H, SH, 'c').

MS : parent ion at 295 m/z (CI), notable fragments found at 149 m/z (EI and CI), 124 m/z (EI), 123 m/z (EI), 106 m/z (EI) and at 78 m/z (EI).

2.2.7 SELF-ASSEMBLY OF PYRIDINE TAGGED ALKANETHIOL MONOLAYERS

Monolayers constructed of 1-(10-mercaptodecyl)isonicotinate were prepared via self-assembly from a stirred 1 mM aqueous solution onto gold electrodes.[13,14] The electrode surface was prepared by polishing the electrode with sequentially finer grades of aluminum oxide with intermittent sonication of the electrode in distilled water. The final polish was with 1.0 μm aluminum oxide. Polishing was continued until a mirror finish was achieved. The working electrode was then electrochemically reduced in 1.0 M $HClO_4$ by applying a constant current of + 10 mA/cm^2 for 15-20 minutes to the electrode. Electrochemical cleaning was performed to prevent the formation of a surface oxide layer

on the gold.[14] The cleaning was performed with an EG&G Princeton Applied Research model 273A galvanostat using a platinum counter electrode and a silver wire pseudo-reference electrode. After the electrodes were prepared, they were placed in a 1 mM aqueous solution of 1-(10-mercaptodecyl)isonicotinate. The electrodes were allowed to soak in the stirred coating solution for 1 day to allow time for complete self-assembly, see Figure 2.2. Studies were also conducted on 2 and 3 day soaking times, however the 1 day soaking proved to be the most reliable and reproducible and was used for most of the analysis. After soaking, the electrodes were rinsed with distilled water, diethyl ether, and finally 1.0 M sodium acetate solution. The chemical and electrochemical properties of the monolayers were investigated via cyclic voltammetry. This step was performed in a single compartment electrochemical cell, with 1.0 M sodium acetate electrolyte, using a monolayer coated gold working electrode, a platinum counter electrode, and a silver/silver chloride reference electrode. After a well ordered monolayer was formed and characterized via cyclic voltammetry,[15-18] cobalt phthalocyanine was then introduced for construction of bi- and multi-layers films.

2.2.8 SELF-ASSEMBLY OF COBALT PHTHALOCYANINE

After the successful formation of monolayers containing 1-(10-mercaptodecyl)isonicotinate, cobalt phthalocyanine was then attached to the pyridine end group, see Figure 2.3. This was accomplished by soaking the electrodes in a stirred 1 mM solution of cobalt phthalocyanine in methylene chloride for 1, 2, and 3 days.[19] After soaking, the electrodes were rinsed with methylene chloride, sonicated in methylene chloride for 10-15 minutes, rinsed again with methylene chloride, distilled water, and

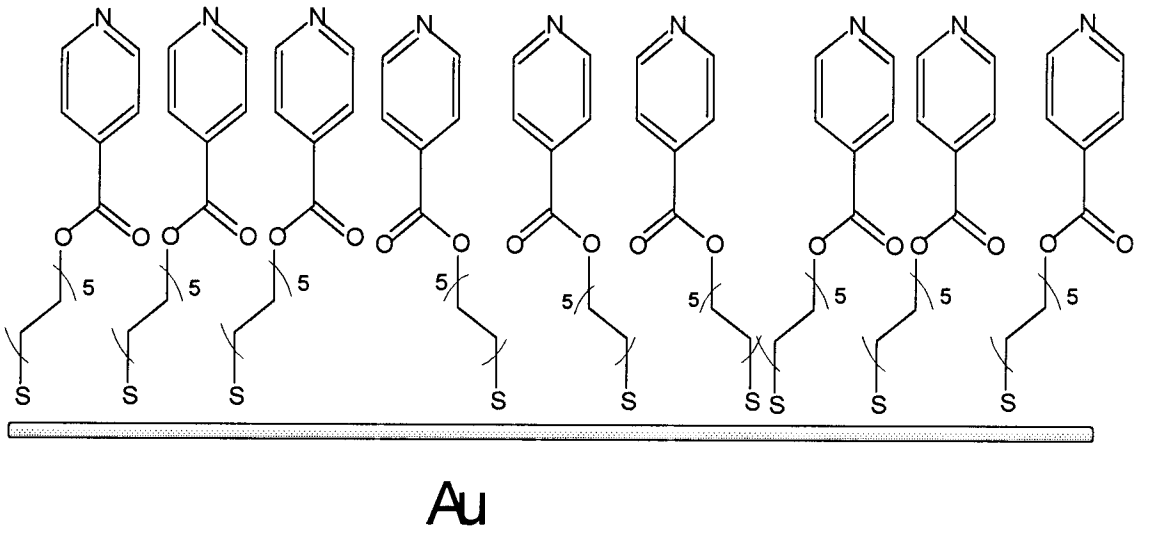

Figure 2.2 : Self-assembly on gold electrodes.

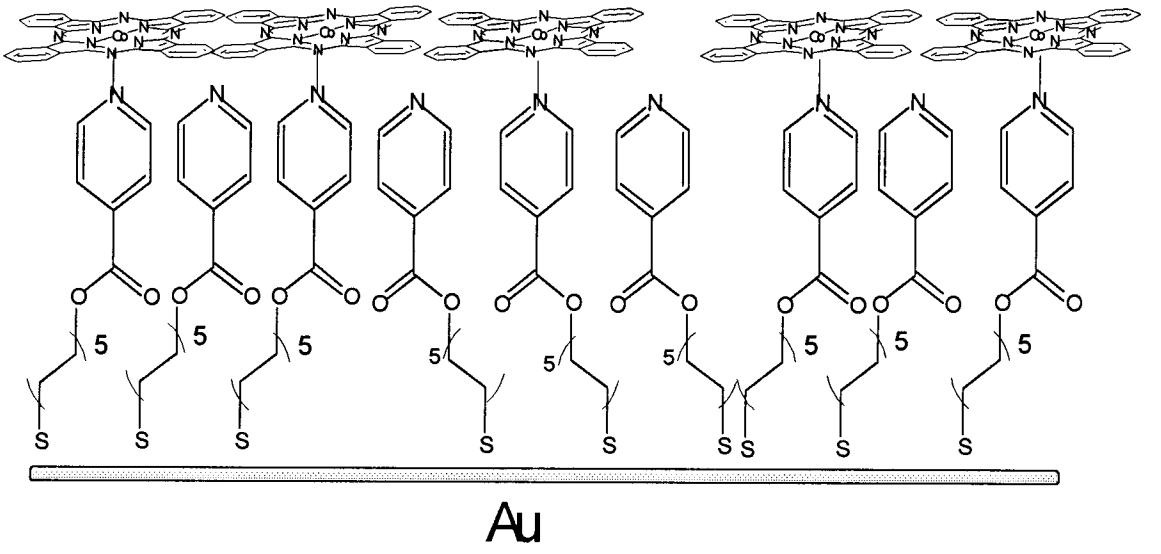

Figure 2.3 : Bi-layer formation.

finally with 1.0 M sodium acetate. The cyclic voltammetry of the 1 day soaking showed the cobalt $2^{+}/3^{+}$ redox couple, indicating that the cobalt phthalocyanine was successfully assembled onto the pyridine end group. The voltammetry on 2 and 3 day soakings, however, showed that the bi-layer had become more ordered, as the peaks in the voltammogram were sharper and easier to integrate. The 2 day soaking proved to be the most reliable and reproducible and was used for most of the analysis.

2.2.9 CONSTRUCTION OF MULTI-LAYER FILMS OF COBALT PHTHALOCYANINES

The successful construction of the cobalt phthalocyanine bi-layer allowed the fabrication of heterogeneous and homogeneous multi-layer films, see Figure 2.4. The bi-layer coated electrodes were first allowed to soak for 2-3 hours in a stirred 1 mM solution of pyrazine in methylene chloride. Pyrazine is known to axially ligate to cobalt in cobalt containing macrocycles[10,19-21] and was used as a spacer group to increase multi-layer order by keeping the large phthalocyanine rings at a fixed distance from each other. The rings need not only to be spatially defined but also parallel to one another. Pyrazine is expected to maintain the ring's co-planarity, thus controlling ring-ring interactions. Also, since the pyrazine is a bidentate, aromatic ligand it was expected to facilitate electron transfer through the layered, phthalocyanine π ring system.[22-24] Following the above outlined protocol for each newly constructed layer, the electrodes were then soaked in a stirred 1 mM solution of cobalt phthalocyanine in methylene chloride for 1-2 days. After three layers of cobalt phthalocyanine had been successfully formed, a layer of cobalt octafluorophthalocyanine was then added forming four layers of phthalocyanine

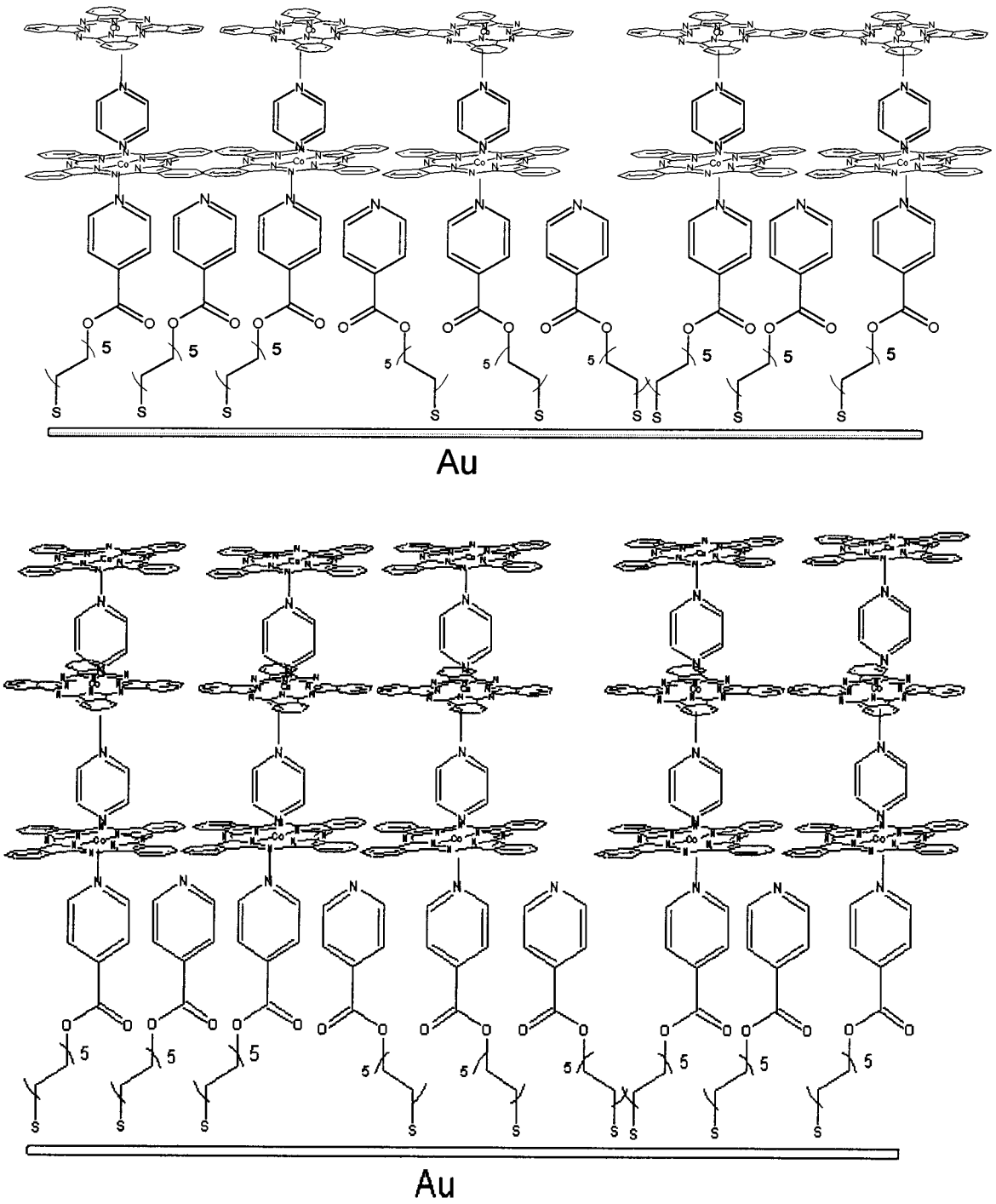

Figure 2.4 : MULTI-LAYER FORMATION

molecules, following the above procedure. Each completed layer was then analyzed via cyclic voltammetry and examined for molecular rectification properties.[25-28]

2.2.10 CONSTRUCTION OF MULTI-LAYER FILMS OF COBALT OCTAFLUOROPHTHALOCYANINE

A layer of cobalt octafluorophthalocyanine was self-assembled onto a monolayer containing 1-(10-mercaptodecyl)isonicotinate from a 1 mM coating solution of cobalt octafluorophthalocyanine in methylene chloride, following the protocol outlined above. The electrode soaking was allowed to continue for 2 days. This bi-layer was constructed to ascertain how this species would self-assemble and how it's formal potential would be altered from solution to self-assembly. This procedure was also necessary to properly identify changes found in the mixed multi-layer voltammograms believed to be characteristic of the cobalt octafluorophthalocyanine. After the bi-layer was successfully assembled, a tri-layer of cobalt octafluorophthalocyanine was constructed, following the protocol outlined above for the construction of multi-layer films. This tri-layer was constructed to support the findings of the cobalt phthalocyanine tri-layers that surface coverage is directly proportional to number of layers. Each completed layer was analyzed via cyclic voltammetry and will be discussed in Chapter 3.

2.3 RESULTS AND DISCUSSION

The self-assembled monolayer and subsequent multi-layers were characterized via cyclic voltammetry. Information obtained from the voltammograms was then used to describe the activity of the bound species on a molecular level; based on faradaic and

non-faradaic currents.[29-33] When the voltammograms were generated, the redox waves were examined for chemical and electrochemical reversibility.[15] In addition, analysis to determine the heterogeneous electron transfer rate constant was conducted using the Laviron method.[34,35] The homogeneous multi-layers of cobalt phthalocyanine showed the expected increase in current response and surface coverage proportional to the number of layers constructed.[22,29] The alternating multi-layers of cobalt phthalocyanine and cobalt octafluorophthalocyanine exhibit an increase in current response and surface coverage with increasing number of layers.

Cyclic voltammetry was used to determine the formal potential of the cobalt phthalocyanines.[13,31] Information such as surface coverage (Γ), standard potential (E^0), peak potential (E_p), peak current (i_p), difference in peak potentials (ΔE_p), ratio of anodic to cathodic currents (i_{pa}/i_{pc}), standard kinetic rate constant (k^0), thermodynamic stability, and electron transfer pathway was obtained from the cyclic voltammograms. All electrochemical data and analysis are included in Chapter 3.

2.3.1 CHARACTERIZATION OF 10-THIODECANOL via NMR

The ^{1}H NMR of 10-thiodecanol in $CDCl_3$ is shown in Figure 2.5. Peaks were assigned based on their chemical shifts, multiplicities, and integrations. The singlet at 5.3 ppm was from the hydrogen directly bound to oxygen and was labeled as peak F. The protons on the methylene group bound to the oxygen gave a triplet at 3.6 ppm, labeled as peak E, and was used as a reference point for identifying the spectra of products in subsequent steps. The methylene group attached to the thiol gave a triplet at 2.6 ppm and was labeled as peak D. The methylene attached to group D gave a distorted triplet at 1.7

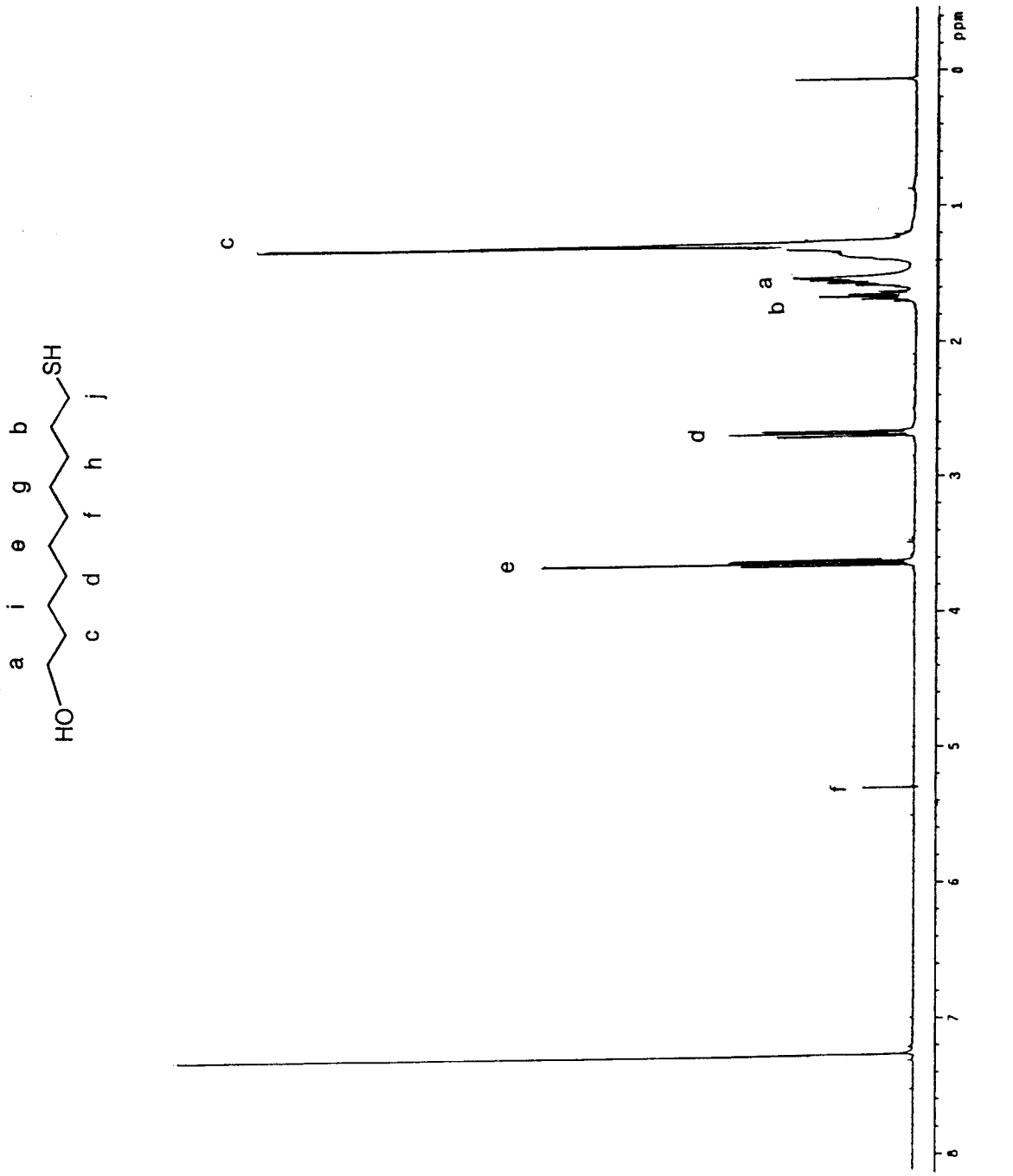

Figure 2.5 : ^{1}H NMR of 10-thiodecanol.

ppm and was labeled as peak B. This group is commonly found close to the thiol's proton and so differences in peak position and shape between spectra were used to determine the success of substitution on the thiol. The thiol's hydrogen gave a broad singlet at 1.5 ppm, labeled as peak A. The appearance of this peak, along with the loss of the bromine peak (3.2 ppm), confirms the successful thiolation of the alkane chain. The final broad singlet at 1.3 ppm, labeled as peak C, is from the methylene hydrogens within the chain. The broadness of this peak is believed to be do to the flexable nature of the alkane chain, which is expected to intensify proton-proton interactions, and was found to broaden many peaks in the ^{1}H NMR spectra taken.

The ^{13}C NMR of 10-thiodecanol in $CDCl_3$ can be seen in Figure 2.6. All observed peaks were singlets and are identified as follows, starting with the carbon attached to the oxygen and progressing towards the thiol: 64.2 ppm (peak A), 34.0 ppm (peak C), 29.8 ppm (peak I), 30.8 ppm (peak D), 30.7 ppm (peak E), 30.6 ppm (peak F), 30.5 ppm (peak G), 30.4 ppm (peak H), 40.4 ppm (peak B), and finally 27.0 ppm (peak J). These peak assessments were used as a template for further ^{13}C NMR peak identification. Of particular interest is the carbon nearest the oxygen. This peaks' position was found to remain fairly constant throughout the synthetic procedure, and so was used to follow the progression of the synthesis.

2.3.2 CHARACTERIZATION OF 10-(1-ADAMANTYL)THIODECANOL via NMR

The ^{1}H NMR of 10-(1-adamantyl)thiodecanol in $CDCl_3$ is presented in Figure 2.7. All expected peaks were observed and identified. The proton bound directly to the oxygen gave a singlet at 5.3 ppm and was labeled as peak A. The protons on the

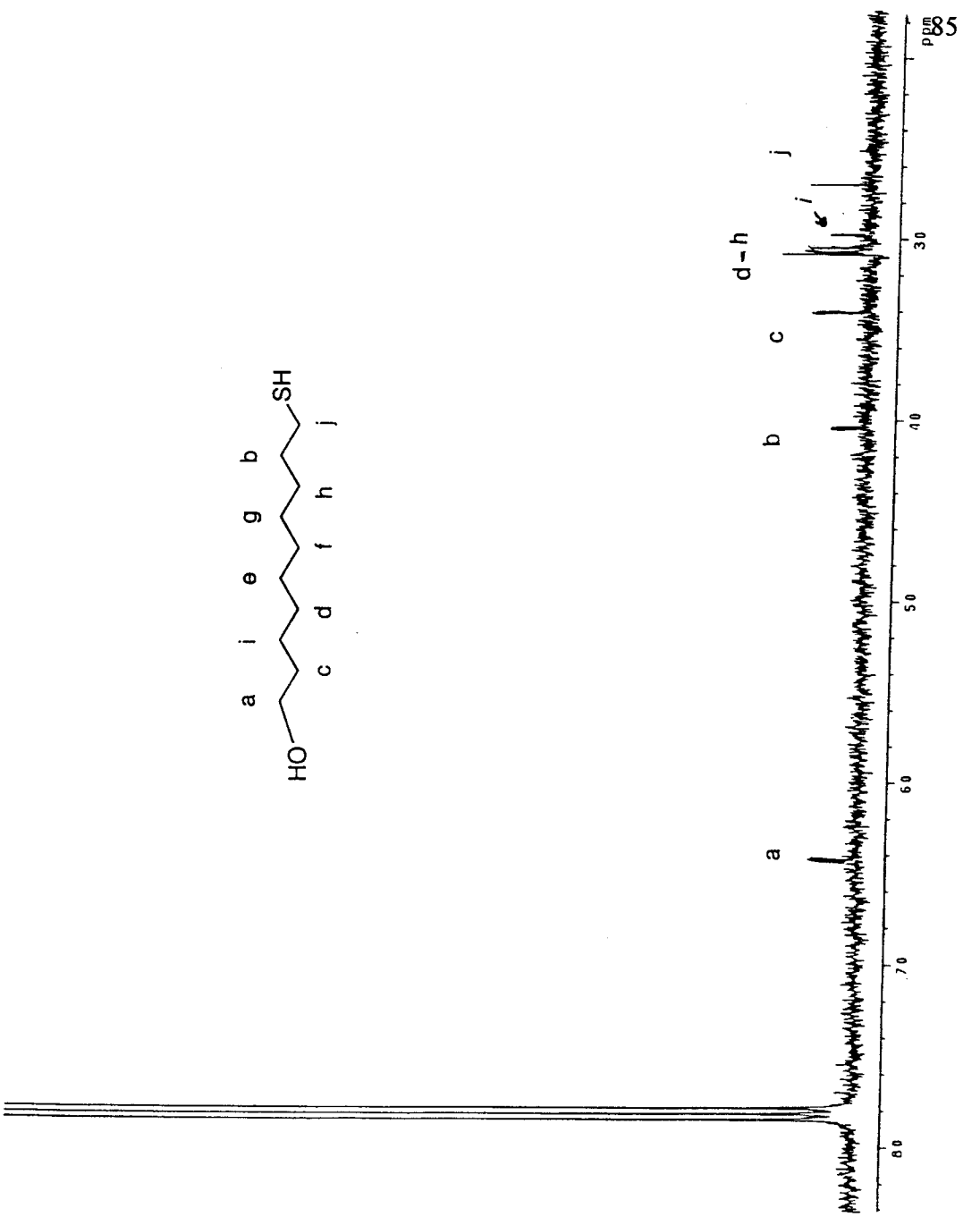

Figure 2.6 : ^{13}C NMR of 10-thiodecanol.

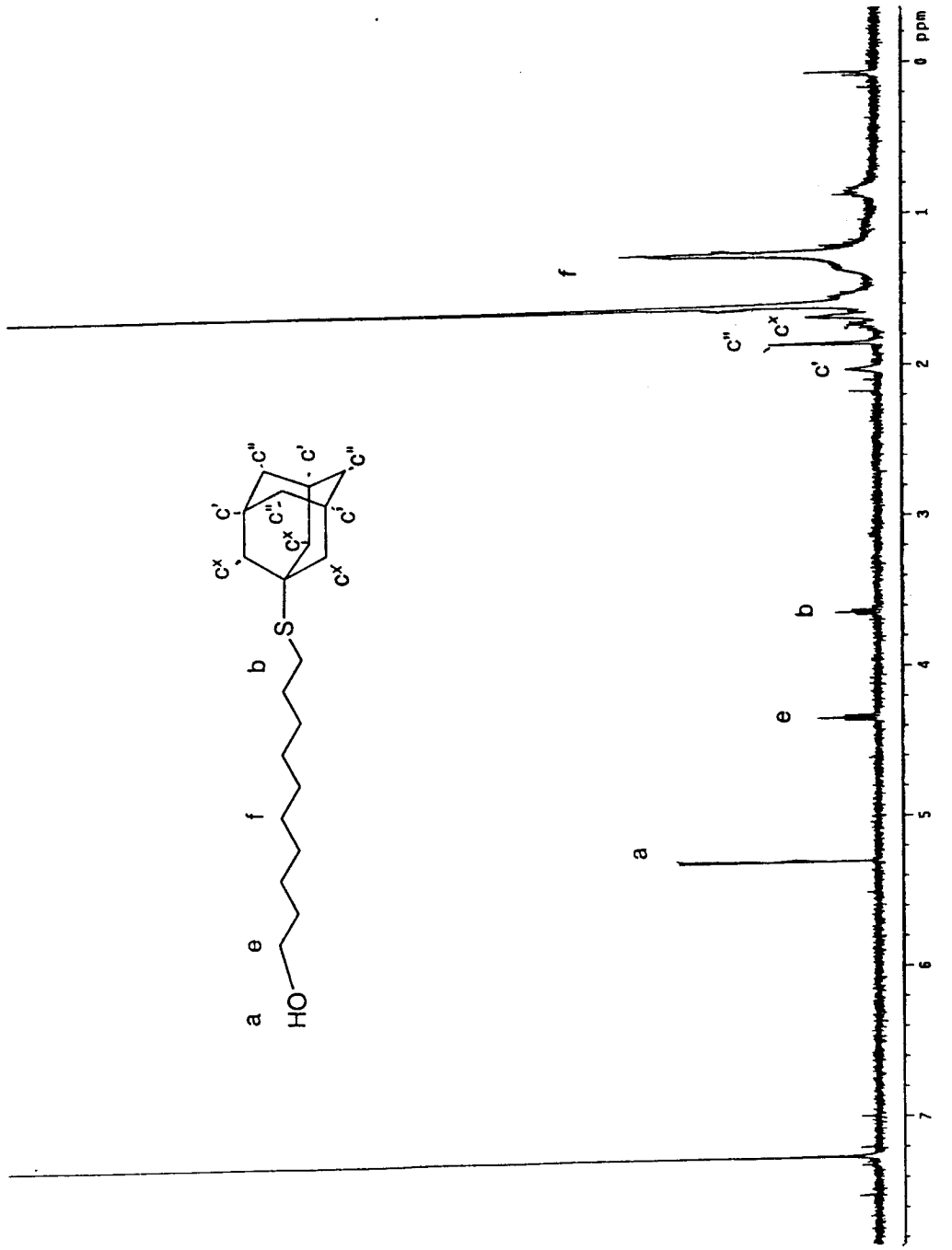

Figure 2.7 : ^{1}H NMR of 10-(1-adamantyl)thiodecanol.

methylene group attached to the oxygen gave a triplet at 4.3 ppm and were labeled as peak E. This peak was shifted slightly upfield, most likely due to the addition of the bulky adamantyl group. The protons on the methylene bound to the sulfur gave a triplet at 3.6 ppm and were labeled as peak B. This peak was found to shift downfield when compared to the 10-thiodecanol. This shift of 1 ppm indicates a significant change in the environment near the methylene group and, along with the appearance of the adamantyl's characteristic peaks, indicates a successful reaction. The adamantyl substituent had three types of proton signals from two sets of three CH_2 groups and one set of three CH groups. The three CH_2 groups closest to the thiol, labeled as C^x, gave a broad singlet at 1.7 ppm. The other CH_2 group, labeled as C", gave a singlet at 1.9 ppm. The CH group gave a broad singlet at 2.0 ppm and was labeled as C'. The proton signals from the middle of the chain were labeled as peak F and gave broad singlets at 1.6 and 1.3 ppm. Due to the intermediates poor solubility and instrumental difficulties analysis via ^{13}C NMR was not performed.

2.3.3 CHARACTERIZATION OF 10-(1-ADAMANTYL)THIODECYL ISONICOTINATE via NMR

The ^1H NMR of 10-(1-adamantyl)thiodecyl isonicotinate in $CDCl_3$ is presented in Figure 2.8. All expected peaks were observed and identified. The protons in the pyridine gave a broad singlet at 8.3 ppm and were labeled as peaks A and D. Two distinct doublets were expected for the 2 types of hydrogens in the pyridine, however, the NMR was undergoing shimming problems and so most peaks were distorted. The appearance of the pyridine hydrogen peaks far downfield and the loss of the alcohol peak confirmed

the attachment of the isonicotinic acid to the thiol-protected chain through an ester coupling. The methylene group bound directly to the oxygen gave a singlet at 4.3 ppm and was labeled as peak E. The methylene group attached to the sulfur was found to shift upfield, resulting in a singlet at 2.9 ppm and was labeled as peak B. The adamantyl proton groups, labeled as above, gave broad singlets at 2.2 and 1.5 ppm for C" and C^{x}, respectively, and a singlet at 2.2 ppm for C'. Unless otherwise noted, all peaks were found to shift slightly downfield, when compared to the 10-(1-adamantyl)thiodecanol, and to sharpen greatly. The proton signals from the middle of the chain were labeled as peak F and gave a broad singlet at 1.4 ppm.

The ^{13}C NMR obtained in $CDCl_3$ can be seen in Figure 2.9. All peaks observed were singlets, however, some were broadened by instrumental problems and residual acetone. The acetone had characteristic peaks at 208 and 32 ppm. The first hydrogens at ring positions 2 and 6 in the pyridine ring, labeled as A, gave a singlet at 150.8 ppm. The other protons at ring positions 3 and 5, labeled as D, gave a singlet at 157.9 ppm. The appearance of these peaks, compared to 10-thiodecanol's ^{13}C NMR, reaffirms the addition of the pyridine group to the chain. The carbon at ring position 4, labeled as H, gave a singlet at 162.8 ppm and the carbon attached to the ketone oxygen gave a singlet at 163.1 ppm and was labeled as peak G. The carbons in the alkane chain were identified as follows starting with the carbon attached to the ester oxygen and progressing towards the sulfur: 54.1 ppm (peak E) this peak shows a considerable shift from that observed in 10-thiodecanol as was expected to be the case with the addition of such large substitutes on either end of the chain and indicates a deshielding of the protons. 35.0 ppm (peak F), 26.8 ppm (peak P), 27.3 ppm (peak J), 32.2 ppm (broadened, peaks K and O), 29.2 ppm

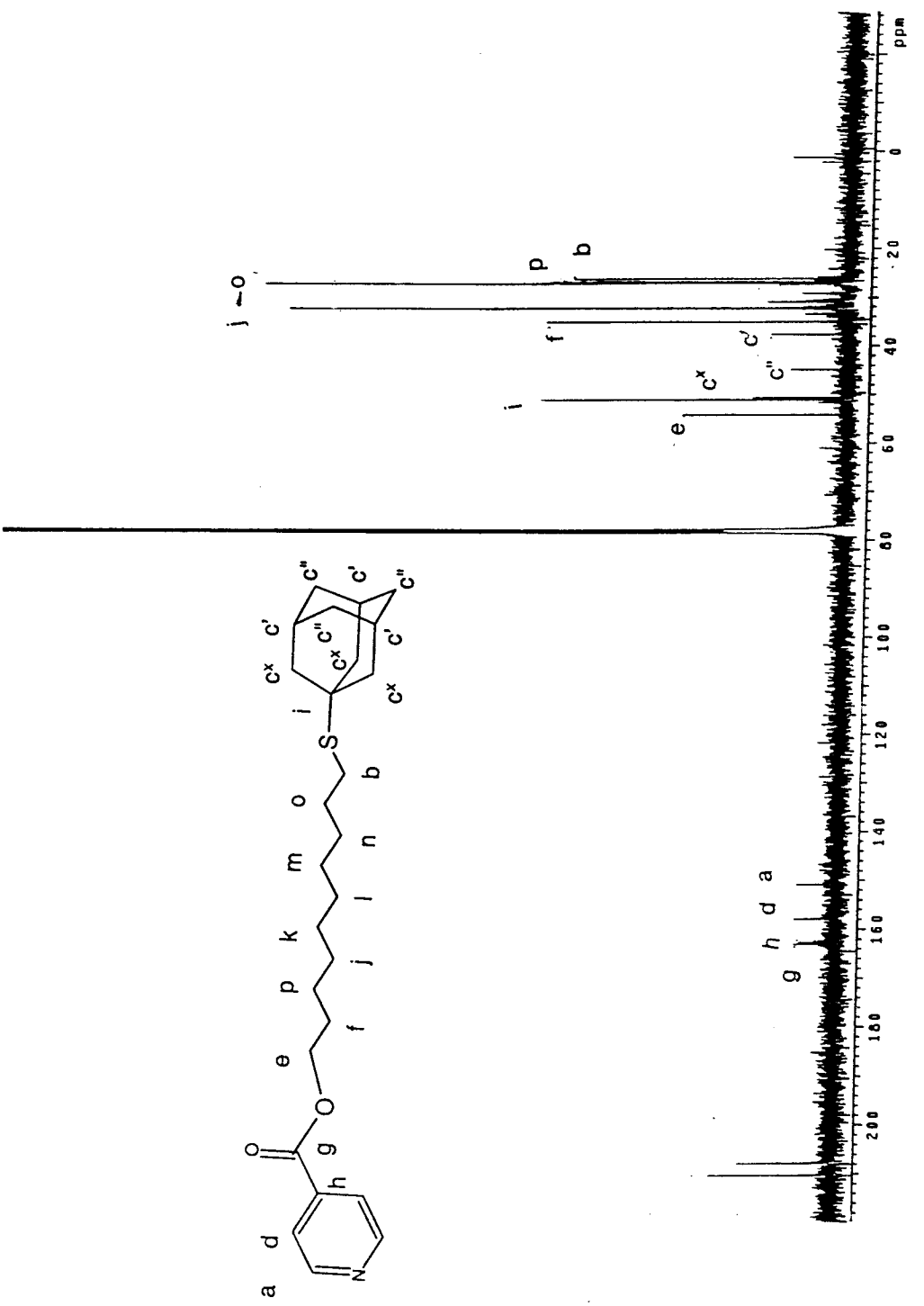

Figure 2.9 : ^{13}C NMR of 10-(1-adamantyl)thiodecyl isonicotinate.

(peak L), 27.1 ppm (peak M), 30.9 ppm (peak N), and 26.1 ppm (peak B). The adamantyl's carbon, labeled as with the ^{1}H NMR, were found to give broad singlets at 50.5 ppm (C^{x}), 44.9 ppm (C"), 37.6 ppm (C'), and at the point of attachment to the sulfur 51.0 ppm (peak I). All ten carbons from the decane chain were assigned, as was the presence of the adamantyl group, indicating that the desired product was formed. This is important in consideration of the inability to acquire a ^{13}C NMR for the 10-(1-adamantyl)thiodecanol and supports the success of the proposed reaction scheme.

2.3.4 CHARACTERIZATION OF 1-(10-MERCAPTODECYL)ISONICOTINATE via NMR and MASS SPECTROMETRY

The ^{1}H NMR of 1-(10-mercaptodecyl)isonicotinate in $CDCl_3$ is represented in Figure 2.10. All expected peaks were observed and identified. The protons in the pyridine gave two distinct doublets at 8.8 ppm and 7.9 ppm and were labeled as peaks A and D, respectively. These peaks became sharper from the 10-(1-adamantyl)thiodecyl isonicotinate spectrum and were easier to identify. The protons on the methylene group nearest the ester oxygen were shifted slightly upfield and gave a triplet at 3.5 ppm, labeled as peak E. This shift is believed to be indicative of the increase in the freedom of motion within the alkane chain and is seen by this proton's shift towards a position similar to that of the unsubstituted 10-thiodecanol. The next triplet at 2.3 ppm, labeled as peak B, is from the methylene hydrogens closest to the thiol. This peak has been greatly shifted upfield, indicating a change in its local environment, which is supported by the distinguishable peak from the methylene group attached to group B. These protons gave broad singlet at 2.2 ppm and were labeled as peak G. The thiol proton, labeled as peak C,

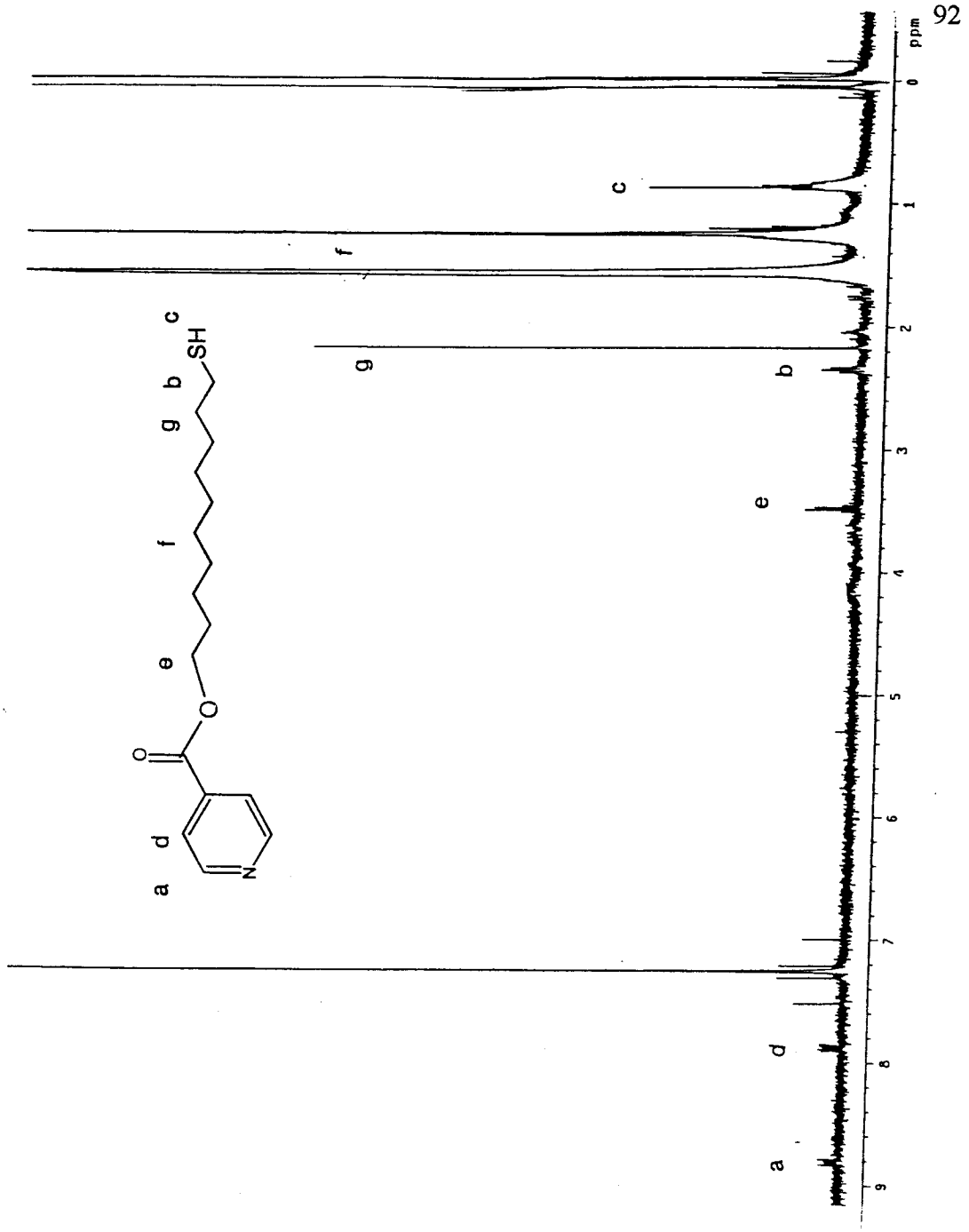

Figure 2.10 : ^{1}H NMR of 1-(10-mercaptodecyl)isonicotinate

is also believed to be shifted upfield and is seen as a broad singlet at 0.9 ppm. The appearance of this peak and the loss of the adamantyl's peaks confirm the deprotection of the thiol. The methylene hydrogens within the chain gave 2 broad singlets at 1.6 and 1.3 ppm and were labeled as peak F. A ^{13}C NMR was unable to be taken due to solubility problems.

Mass Spectrometry (EI) : Although the plot of ion current versus time as a function of the temperature of the probe initially was expected to show 1 peak, 2 peaks were seen in this product. The first peak is attributed to the analyte, see Figure 2.11, while the second peak was found to be from instrumental contaminants. This made definitive labeling of the parent ion peak arguable, however, the product's identity was determined by ascertaining the fragmentation patterns listed in Table 2.1. Since ion fragmentation was used, whenever possible, the fragmented ion's mass is cited; i.e. if $(CH_2)_{10}SH$ is lost from the molecular ion the resulting ion would be at m/z 122. Based on the first peak in the m/z plot the molecular ion (m/z 295) is not seen at an acceptable level, i.e. the signal-to-noise ratio is too low. However, the following fragment ions: pyridine-(C=O)-$O^{+\cdot}$-(CH)=(CH_2) (m/z 149), pyridine-(C=OH^+)-OH (m/z 124), pyridine-(C=O)-$OH^{+\cdot}$ (m/z 123), pyridine-C≡O^+ (m/z 106), and pyridine$^+$ (m/z 78) were observed. The most abundant signals are at m/z 123 (100%) and at m/z 106 (25%). These mass values correlate with pyridine-(C=O)-OH^+ and pyridine-C≡O^+, respectively. The ions at m/z 123 is believed to be from a McLafferty rearrangement at the carboxylic group resulting in a charged hydroxyl ion. This hypothesis is supported by the highly conjugated region at the carboxylic group, which theoretically should be able to account for the placement of charge. The peak at m/z 106 is believed to be from the loss of the

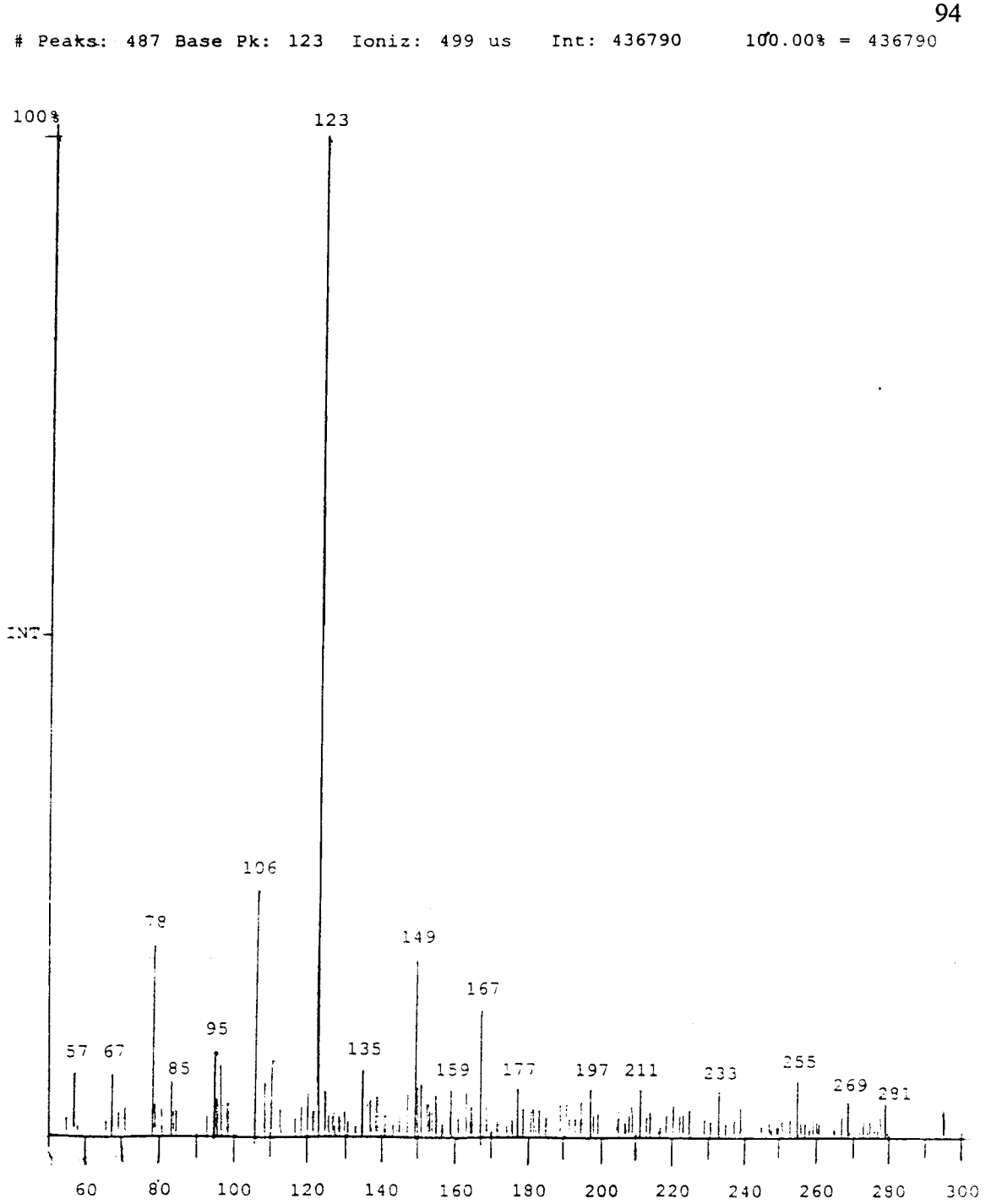

Figure 2.11 : Mass spectrum (EI) of 1-(10-mercaptodecyl)isonicotinate.

Table 2.1 : Mass Spectrometry fragments

and their respective mass to charge ratios.

SPECIES DETECTED	m/z RATIO
parent ion	295
pyridine-C-(C=O)-O^+-(CH)=(CH_2)	149
pyridine-C-(C=OH^+)-OH	123
pyridine-C-(C=O)-OH^+	122
pyridine-C-(C≡O)$^+$	106
pyridine$^+$	78

ether chain forming a triple bond between the pyridyl carbon and the oxygen. The loss of the chain is readily acceptable in this configuration. Both of these hypothesized fragmented species are deemed to be reasonable and realistic. Although the long chain and the thiol were not evident, a peak at m/z 149 is believed to be from a methylene chain of two carbons attached to the pyridine-carboxylic group. The presence of these two carbons indicates that a chain was attached to the isonicotinic acid and therefore the whole chain should have been attached. This conclusion is further supported by the NMR data. The peak at m/z 124 is believed to be from a double hydrogen transfer to the pyridine-carboxylic group. This would form from the lost of the decane-thiol chain. The final main peak at m/z 78 is believed to be from a fragmented pyridine with a positive charge. Chemical ionization (CI) was then used to find the parent ion because CI is a gentler ionization technique, see Figure 2.12. The parent ion was detected at m/z 295 at 47+ %, along with a fragment at m/z 149 at 100% identified above. While other peaks were observed in the CI spectrum, gross contaminants in the system made complete analysis difficult.

2.4 CONCLUSIONS

The pyridine tagged alkanethiol chain has been successfully synthesized and characterized. ^{1}H and ^{13}C NMR, along with mass spectrometry, have been used to confirm the identities and purity of all products, when possible. The formation of monolayer films of 1-(10-mercaptodecyl)isonicotinate, and the subsequent construction of multi-layer films of cobalt phthalocyanine, have also been successful. These systems will be discussed in greater detail in Chapter 3.

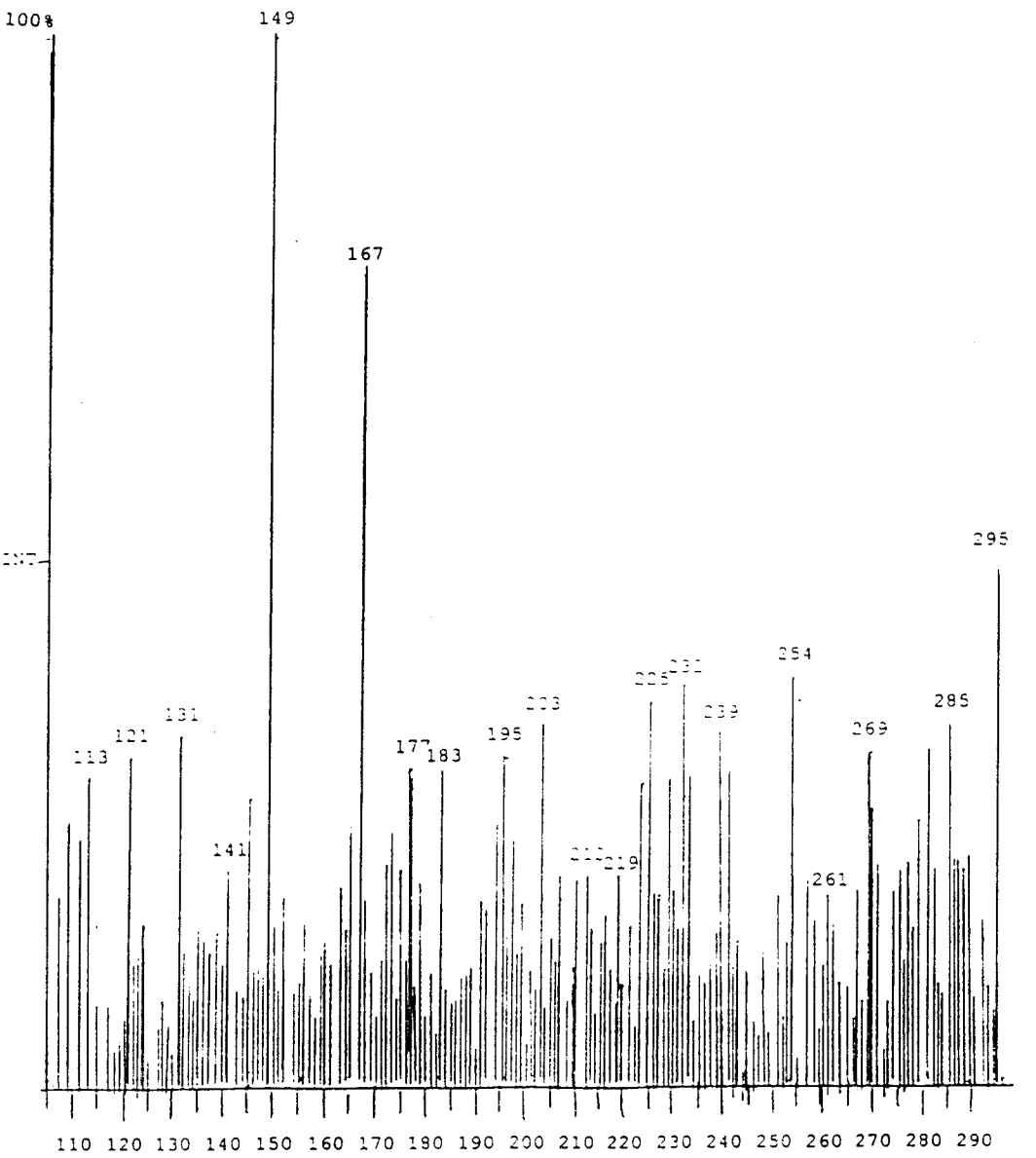

Figure 2.12 : Mass spectrum (CI) of 1-(10-mercaptodecyl)isonicotinate.

2.5 OTHER ATTEMPTED SYNTHETIC PROCEDURES

The first attempted reaction pathway was the nucleophilic displacement of bromine from 1,12 dibromododecane using sodium hydrosulfide in 80% DMSO/20% H_2O.[13,36] NaSH easily cleaved the bromine from the alkane chain, resulting in a ω-bromoalkanethiol. The crude product was then extracted into methylene chloride, washed with distilled water and brine, followed by drying over sodium sulfate. The methylene chloride layer was then removed under reduced pressure. The crude product was found to contain a mixture of 12-thio-1-bromododecane, 1,12-dithiododecane, ω-thio-1-bromododecyl disulfide, and some starting material. A common problem encountered in this reaction was the formation of the disulfide, which was very difficult to separate from the thiol. Products were purified and separated via flash column chromatography in 90%/10% hexane/ethyl acetate. The clean products were then characterized via ^{1}H and ^{13}C NMR, and MS. Unfortunately, the analysis confirmed the existence of a disulfide. Initially the product was a waxy liquid, but over a few days the product became a thick yellow wax-like solid; which was totally intractable in all organic solvents.

Another attempted synthetic procedure involved the classic Williamson ether addition of 12-bromododecanol to 4-pyridylcarbinol. In this reaction scheme, 4-pyridylcarbinol was reacted with 12-bromododecanol in the presence of sodium hydride and methylene chloride. The alcohol was protected using chlorotetramethylsilane in tetrahydrofuran and triethylamine (used as a scavenger). The product of this reaction was then added, following the Williamson ether addition protocol,[7,11] to 4-pyridylcarbinol by stirring the solutions in a mixture of sodium hydride and methylene chloride, followed by

working up the solution in brine. This product was then purified via flash column chromatography and the alcohol was deprotected using tetrabutylammonium fluoride in tetrahydrofuran. Next, the alcohol was brominated using PBr_3 in a 3 fold excess, in tetrahydrofuran. Finally, the brominated alkane was thiolated using sodium hydrosulfide in 3 fold excess ran in 80%/20% dimethylsulfoxide/distilled water. This product was then purified via flash column chromatography in 70%/30% hexane/ethyl acetate and characterized via ^{1}H & ^{13}C NMR, and MS. While the analysis appeared promising, and the product was identified as the desired thiol, the product solidified in air and could not be re-dissolved in organic solvents.

References

(1) Simpson, T.; Revell, D.; Cook, M.; Russell, D. *Langmuir* **1997**, 13, 460-64.

(2) Bain, C.; Evall, J.; Whitesides, G. *J. Am. Chem. Soc.* **1989**, *111*, 7155.

(3) Li, D.; Swanson, B.; Robinson, J.; Hoffbauer, M. *J. Am. Chem. Soc.* **1993**, *115*, 6975-6980.

(4) Anderson, T.; Komplin, G.; Pietro, W. *J. Phys. Chem.* **1993**, *97*, 6577-6578.

(5) Perrin, D.; Armarego, W.; Perrin, D. *The Purification of Laboratory Chemicals*; Pergamon: New York, 2nd Ed., **1980.**

(6) Nishimura, O.; Kitada, C.; Fukino, M.; *Chem. Pharm. Bull.* **1978**, *26*, 1576-1585.

(7) McMurry, J. *Organic Chemistry*; Brooks/Cole Publishers: California, 3rd Ed., **1992**.

(8) Durst, H.; Gokel, G. *Experimental Organic Chemistry*; McGraw-Hill: New York, 2nd Ed., **1987**.

(9) Pasto, D.; Johnson, C.; Miller, M. *Experiments and Techniques in Organic Chemistry*; Prentice-Hall: New Jersey, **1992**.

(10) Cotton, F.; Wilkinson, G. *Advanced Inorganic Chemistry*; Wiley: New York, 4th Ed., **1980**.

(11) March, J. *Advanced Organic Chemistry*; Wiley: New York, 4th Ed., **1992**.

(12) Peck, S.; Curtin, L.; Tender, L.; Carter, M.; Terrill, R.; Murray, R.; Collman, J.; Little, W.; Duan, H.; Hermann, A. *J. Am. Chem. Soc.* **1995**, *117*, 1121-1126.

(13) Bard, A.; Faulkner, L. *Electrochemical Methods*; Wiley: New York, **1980**.

(14) Murray, R. *Molecular Design of Electrode Surfaces*; Wiley: New York, **1992**.

(15) Kissinger, P.; Heineman, W. *J. Chem. Educ.* **1983**, *60*, 702-706.

(16) Evans, D. *Acc. Chem. Res.* **1977**, *10*, 313-319.

(17) Creuger, S.; Hockett, L.; Rowe, G. *Langmuir* **1992**, *8*, 854-861.

(18) Widrig, C.; Chinkap, C.; Porter, M. *J. Electroanal. Chem.* **1991**, *310*, 335-359.

(19) Hutchinson, J.; Posthlewaithe, T.; Murray, R. *Langmuir* **1993**, 9, 3277 -3283.

(20) Orihashi, Y.; Ohro, H.; Tsuchida, E. *Molecular Crystals and Liquid Crystals*, **1988**, 160, 139-149.

(21) Bear, J.; Li, Y.; Han, B.; Van Camelbecke, E.; Kadish, K. M. *Inorg. Chem.* **1996**, *35*, 3053-3055.

(22) Kadish, K. M.; Adamian, V.; Van Camelbecke, E.; Tan, Z.; Tagliatesta, P.; Bianco, P.; Boschi, T.; Yi, G.; Khan, M.; Richter-Addo, G. *Inorg. Chem.* **1996**, *35*, 1343-1348.

(23) Bear, J.; Han, B.; Huang, S.; Kadish, K. M. *Inorg. Chem.* **1996**, *35*, 3012-3021.

(24) Willicut, R.; McCarley, R. *J. Am. Chem. Soc.* **1994**, *116*, 10823-824.

(25) Finkleu, H.; Hanshew, D. *J. Am. Chem. Soc.* **1992**, *114*, 3173-3178.

(26) Bear, J.; Han, B.; Huang, S. *J. Am. Chem. Soc.* **1993**, *115*, 1175-1177.

(27) Marks, T. *Science* **1985**, 227, 881-888.

(28) Ulman, A. *An Introduction to Ultrathin Organic Films*; Academic Press: New York, **1994**.

(29) Anson, F. *Anal. Chem.* **1966**, *38*, 54-57.

(30) Anson, F.; Osteryoung, J. *J. Chem. Educ.* **1983**, *60*, 293-296.

(31) Evans, D. *J. Chem. Educ.* **1983**, *60*, 290-293.

(32) Heineman, W. *J. Chem. Educ.* **1983**, *60*, 305-308.

(33) Nicholson, R; Shain, I. *Anal. Chem.* **1964**, *36*, 706-723A.

(34) Laviron, E. *J. Electroanal. Chem.* **1979**, *100*, 263-270.

(35) Laviron, E. *J. Electroanal. Chem.* **1979**, *101*, 19-28.

(36) Poirier, G.; Pylant, D. *Science* **1996**, *272*, 1145-1148.

(37) Zak, J.; Yuan, H.; Ho, M.; Woo, L.; Porter, M. *Langmuir* **1993**, 9 2772-2774.

CHAPTER 3 : ELECTROCHEMICAL INVESTIGATION

3.1 INTRODUCTION

The final steps in this project were the electrochemical investigations of monolayers formed from pyridine tagged alkanethiols and the subsequent construction of heterogeneous and homogeneous multi-layer films containing cobalt phthalocyanine and cobalt octafluorophthalocyanine. The synthesis of these layers was previously discussed in Chapter 2.

The pyridine tagged alkanethiol was chosen to make use of the thiol's ability to form strong covalent bonds to gold via chemisorption. This process will keep the monolayer and the extensions made to the chain firmly in place. A strong anchoring group was needed to limit desorption of the multi-layer films. The long alkane chain, consisting of ten carbons, was used to take advantage of the increase in van der Waals interactions inherent in carbon chains placed in close proximity to each other. The packing and ordering of these chains was expected to be fairly high, with typical literature values of the surface coverage for similar molecules being $3\text{-}5 \times 10^{-11}$ ($mole/cm^2$).[1-3] Although longer chains could have been used, they may have decreased the electron transfer kinetics of the electroactive end groups to unacceptable values. Likewise, shorter chains could have been used, but were expected to possess a lesser degree of order. Future work would be needed to confirm these hypotheses.

The ten carbon length chain was expected to be tightly packed. Therefore, the resolution of electrochemical signals from isolated sites may have been complicated. To overcome this common problem, electroinactive diluent could have been used to separate

neighboring electroactive end groups. This is a common practice when studying surface confined monolayers. However, the purpose of this investigation was the study of multi-layers, and the use of diluent would have reduced the number of active sites available for the cobalt phthalocyanine to bind to. It is believed that this would have lowered the order and packing of the multi-layers. The carboxylic acid was used near the end group to create a bulkier end on the chain, thus spacing the electroactive end groups a distance apart while maintaining chain orientation and packing.

The pyridine end group was used because the nitrogen contains a lone pair of electrons and is known to axially bind to cobalt ions.[4] This would cause the phthalocyanines to arrange in a planar, head-to-tail fashion. The pyridine was also expected to be electroactive, although this was not a requirement for an effective end group. An electroactive end group proved to be advantageous because it allowed for the monitoring of changes in its electrochemical response as a function of changes in environment. The aromatic ring of the pyridine was also expected to increase the activity of the end group, especially in coordination with the carboxylic acid group, creating an extended π-network and facilitating electron transfer through the conjugated bonds.

Cobalt phthalocyanine was selected for construction of molecular multi-layers for several reasons. It has the ability to stack in a co-planar arrangement, is cost effective, and has a readily discernible $2^{+}/3^{+}$ redox couple. The ring's oxidation was also expected to be observable and both the metal's and the ring's redox processes could then be used to monitor the completeness of multi-layer formation. In addition, cobalt phthalocyanine has been shown to be electronically conductive, when used in thin layer and polymer films and so was expected to possess the same, if not enhanced, characteristics when used

in self-assembled molecular layers. Cobalt is also known to covalently bind to nitrogen containing ligands and is expected to form strong bonds to the pyridine end group, as well as the pyrazine spacer.[4]

The pyrazine spacer was used to maintain the extended π-system between layers of cobalt phthalocyanines, thereby enhancing electronic communications between the rings. Pyrazine was used to achieve this goal mainly because it is an aromatic and rigid bidentate ligand. Its rigidity was expected to keep the layers tightly packed and well ordered. This should allow for the coordination of other molecules and maintain electronic communication between the rings. This is considered vital to the construction of the SAM.

The construction of a molecular rectifier was also a consideration in this investigation and so cobalt octafluorophthalocyanine was used because the electron withdrawing fluorine atoms altered the redox potential of the phthalocyanine ring and the cobalt $2^+/3^+$ couple. The addition of a cobalt octafluorophthalocyanine outer layer was expected to create a capacitor within the multi-layer by collecting charge at this outer layer and holding it until the fluorinated ring could be oxidized. Theoretically, this would then send the charge through the other layers and oxidized these layers at a potential greater than necessary. This would facilitate electron transfer through these inner layers and the transfer of charge would encounter less resistance from the layers. An increase in the electrochemical response from the system would then be expected. A system may be considered a molecular rectifier when such an increase in current response is observed.

3.2 ELECTRODE PREPARATION

Several gold electrodes were selected and polished for approximately 20 minutes on a disk polishing wheel, using a flocked twill polishing cloth wetted with a 1 μM aluminum oxide suspension. The polished electrodes were then sonicated for 15 minutes, in distilled water to remove residual aluminum oxide. A well polished electrode was formed when the electrode surface was determined to be free of large imperfections and scratches and had obtained a mirror finish, under a SuperVision 10x magnifying lens.

The electrode's surface was fully reduced in order to obtain a gold surface which was free of contaminants. This procedure ensured that the electrode surface was reproducible between different electrodes and that in the self-assembly step, the electrode surface is in an optimal state for molecular bonding. The electrode was reduced in a solution of 1 M $HClO_4$ on an EG&G Princeton Applied Research galvanostat (model 273) at a constant current of + 10 mA/cm^2 for 15 minutes, using a platinum wire as the counter electrode and a silver wire as the reference electrode. The working electrodes were then sonicated for 5 minutes in distilled water and then allowed to soak in the coating solution for the appropriate length of time (see Chapter 2).

Two types of electrodes were chosen for analysis, as discussed in Chapter 2. The first type was prefabricated from BioAnalytical Systems which had a smaller surface area of 0.0201 cm^2 than that of the second type. The second type was homemade and had a surface area of 0.0710 cm^2. The electrodes were found to have a working area twice their geometric area by the method of Soriaga et al.[5]

3.3 SOLUTION ELECTROCHEMISTRY

Prior to examining samples containing analyte, each electrode was used to examine 1 M solution of the sodium acetate electrolyte. A silver/silver chloride aqueous reference electrode and a platinum counter electrode were employed in the solution voltammetry experiments. A blank solution of 0.1 M TBAP in methylene chloride was also examined, using a silver/silver ion non-aqueous reference electrode and a platinum counter electrode. It was necessary to examine the electrolyte solutions to establish the purity and potential window (i.e. the potential between electrolyte reduction and oxidation) of the blank electrolyte solutions.

Solution voltammetry was also conducted on samples of a 1 mM aqueous solution of 1-(10-mercaptodecyl)isonicotinate and 1 mM solutions of pyrazine, cobalt phthalocyanine and cobalt octafluorophthalocyanine in methylene chloride. The pyridine tagged alkanethiol was conducted in a 1 M aqueous solution of sodium acetate and all other solution voltammetry was conducted in a 0.1 M solution of TBAP in methylene chloride. The solution experiments were conducted using a platinum working electrode (cleaned in hot nitric acid), platinum counter electrode, and either silver/silver chloride aqueous reference electrode or silver/silver ion non-aqueous reference electrodes. Prior to electrochemical analysis, and between all experiments, the solutions were deoxygenated by sparging with argon for 10-20 minutes.

The solution voltammetry of the above species were examined to establish a template voltammogram for qualitative comparison to monolayer investigations and to determine the potential of the redox couples. The redox couples could then be assigned with greater certainty in the voltammetry of the adsorbed species. The formal potential

of the redox couple was distinctive for each species and was greatly influenced by such experimental parameters as the stability of the reference electrode, solvent (electrolyte) purity, and adsorbed versus solution samples. Therefore, the redox couples of the adsorbed samples were expected to be shifted from that of the solution analysis.

3.3.1 VOLTAMMETRY OF ELECTROLYTE SOLUTIONS

The sodium acetate electrolyte was found to have a stable, optimum range of + 1 volt to – 1 volt. However most scans were conducted from + 700 mV to – 700 mV as electrolyte breakdown occurred at + 1100 mV and –1100 mV. Voltammetry using 0.1 M solutions of TBAP, in methylene chloride, were conducted from + 1800 mV to – 1800 mV, even though solvent breakdown occurred at + 2000 mV and – 2000 mV. The potential windows were determined by the absence of Faradaic processes beyond the chosen values. The ranges the voltammetric scans were conducted in were limited because of concerns over monolayer desorption.

3.3.2 SOLUTION VOLTAMMETRY OF 1-(10-MERCAPTODECYL)ISONICOTINATE

This solution was scanned from + 800 mV to – 900 mV at scan rates of 10, 50, 100, 500, 1000, 2000, and 3000 mV/s, see Figure 3.1. A pair of anodic and cathodic peaks were observed at an average peak position of + 630 mV. The anodic peak was easily observed, and appeared to be very broad. Three cathodic peaks were observed at + 120 mV, - 160 mV, and – 450 mV. The cathodic peaks were found to change in relative intensity with increasing scan rate. This is indicative of a complex irreversible chemical process whose mechanism was not determined in this investigation.

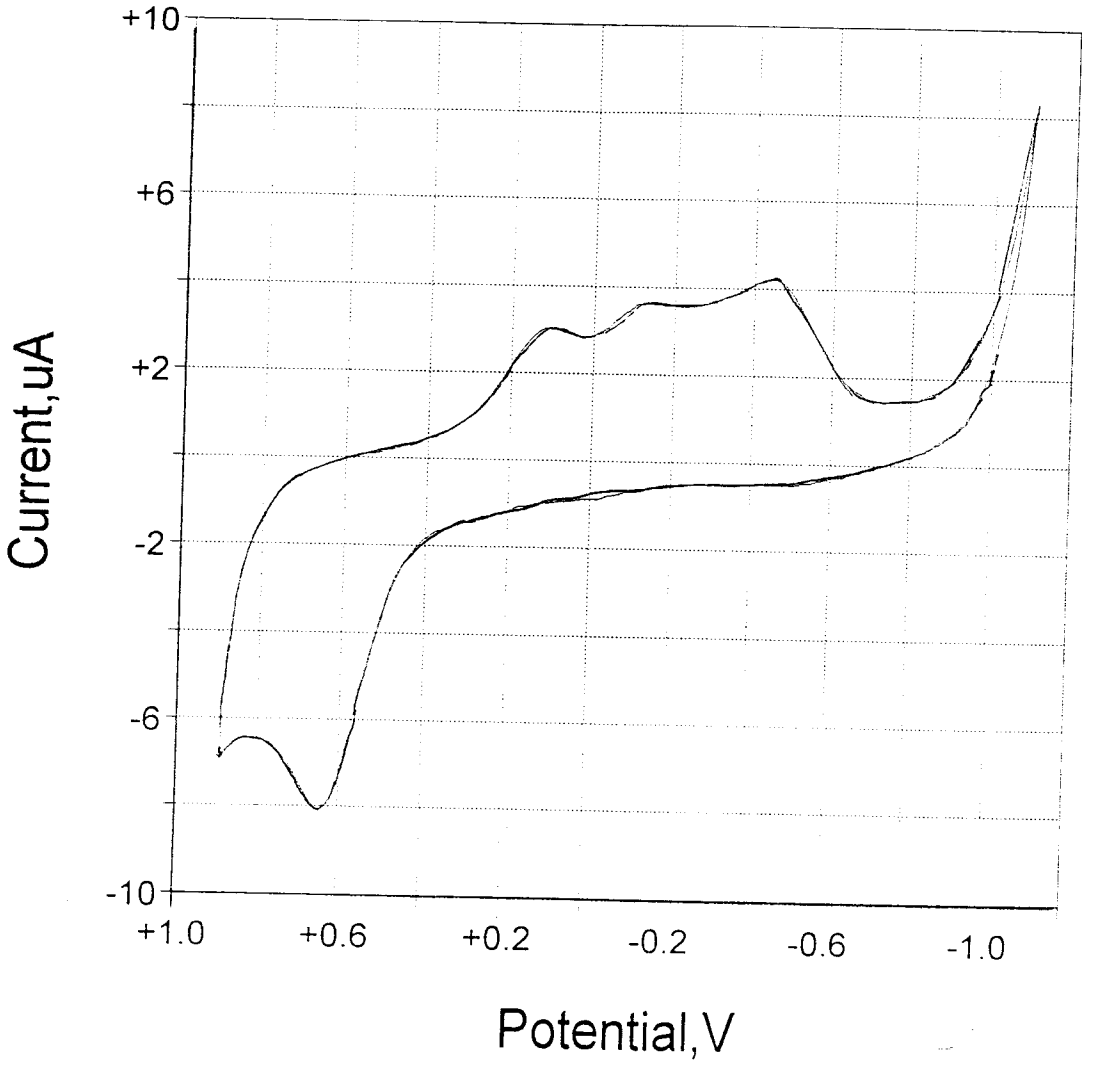

Figure 3.1 : Cyclic voltammogram of a 1 mM solution of 1-(10-mercaptodecyl)isonicotinate in 1 M sodium acetate using a platinum working electrode. Scan rate: 0.1 V/s. Temperature: 20 °C. Reference electrode: Ag/AgCl. Counter electrode: platinum wire.

3.3.3 SOLUTION VOLTAMMETRY OF COBALT PHTHALOCYANINE

The solution was scanned over the potential range of + 1 volt to –2 volt and the voltammetry was examined at scan rates of 10, 50, 100, 500, and 1000 mV/s, see Figure 3.2. The anodic scans proved uninteresting and unremarkable, resembling the electrolyte blank. The cobalt phthalocyanine ring oxidation was expected to occur anodically, but was not observed within the range scanned. The cathodic scans showed the appearance of the cobalt's redox processes. Several pairs of anodic and cathodic peaks were observed at average peak positions of (–391, -315 mV cobalt's 2^+,3^+ couple), (-900, -587 mV O_2), and (-1391, -1326 mV cobalt's 1^+,2^+ couple). The peak maximums of all of the peaks were easily observed. The peaks at (-900, -587 mV) are probably due to the presence of oxygen, given the potential, shape and intensity of the peaks. Again, the solution run was needed to establish the relative position of the metal's redox couples, and to determine if the ring's oxidation could be observed. The best average ΔE_p was found to be 76, which correlates to an electrochemical reversible process. The ΔE_p was found to remain fairly constant with increasing scan rate, varying by 5-10 mV. The i_{pa}/i_{pc} ratio was found to be approximately equal to one, indicating a chemically reversible process. These assignments should not be construed as absolute, as the redox peaks were found to lie on a sloping background.

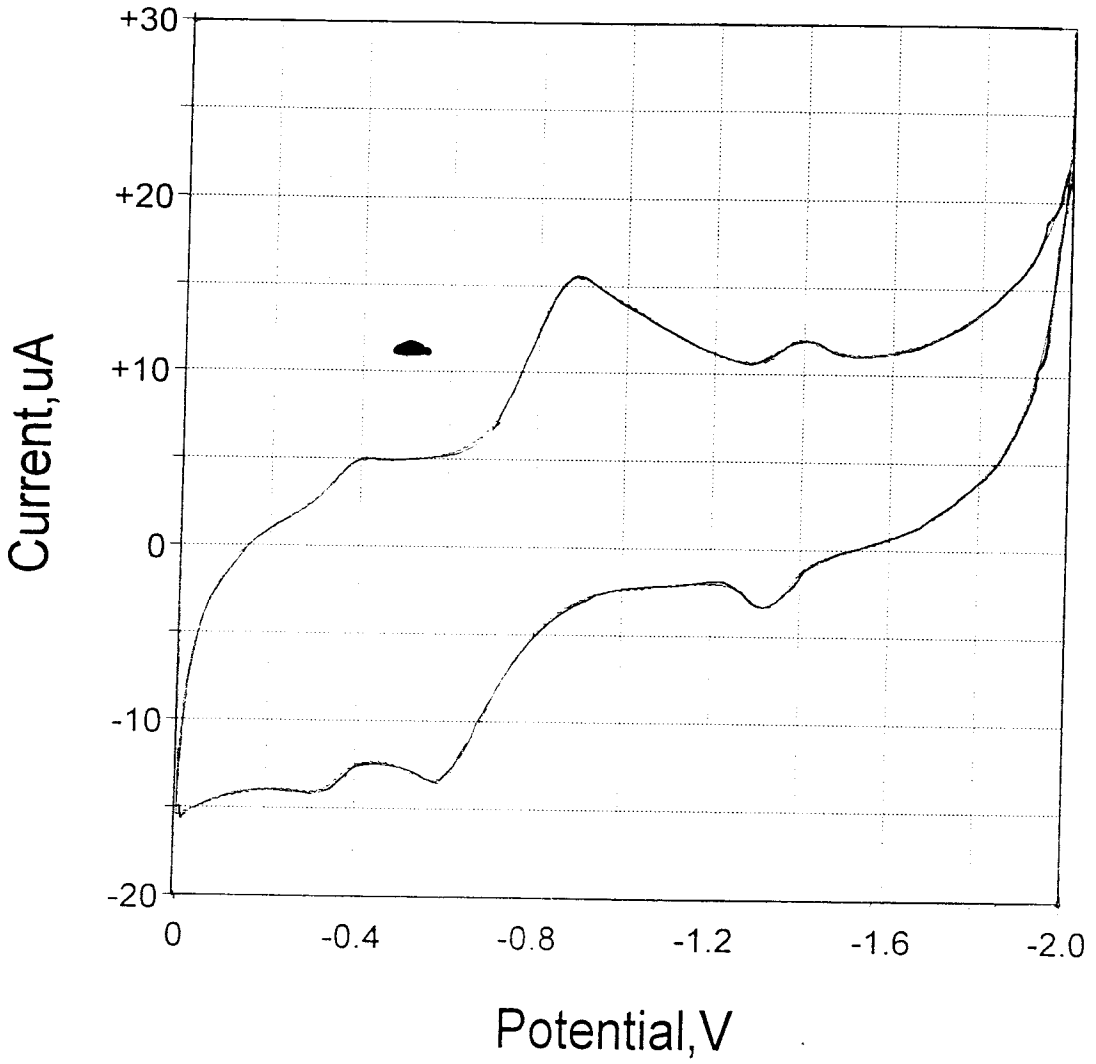

Figure 3.2 : Cyclic voltammogram of a 1 mM solution of cobalt phthalocyanine and 0.1 M TBAP in methylene chloride in using a platinum working electrode. Scan rate: 0.1 V/s. Temperature: 20 °C. Reference electrode: Ag/Ag^{+} in THF. Counter electrode: platinum wire.

3.3.4 SOLUTION VOLTAMMETRY OF COBALT OCTAFLUOROPHTHALOCYANINE

The solution was scanned over a potential range of + 1 volt to –2 volt at scan rates of 50, 100, and 1000 mV/s, see Figure 3.3. A pair of anodic and cathodic peaks were observed at average peak positions of + 1150 and – 141 mV, however the cobalt octafluorophthalocyanine was not highly soluble in methylene chloride; which caused the peak position to vary greatly from scan to scan. The peak maxima of all observable peaks were easily assessed. The observed peaks were very broad and any assessment is qualitative at best, however the solution run was needed to establish the relative position of the metal's redox couple, and to determine if the ring's oxidation could be observed. Unlike the cobalt phthalocyanine, the fluorinated species' ring oxidation was easily observed with an average peak position of + 1100 mV. The best average ΔE_p was found to be 990 mV, which correlated to an electrochemical irreversible process. The ΔE_p was found to increase with increasing scan rate by 30-50 mV. The i_{pa}/i_{pc} ratio was found approximately equal to one, indicating a chemically reversible process. The chemical and electrochemical reversibility was difficult to determine with absolute certainty, as the large redox waves each appeared to contain two peaks.

3.3.5 SOLUTION VOLTAMMETRY OF PYRAZINE

Pyrazine was found to be electroinactive, i.e. no peaks were observed in the voltammograms, and so it was not expected to be electroactive within the monolayer studies. This is advantageous as the pyrazine did not complicate the multi-layer voltammetry.

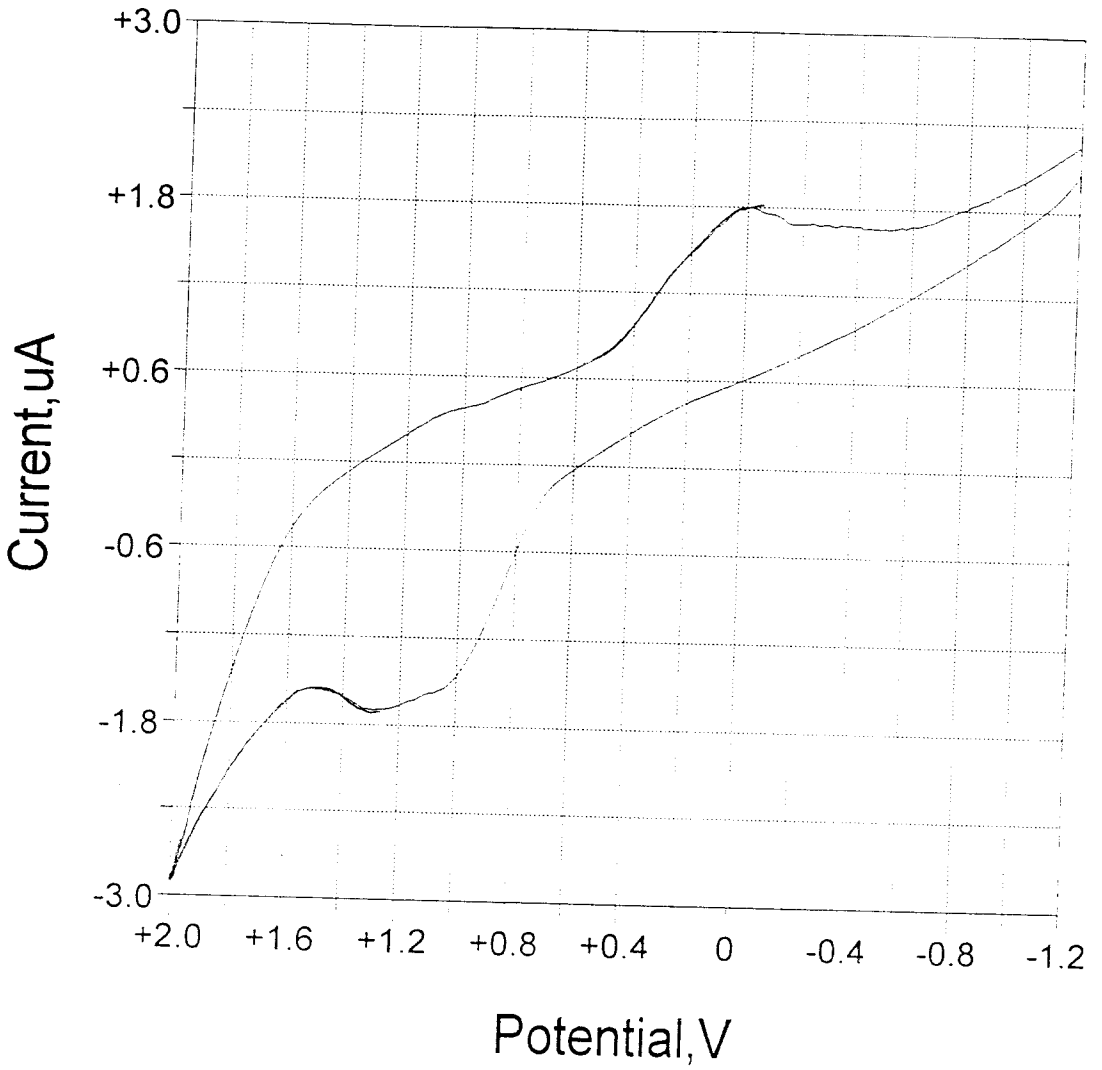

Figure 3.3 : Cyclic voltammogram of a 1 mM solution of cobalt octafluorophthalocyanine and 0.1 M TBAP in methylene chloride using a platinum working electrode. Scan rate: 0.1 V/s. Temperature: 20 °C. Reference electrode:Ag/Ag^{+} in THF. Counter electrode: platinum wire.

3.4 VOLTAMMETRY OF PYRIDINE TAGGED ALKANETHIOL MONOLAYERS

After following the outlined (see Chapter 2) soaking and rinsing procedure, the electrodes were placed into deaerated 1 M aqueous sodium acetate solutions and cyclic voltammograms were obtained at scans of 25, 50, 100, 200, and 500 mV/s from +700 mV to –1000 mV/s. Voltammograms taken beyond this range did not provide any additional information, see Figure 3.4. A redox couple was found to exist in the anodic scans, and is believed to exhibit a chemical/electrochemical (CE) redox mechanistic process. The mechanistic classification is based on the appearance of an anodic peak after the formation of the cathodic peak and on the profile of a plot of i_{pa}/i_{pc} versus scan rate, see Figure 3.5. The plot's profile matches that of a CE defined process according to literature criteria, however these methods of identification are qualitative only and used to help assess the possible chemical and electrochemical processes occurring at the surface. To obtain a definite identification, a more extensive analysis would be needed including the use of other electrochemical techniques, e.g. AC impedance. Plots of ΔEp versus scan rate and ip versus scan rate were constructed based on the voltammograms to establish electrochemical reversibility and to determine if the adsorbed species were surface confined, respectively, see Figures 3.6 and 3.7. The surface coverage was also determined, and found to be comparable to values found in the literature.[6,7]

The 1-(10-mercaptodecyl)isonicotinate was found to be chemically irreversible, with an i_{pa}/i_{pc} ratio not equal to one. The peak currents were also found to be linear with respect to scan rate, although the peak maximums were difficult to assess. This relationship indicated a diffusionless process, i.e. a response from adsorbed species. The

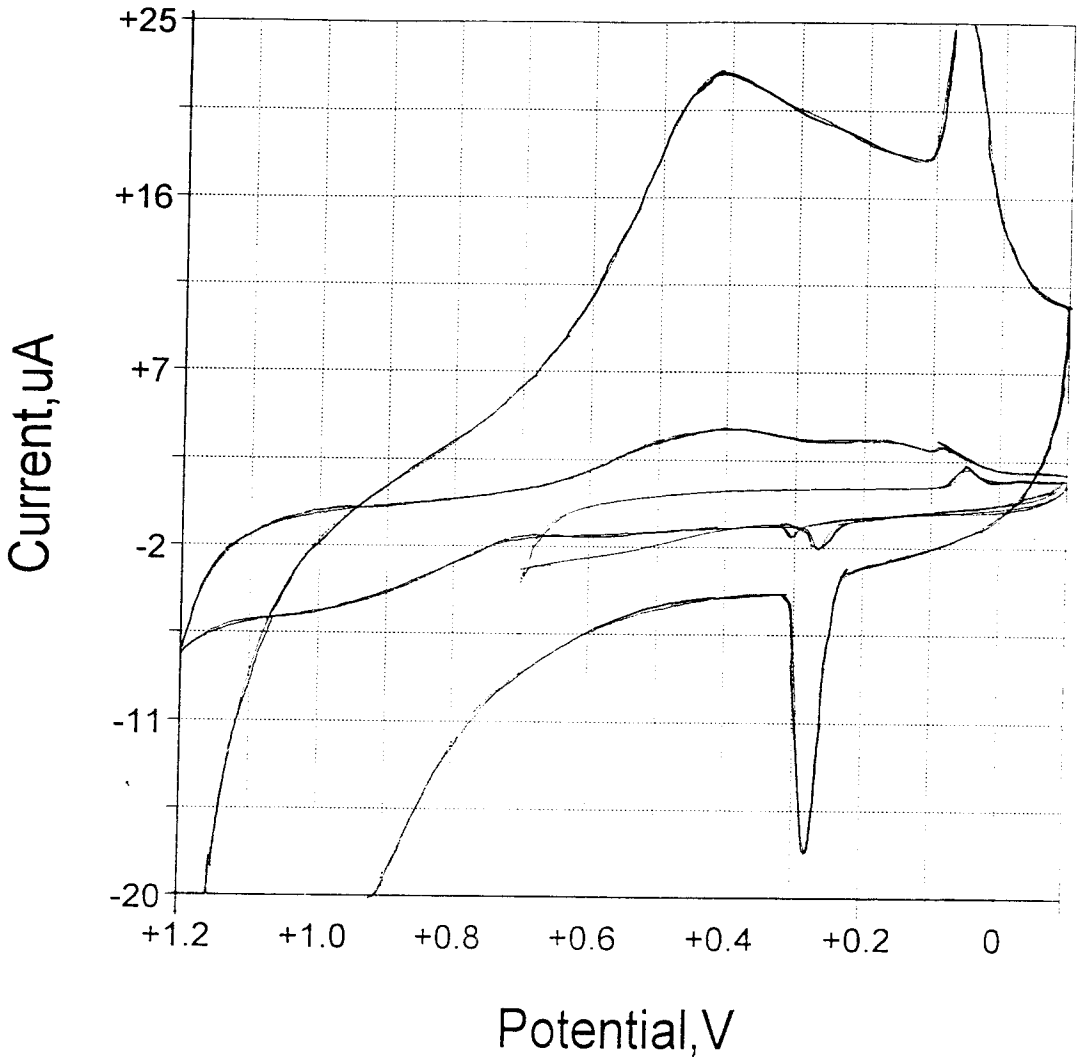

Figure 3.4 : Cyclic voltammograms of a self-assembled monolayer of 1-(10-mercaptodecyl)isonicotinate in a 1 M solution of sodium acetate on a gold working electrode. Scan rates: 0.05, 0.1, and 0.5 V/s. Temperature: 20 °C. Reference electrode: Ag/AgCl. Counter electrode: platinum wire.

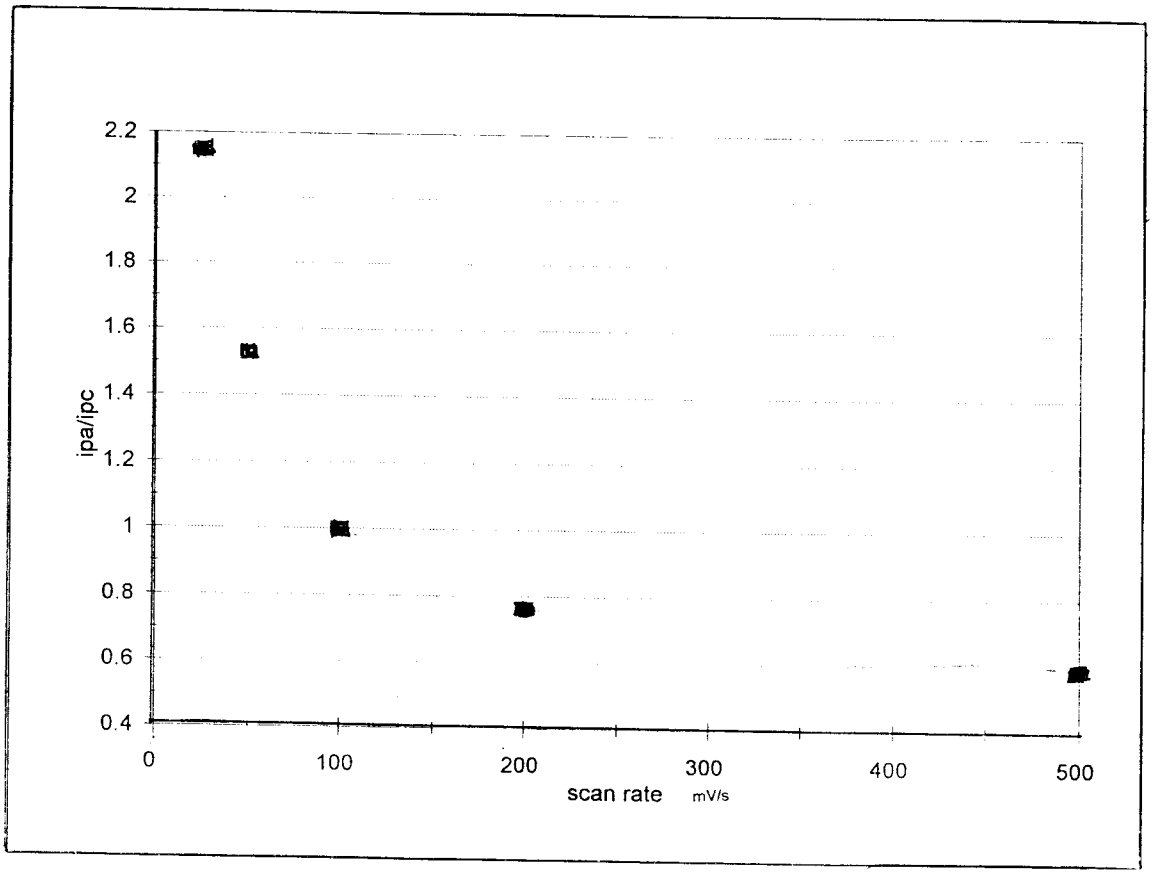

Figure 3.5 : Plot of i_{pa}/i_{pc} vs scan rate for a monolayer containing 1-(10-mercaptodecyl)isonicotinate.

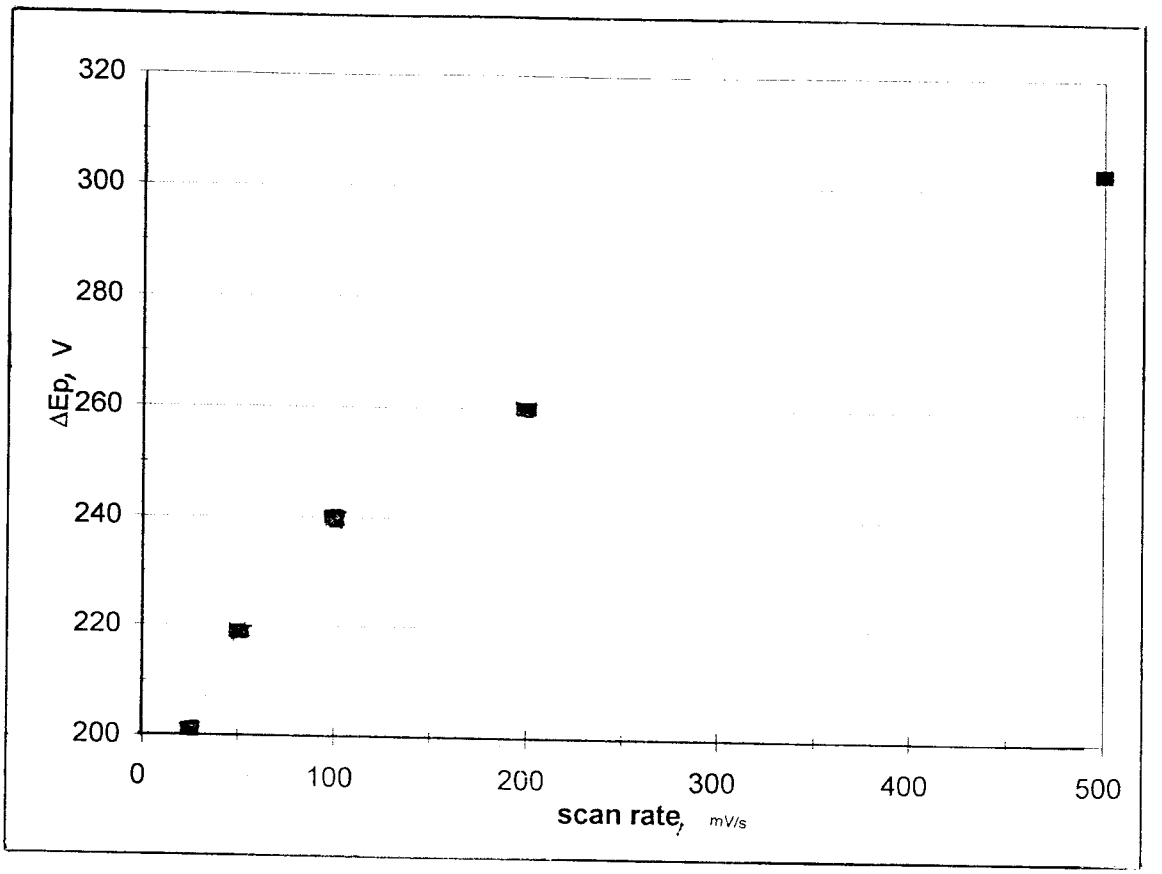

Figure 3.6 : Plot of ΔE_p vs scan rate for a monolayer containing 1-(10-mercaptodecyl)isonicotinate.

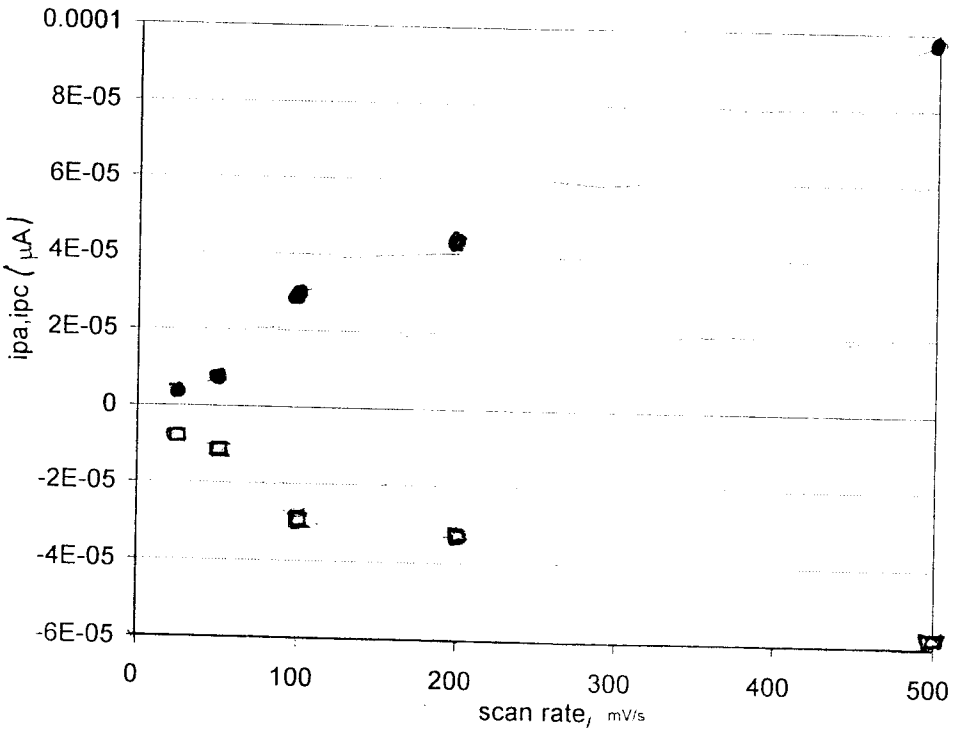

Figure 3.7 : Plot of (i_{pa}, i_{pc}) vs scan rate for a monolayer containing 1-(10-mercaptodecyl)isonicotinate.

electron transfer was also found to be electrochemically irreversible since the ΔE_p increased with increasing scan rate. The anodic peak was observed at 280 mV and the cathodic was observed at 70 mV, at a scan rate of 100 mV/s. The peak positions were found to drift slightly from electrode to electrode on an average of 10-20 mV. The E_{fwhm} was determined at scan rates of 50, 100 and 500 mV/s; calculated to be 32.2, 64.7, and 71.5 mV for the anodic peak and 50.4, 72.8, and 90.0 mV for the cathodic peak. The surface coverages, calculated by integrating the anodic or cathodic peak, were found to closely agree between electrodes with an average range of 1-5 $\times$ 10^{-10}(mole/cm^2). These values were slightly higher than reported literature values of other heterocyclic derivatives attached to alkane chains.[6,8] This could have been a result of not using diluent, which increased the activity of the monolayer.

3.5 VOLTAMMETRY OF COBALT PHTHALOCYANINE BI-LAYER FILMS.

After following the outlined (see Chapter 2) soaking and rinsing procedure, the electrodes were placed into deaerated sodium acetate electrolyte solution and cyclic voltammograms were taken at scans of 25, 50, 100, 200, 300, 500, and 1000 mV/s from +700 mV to –900 mV. Scans taken beyond this potential range did not provide any additional information, see Figure 3.8. The redox couple for the original monolayer was found to exist in the anodic scans and is believed to exhibit a chemical/electrochemical (CE) redox mechanism which was still observed in the bi-layer. A new redox couple appeared in the cathodic range which is assigned as the cobalt's $2^+/3^+$ couple. The ring based oxidation existed too close to the solvent breakdown to be able to derive any

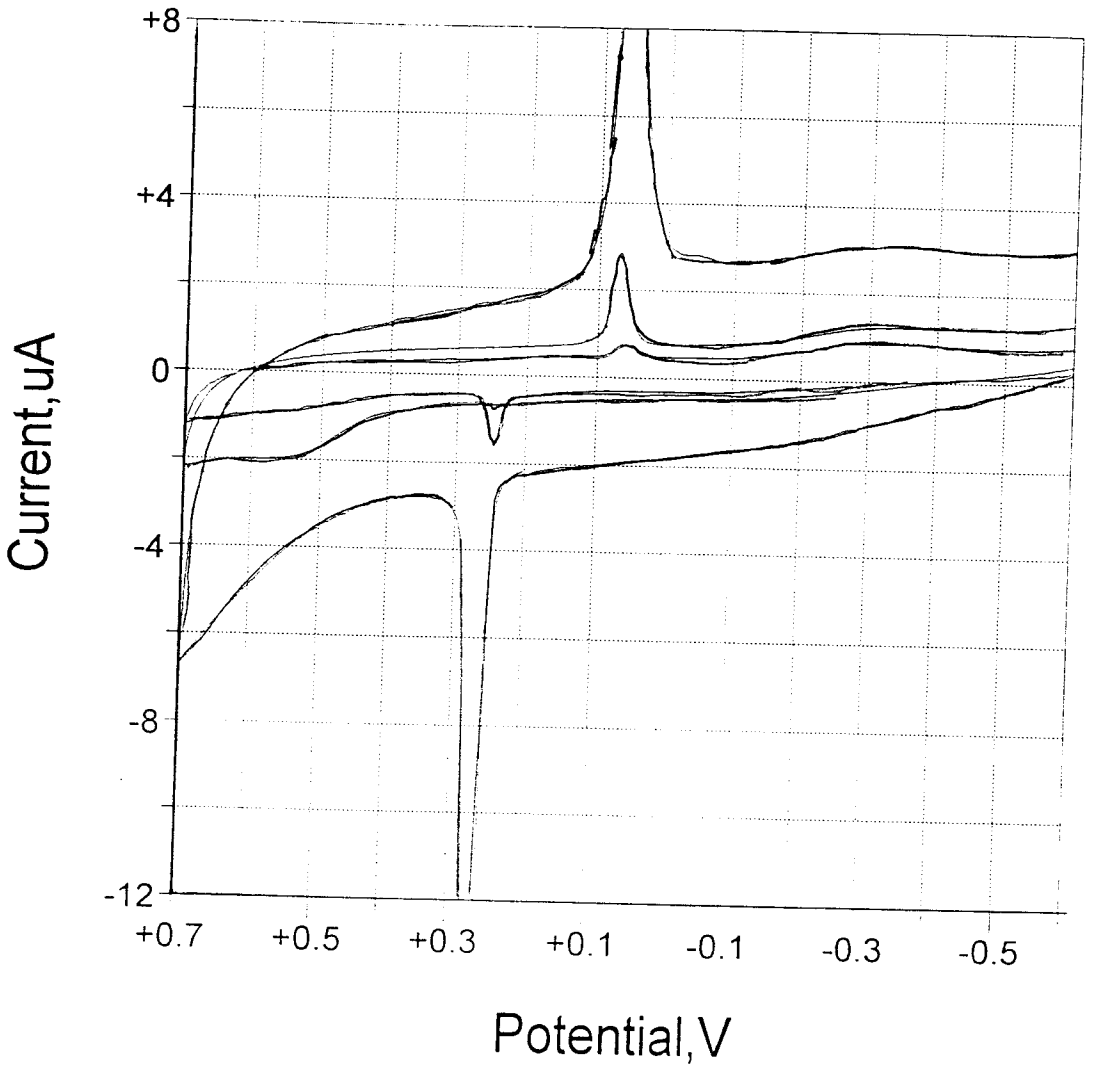

Figure 3.8 : Cyclic voltammograms of self-assembled bi-layers consisting of cobalt phthalocyanine on a monolayer of 1-(10-mercaptodecyl)isonicotinate in a 1 M solution of sodium acetate at a gold working electrode. Scan rates: 0.05, 0.1, and 0.5 V/s. Temperature: 20 °C. Reference electrode: Ag/AgCl. Counter electrode: platinum wire.

kinetic or electrochemical information from this peak, since the peak broadened and shifted into the background at increasing scan rates, but it was observed for some experiments at + 515 mV. Therefore, the appearance of this peak was used for qualitative purposes only.

Plots of ΔEp versus scan rate and ip versus scan rate were taken based on the voltammograms to establish the electrochemical reversibility and determination of the absence of diffusion for of the adsorbed species, respectively, see Figures 3.9 and 3.10. The anodic scan showed a sharpening of the monolayer's peaks compared to the free monolayer's CV. The cobalt's $2^+/3^+$ peaks were very broad and the reported values are an approximation, used to establish trends in analysis rather than absolute identification. Their assignments were based on the solution voltammetry presented earlier and the kinetics of this couple was determined by the method of Laviron.[9] The surface coverage was also determined by integrating the cathodic peak for all peaks and found to be comparable to values found in the literature.[10,11]

The 1-(10-mercaptodecyl)isonicotinate peaks were found to be chemically irreversible, with an i_{pa}/i_{pc} ratio less than one. This indicated the occurrence of an underlying chemical process occurring within the monolayer. The results of the monolayer mechanistic analysis may indicate that a chemical change (e.g. molecular rearrangement or hybridization) was preceding the electrochemical redox process. The mechanistic analysis is still only a qualitative assessment, without the support of more extensive analysis. The monolayer is also appearing to become less chemically irreversible, as this deviation from unity is not as great as was found in the initial

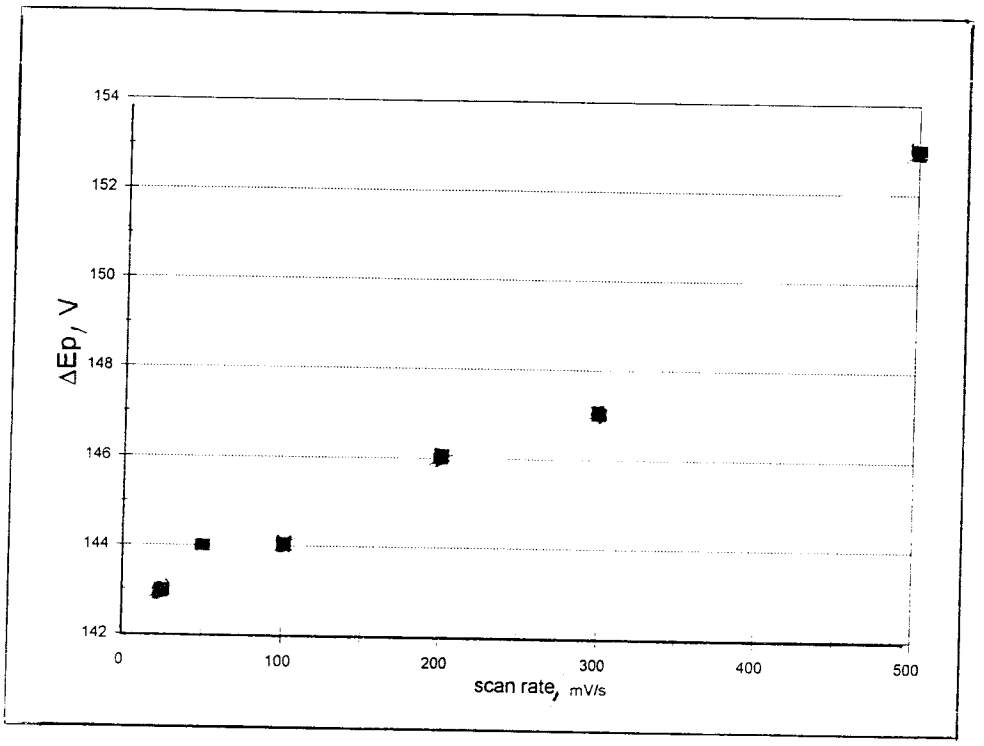

Figure 3.9 : Plot of ΔE_p vs scan rate for the Co-PC bi-layer.

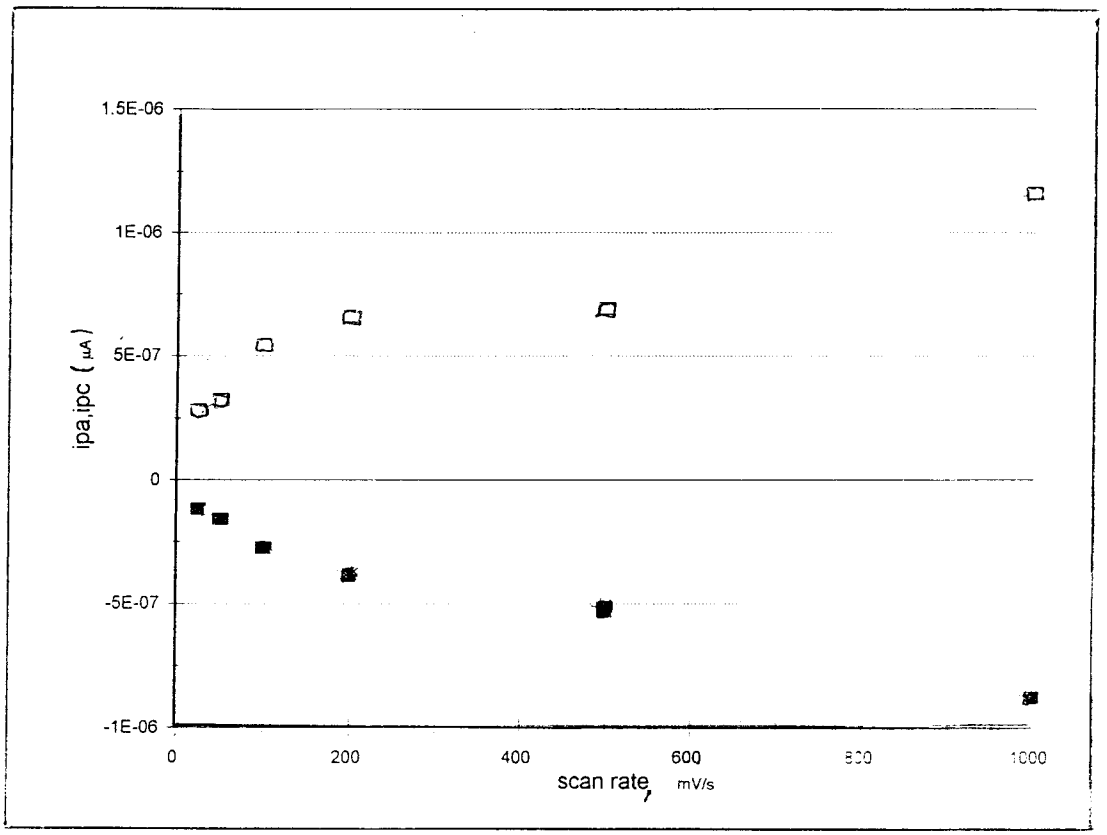

Figure 3.10 : Plot of (i_{pa}, i_{pc}) vs scan rate for the Co-PC bi-layer.

monolayer voltammograms. This may be due to a shielding of the monolayer from the electrolyte solution, by the phthalocyanine rings. This species was also found to be electrochemically irreversible since the ΔE_p increased with increasing scan rate. The anodic peak was observed at 240 mV and the cathodic was observed at 40 mV, at a scan rate of 100 mV/s. The peak positions were found to slightly drift from electrode to electrode on an average of 10 mV and to shift slightly to more cathodic potentials compared to the monolayer. This shift may indicate that the layer was becoming easier to oxidize with the addition of the cobalt phthalocyanine layer. The E_{fwhm} was determined at scan rates of 50, 100 and 500 mV/s calculated to be 17.5, 20.2, and 35.9 mV for the anodic peak and 38.3, 35.9, and 45.5 mV for the cathodic peak. This quantified the sharpening of the anodic peaks from the pyridine tagged alkanethiol couple and was believed to be indicative of a decrease in interactions between the neighboring pyridine groups. This was expected as the cobalt phthalocyanine should inhibit these interactions, i.e. communications between neighboring pyridine end groups. Another possible explanation for the peak sharpening is an underlying structural rearrangement at the monolayer.[7] The surface coverages based on the pyridine tagged alkanethiol redox couple was found to closely agree between different electrodes with an average range of 1-3 $\times$ 10^{-10} (mole/cm^2). These values were found to be similar to those determined in the monolayer study.

The cobalt $2^+/3^+$ peaks were found to be chemically irreversible, with an average i_{pa}/i_{pc} ratio not equal to one. The determination of chemical reversibility for this species is complicated by the fact that the electrochemical response of the cobalt phthalocyanine catalyzes O_2 in solution, which exist in trace quantities even in a deoxygenated solution.[11]

This species was also found to be electrochemically irreversible since the ΔE_p increased with increasing scan rate. The anodic peak was observed at – 170 mV and the cathodic peak was observed at – 350 mV with an electron transfer rate constant (k_s) of 0.425 s^{-1}, at a scan rate of 100 mV/s. These kinetic rate constants were found to be similar to values found in the literature.[11] The peak positions were found to drift slightly from electrode to electrode on an average of 10-30 mV. The ring oxidation was observed at approximately + 550 mV for 500 mV/s, but it was neither easily nor consistently observed. The surface coverages, based on the $2^+/3^+$ peak area, were found to be fairly consistent between electrodes with an average range of 2-4 $\times$ 10^{-10}(mole/cm^2). The surface coverages of the cobalt phthalocyanine were approximately an order of magnitude greater than originally expected, based on comparison of work performed by Murray et al[11]concerning monolayers of macrocycles. This difference may be due to the catalysis of oxygen or to the different methods employed to attach the macrocycle to the electrode. However, the surface coverages were in close agreement to a similar study performed by Chidsey et al.[8] These comparisons were performed to determine if the cobalt phthalocyanine would follow the trends observed in the literature. These results indicate a successfully constructed bi-layer film. The peak currents were also found to be fairly linear with respect to the scan rate indicating a diffusionless system.

3.6 VOLTAMMETRY OF COBALT PHTHALOCYANINE TRI-LAYER

After following the outlined (see Chapter 2) soaking and rinsing procedure, the electrodes were placed into deaerated in sodium acetate electrolyte solution and cyclic voltammograms were taken at scans of 25, 50, 100, 200, and 500 mV/s from +700 mV to

–900 mV. Scans taken beyond this potential range did not provide any additional information, see Figure 3.11. The metal center's $2^+/3^+$ redox couple was found to double in surface coverage (based on the first layer) as expected. These peaks were also much broader then the first layer's, and so determining the exact peak maximum is subjective to interpretation. This may be a result of a broad distribution in the potentials of the cobalt phthalocyanines as additional layers are assembled.

Plots of ΔEp versus scan rate and ip versus scan rate were taken based on the voltammograms to establish the electrochemical reversibility and to determine the absence of diffusion of the adsorbed species, respectively, see Figures 3.12 and 3.13. The anodic peaks from the monolayer were found to again sharpen and the cobalt phthalocyanine peaks broaden. The ring oxidation was also observed in some experiments. The surface coverage based on peak area was also determined and found to be comparable to values found in the literature.[8,11]

The 1-(10-mercaptodecyl)isonicotinate peaks were now found to be chemically reversible, with an i_{pa}/i_{pc} ratio approximately equal to one. This is probably due to shielding of the pyridine groups from the electrolyte by the densely packed phthalocyanine layers. With the subsequent addition of more phthalocyanines, electrolyte solution interactions with the monolayer are strongly diminished. This results in the phthalocyanines preventing, or greatly impeding, the migration of the electrolyte to the monolayer. The monolayer species was also found to be electrochemically irreversible since the ΔE_p increased with increasing scan rate. The anodic peak was observed at + 220 mV and the cathodic was observed at 0 mV at a scan rate of 100 mV/s. The peak positions were found to drift slightly from electrode to electrode on an average

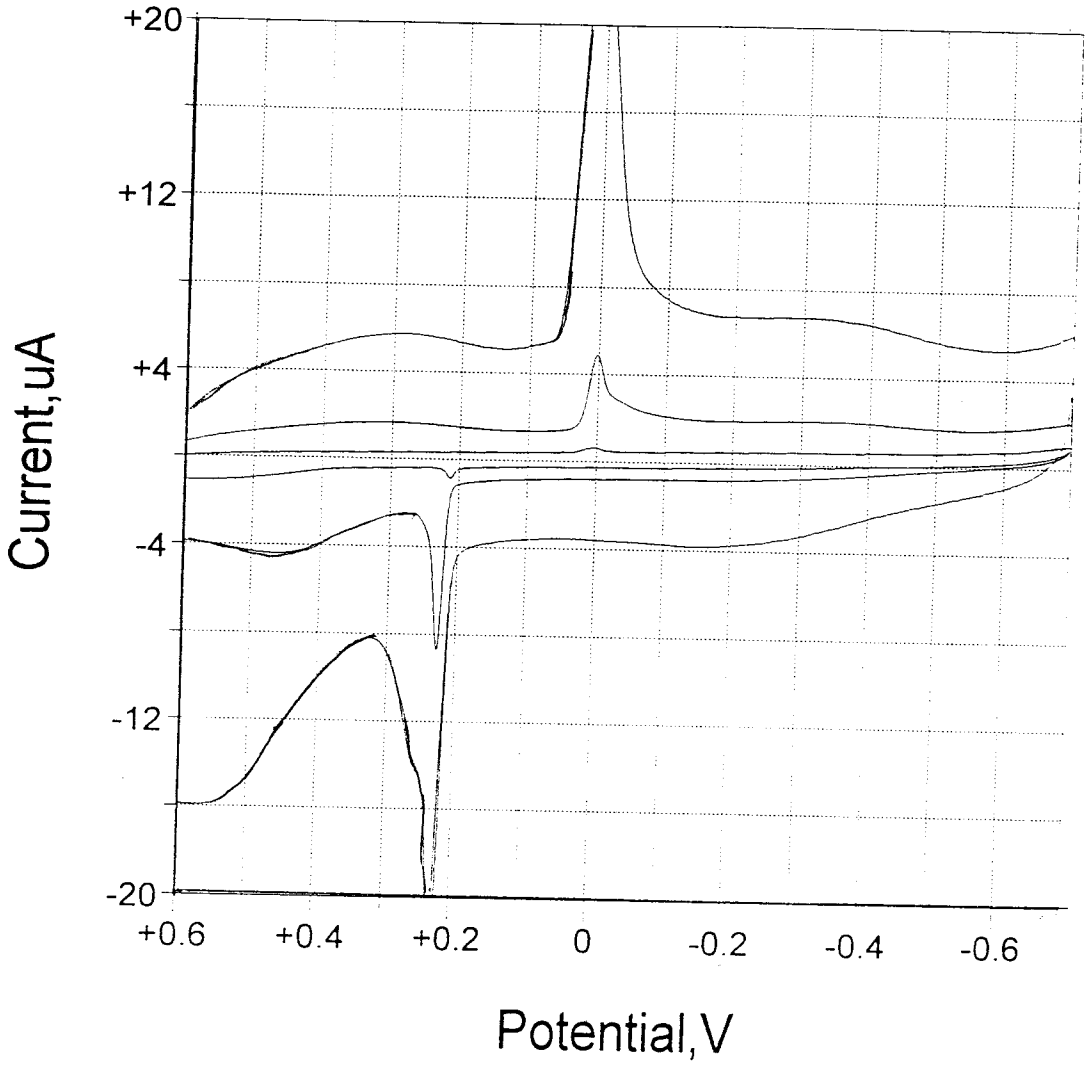

Figure 3.11 : Cyclic voltammograms of self-assembled tri-layer consisting of two layers of cobalt phthalocyanine on a monolayer of 1-(10-mercaptodecyl)isonicotinate in a 1 M solution of sodium acetate at a gold working electrode. Scan rates: 0.05, 0.1, and 0.5 V/s. Temperature: 20 °C. Reference electrode: Ag/AgCl. Counter electrode: platinum wire.

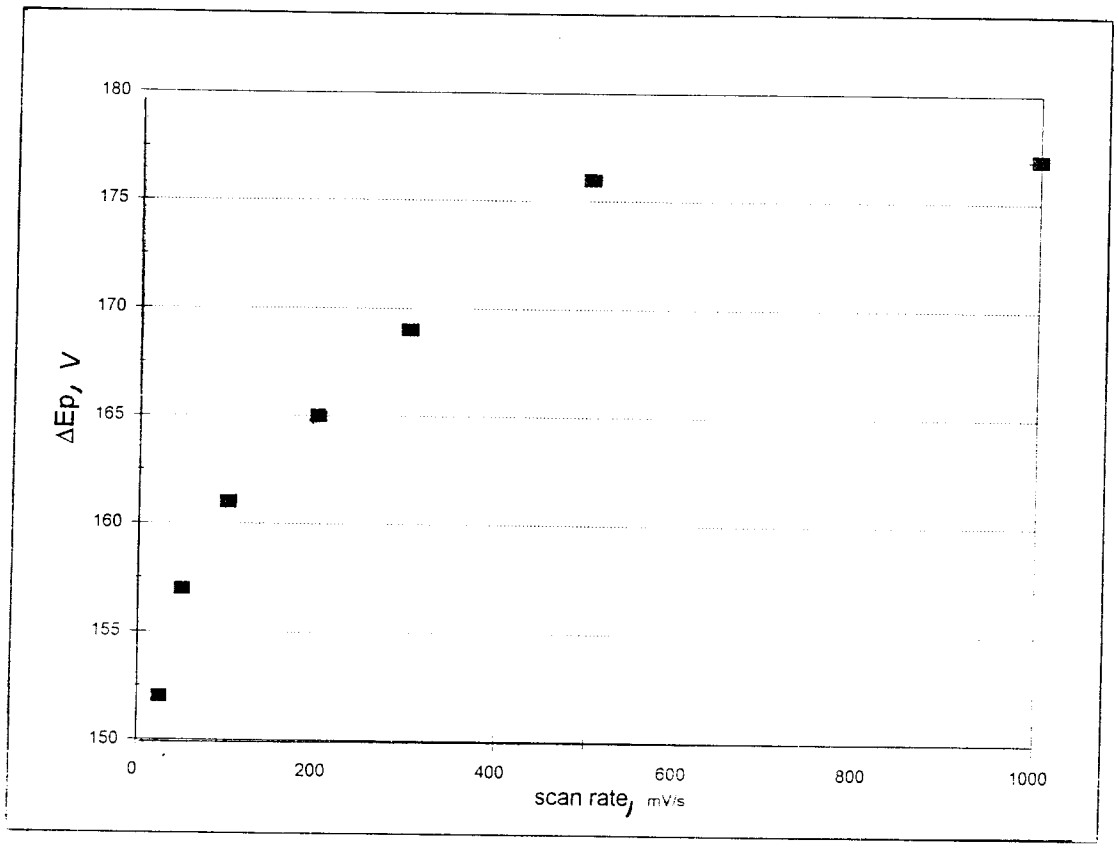

Figure 3.12 : Plot of ΔE_p vs scan rate for the Co-PC tri-layer.

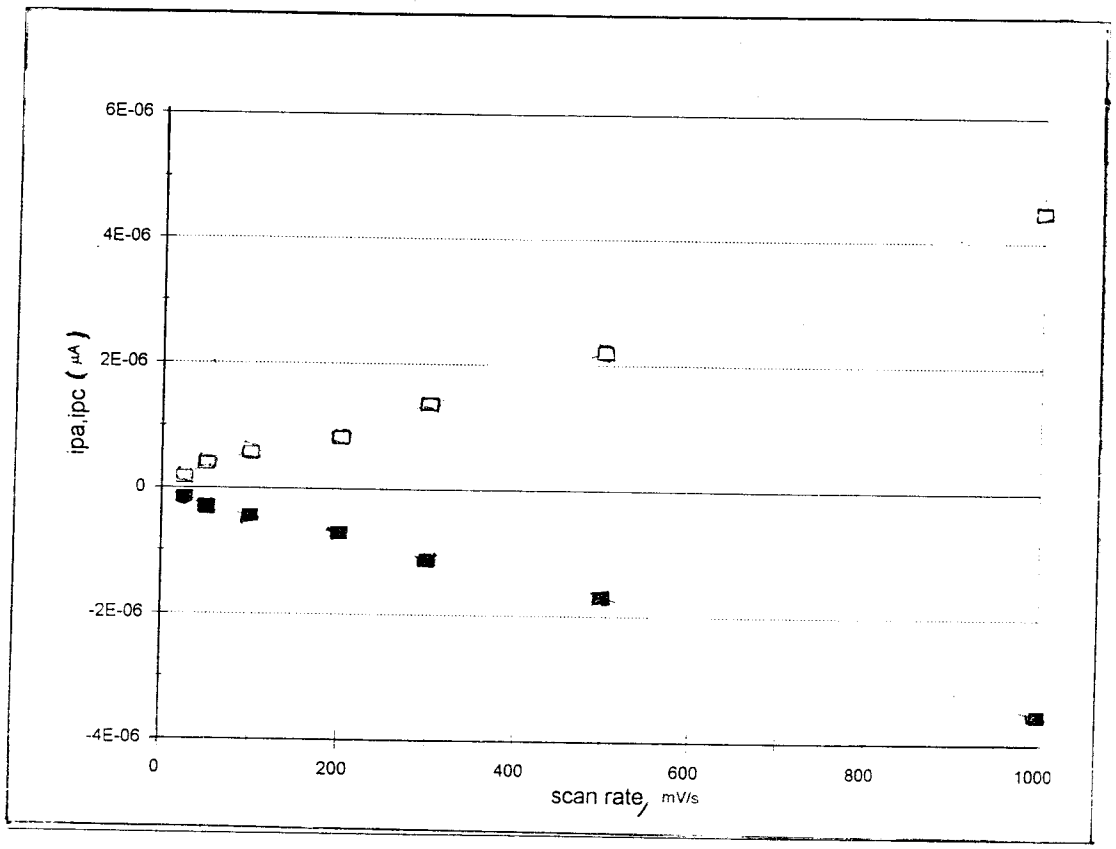

Figure 3.13 : Plot of (i_{pa}, i_{pc}) vs scan rate for the Co-PC tri-layer.

of 5-10 mV. This shift to more cathodic potentials furthered the observed trend that the monolayer becomes easier to oxidized with increasing number of layers. The E_{fwhm} was determined at scan rates of 50, 100 and 500 mV/s calculated to be 13.5, 13.7, and 17.1 mV for the anodic peak and 17.6, 35.0, and 43.3 mV for the cathodic peak. These values quantitate the monolayer peak sharpening observed and illustrate that the peaks are continuing to sharpen with increasing number of layers. These results support the tentative assumption that the monolayer interactions with the electrolyte are diminishing, or that the monolayer is undergoing a structural rearrangement upon coordination to the cobalt phthalocyanines. The surface coverages based on these peaks were found to closely agree between electrodes and the bi-layer results, with an average range of 1-3 $\times$ 10^{-10} (mole/cm^2). These results show that the monolayers' surface coverage is independent of the cobalt phthalocyanine layers.

The cobalt $2^+/3^+$ peaks were found to become chemically reversible, with an average i_{pa}/i_{pc} ratio approximately equal to one, although the broadness of these peaks might have been the cause of this. This species was also found to be electrochemically irreversible since the ΔE_p increased with increasing scan rate. The anodic peak was observed at – 210 mV and the cathodic peak was observed at – 380 mV with an electron transfer rate constant (k_s) of 0.425 s^{-1}, at a scan rate of 100 mV/s. The rate constant has not changed between bi- and tri-layer formation, implying that there is extensive electronic communication between the phthalocyanine molecules. The cobalt's redox couple peaks were found to shift by 40-50 mV cathodically. A slight shift to more cathodic potentials is observed in the $2^+/3^+$ couple when compared to the bi-layer. This may be a result of the broadness of the peaks, where determining the absolute peak

potential was difficult. It is also possibly due to dimer formation, where the cobalt ion became easier to oxidize due to the increasing number of overlapping π-clouds. This shift also implies that the rings are strongly interacting between layers, as was the desired outcome. The peak positions were found to slightly drift from electrode to electrode on an average of 20-30 mV. The surface coverages based on these peaks were found to be fairly consistent between electrodes with an average range of 5-8 $\times$ 10^{-10} (mole/cm^2). The surface coverages based on the $2^+/3^+$ couple were found to double in value from the first phthalocyanine layer, indicating the successful addition of another layer of phthalocyanines. The ring oxidation peak was seen at approximately 520 mV, but it was neither easily nor consistently observed. When these peaks were observed they were found to lie along the sloping background and so their surface coverage was not calculated. This process was also observed to shift to less anodic potentials when compared to the bi-layer, indicating the rings are experiencing an increase in π-π interactions. The peak currents of these peaks were also found to be fairly linear with respect to the scan rate indicating the surface confinement of the cobalt phthalocyanines.

3.7 VOLTAMMETRY OF COBALT PHTHALOCYANINE-TETRA-LAYER

After following the outlined (see Chapter 2) soaking and rinsing procedure, the electrodes were placed into deaerated electrolyte solution and cyclic voltammograms were taken at scans of 25, 50, 100, 200, and 500 mV/s from +700 mV to –900 mV. Scans taken beyond this potential range did not provide any additional information, see Figure 3.14. The metal's redox couple was now found to have an area 3 times greater

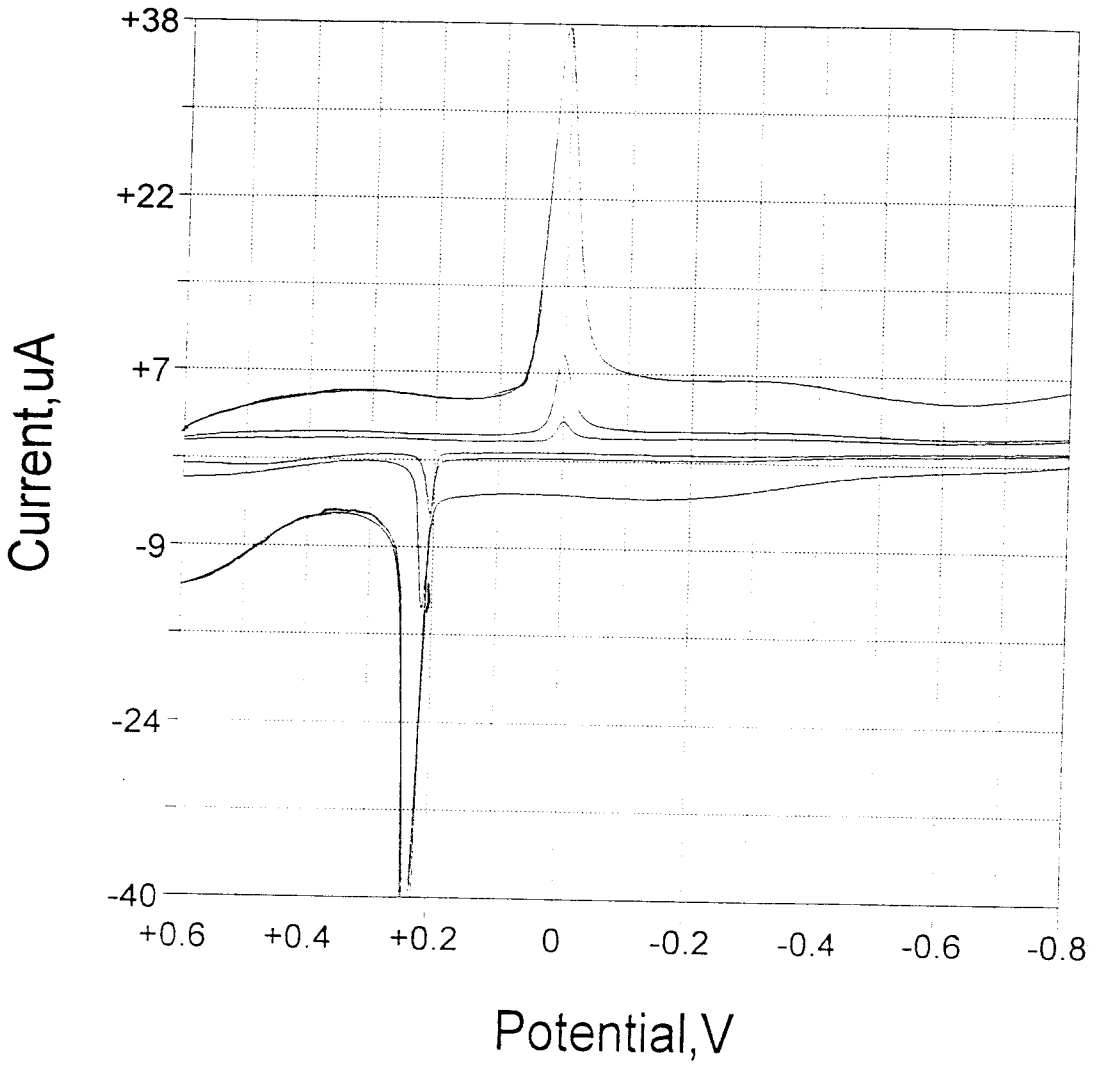

Figure 3.14 : Cyclic voltammograms of self-assembled multi-layers consisting of three layers of cobalt phthalocyanines on a monolayer of 1-(10-mercaptodecyl)isonicotinate in a 1 M solution of sodium acetate at a gold working electrode. Scan rates: 0.05, 0.1, and 0.5 V/s. Temperature: 20 °C. Reference electrode: Ag/AgCl. Counter electrode: platinum wire.

than that of the first layer, as expected. Again the peaks were very broad and determining the peak maximum was very difficult.

Plots of ΔEp versus scan rate and ip versus scan rate were taken based on the voltammograms to establish the electrochemical reversibility and to establish the absence of diffusion of the adsorbed species, respectively, see Figures 3.15 and 3.16. The surface coverage was also determined, and found to be comparable to values found in the literature.

The 1-(10-mercaptodecyl) isonicotinate peaks were found to be chemically reversible, with an i_{pa}/i_{pc} ratio approximately equal to one. This most likely indicates that the phthalocyanines have now completely blocked the monolayer from the electrolyte and/or structural rearrangement of the monolayer is complete. This species was also found to be electrochemically irreversible since the ΔE_p increased with increasing scan rate. The anodic peak was observed at 210 mV and the cathodic peak was observed at 0 mV, at a scan rate of 100 mV/s. These peaks are no longer showing any shift in potential with additional layers. The peak positions were found to slightly drift from electrode to electrode on an average of 10-20 mV. The E_{fwhm} was determined at scan rates of 50, 100 and 500 mV/s calculated to be 14.5, 17.5, and 19.1 mV for the anodic peak and 22.7, 23.5, and 45.3 mV for the cathodic peak. Although these results show that the peaks are very sharp, they do not show a considerable decrease when compared to the tri-layer. This supports the hypothesis that the monolayer/electrolyte interactions have been terminated and that any structural rearrangements have reached a hiatus. The surface coverages based on these peaks were found to closely agree between electrodes and the previous results, with an average range of 1-3 $\times 10^{-10}$ (mole/cm^2). This result establishes

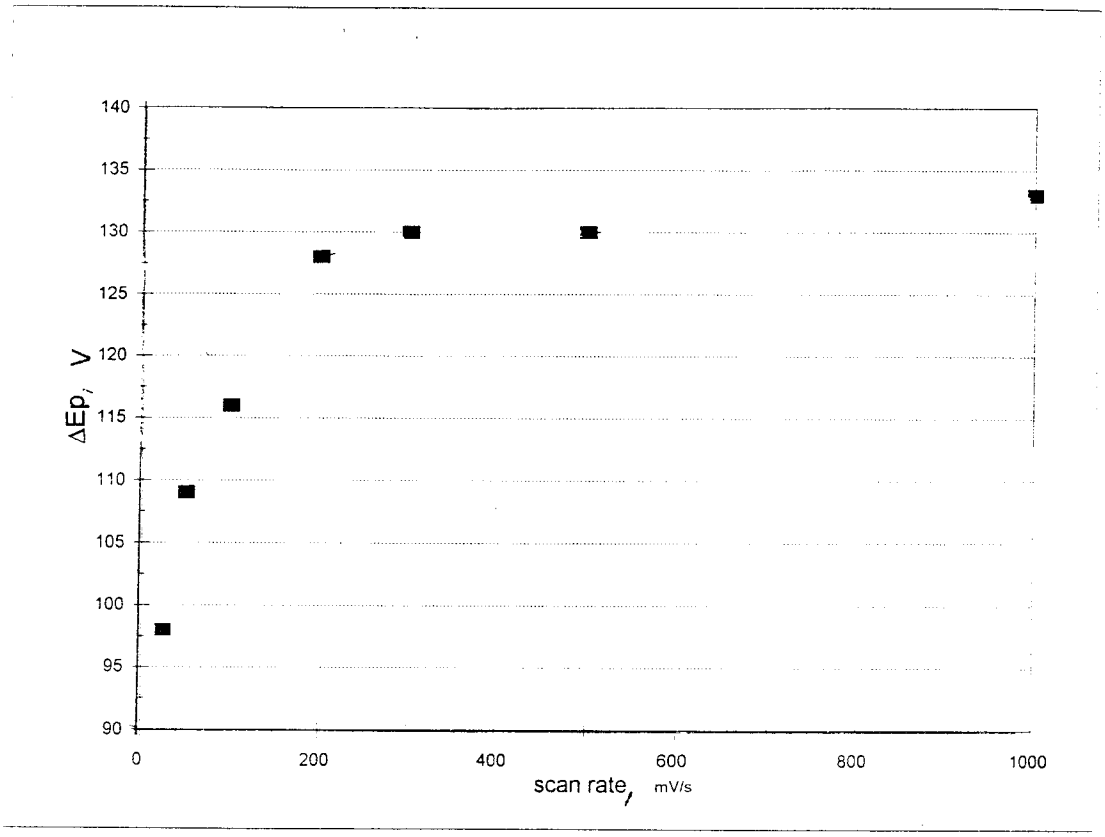

Figure 3.15 : Plot of ΔE_p vs scan rate for the Co-PC tetra-layer.

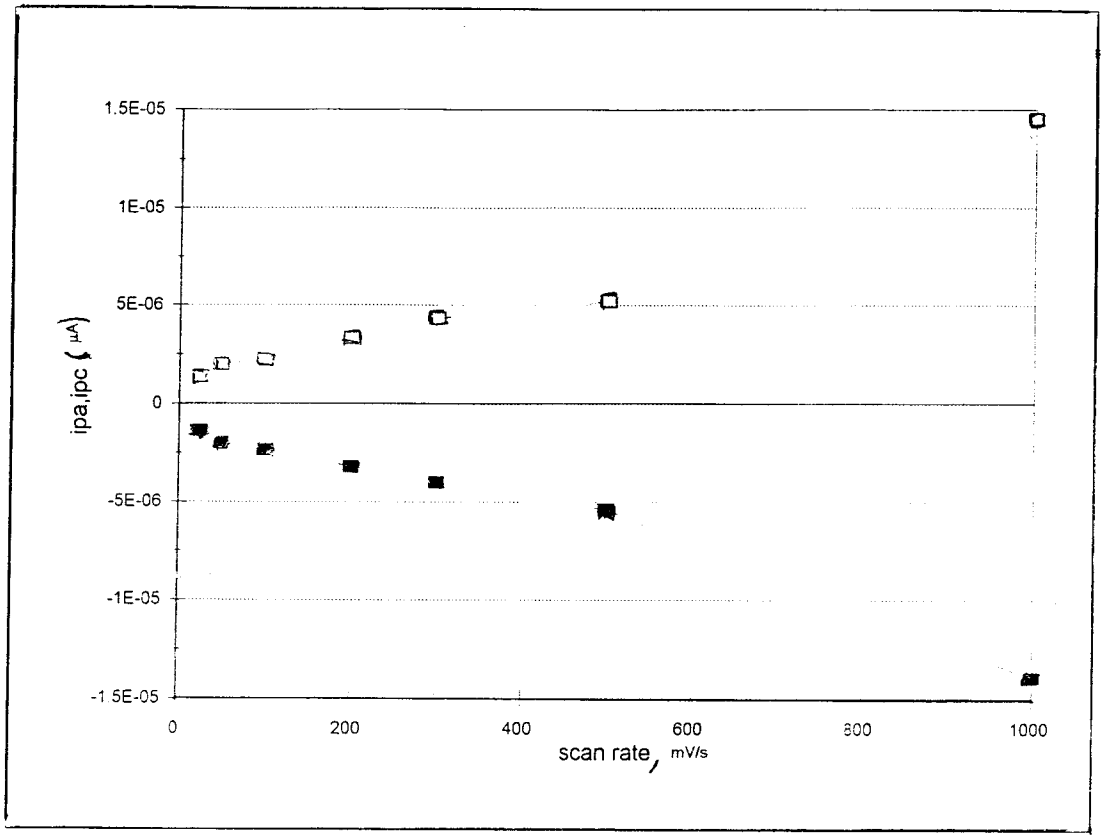

Figure 3.16 : Plot of (i_{pa}, i_{pc}) vs scan rate for the Co-PC tetra-layer.

the trend that the monolayers' surface coverage is independent of the number of cobalt phthalocyanine layers.

The cobalt $2^+/3^+$ peaks were found to be chemically reversible, with an average i_{pa}/i_{pc} ratio approximately equal to one. This species was also found to be electrochemically irreversible since the ΔE_p increased with increasing scan rate. The anodic peak was observed at – 260 mV and the cathodic peak was observed at – 400 mV with an electron transfer rate constant (k_s) of 0.479 s^{-1}, at a scan rate of 100 mV/s. Although a slight change in the rate constant is calculated between the tri- and tetra-layer, this is not a significant difference and is most likely due to the broadness of the peaks. This difference does, however, further support the proposed hypothesis that there is extensive communication between the multiple phthalocyanine layers, resulting in a relatively fast electron transfer is occurring through these layers. A slight shift, 10-20 mV, to more cathodic potentials is observed in the $2^+/3^+$ couple when compared to the tri-layer. Again, this may be a result of the broadness of the peaks and possibly to the increased number of overlapping π-clouds. The peak positions were found to slightly drift from electrode to electrode on an average of 30-40 mV. The surface coverages, based on peak areas, were found to be fairly consistent between electrodes with an average range of 7-10 $\times$ 10^{-10} (mole/cm^2). The surface coverages based on the $2^+/3^+$ couple were found to triple in value from the first phthalocyanine layer, indicating the successful addition of another layer of phthalocyanines. The ring oxidation was seen at approximately 500 mV, but it was neither easily nor consistently observed. This process was also observed to shift to less anodic potentials when compared to the tri-layer, indicating the rings are experiencing an further increase in π-π interactions. The peak

currents of these peaks were also found to be fairly linear with respect to the scan rate indicating the surface confinement of the cobalt phthalocyanines.

3.8 COBALT OCTAFLUOROPHTHALOCYANINE MULTI-LAYERS

To ensure that the peaks observed in the mixed multi-layers discussed below are indeed the result of bound cobalt octafluorophthalocyanine species, self-assembled mono- and multi-layers were formed following the same procedure as that of the unfluorinated derivative. A bi-layer consisting of cobalt octafluorophthalocyanine was constructed onto a monolayer of the pyridine tagged alkanethiol. Cyclic voltammograms were taken at scans of 25, 50, 100, 200, and 500 mV/s from +1500 mV to –1500 mV. Scans taken beyond this potential range did not provide any additional information, see Figure 3.17.

Plots of ΔEp versus scan rate and ip versus scan rate were taken based on the voltammograms to establish the electrochemical reversibility and the absence of diffusion of the adsorbed species, respectively, see Figures 3.18 and 3.19. The surface coverage was also determined from the cobalt $2^+/3^+$ peak area. The monolayer results were in agreement with results presented earlier and so will not be presented in this section with the bi-layer.

The 1-(10-mercaptodecyl)isonicotinate peaks were found to be chemically reversible, with an i_{pa}/i_{pc} ratio approximately equal to one. While this trend was not observed to occur in the phthalocyanine study until the tri-layer was formed, its occurrence here indicates that the octafluorophthalocyanine is better at shielding the monolayer from solution. This is expected as the octafluorophthalocyanine is larger than

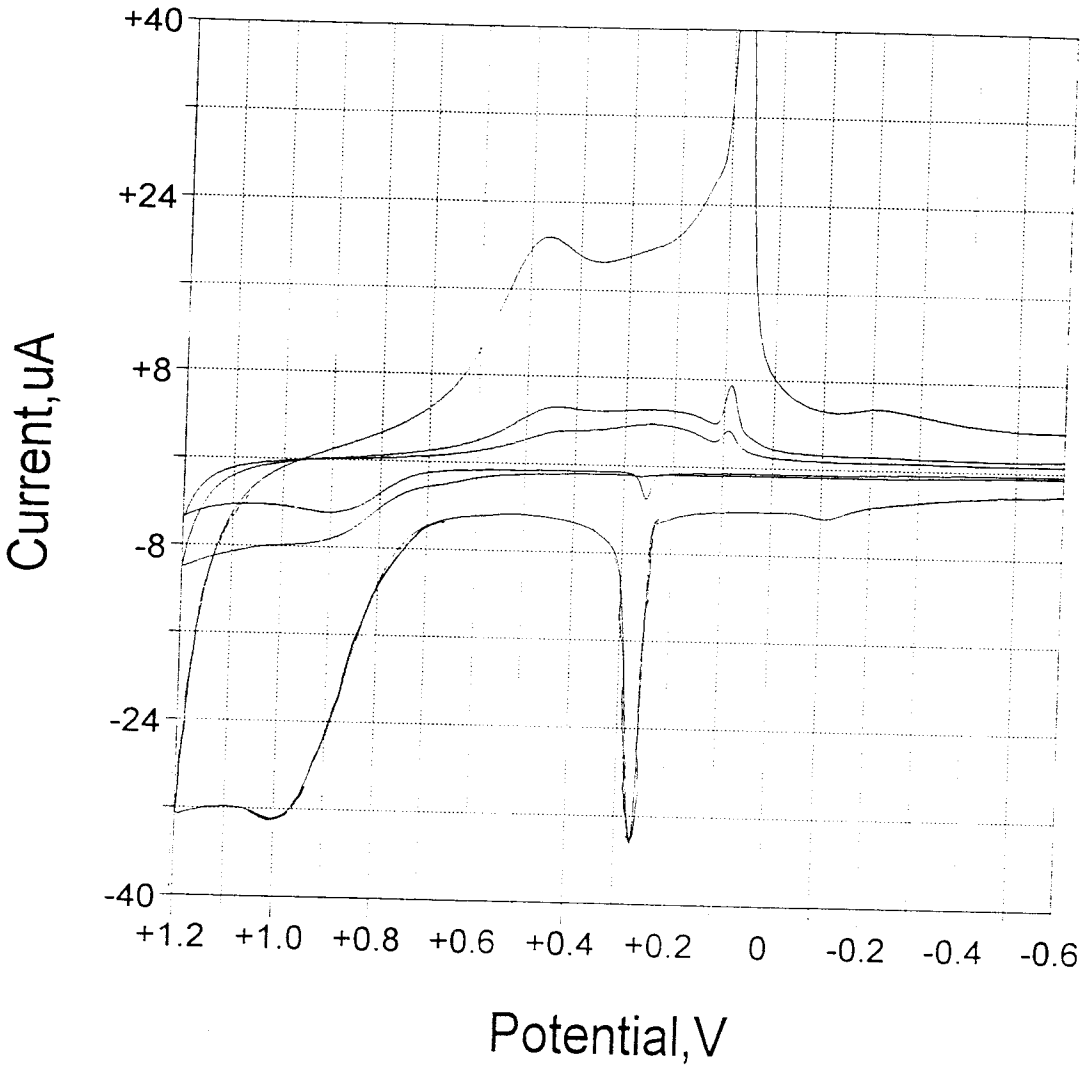

Figure 3.17 : Cyclic voltammograms of a self-assembled bi-layer consisting of cobalt octafluorophthalocyanines on a monolayer of 1-(10-mercaptodecyl)isonicotinate in a 1 M solution of sodium acetate at a gold working electrode. Scan rates: 0.05, 0.1, and 0.5 V/s. Temperature: 20 °C. Reference electrode: Ag/AgCl. Counter electrode: platinum wire.

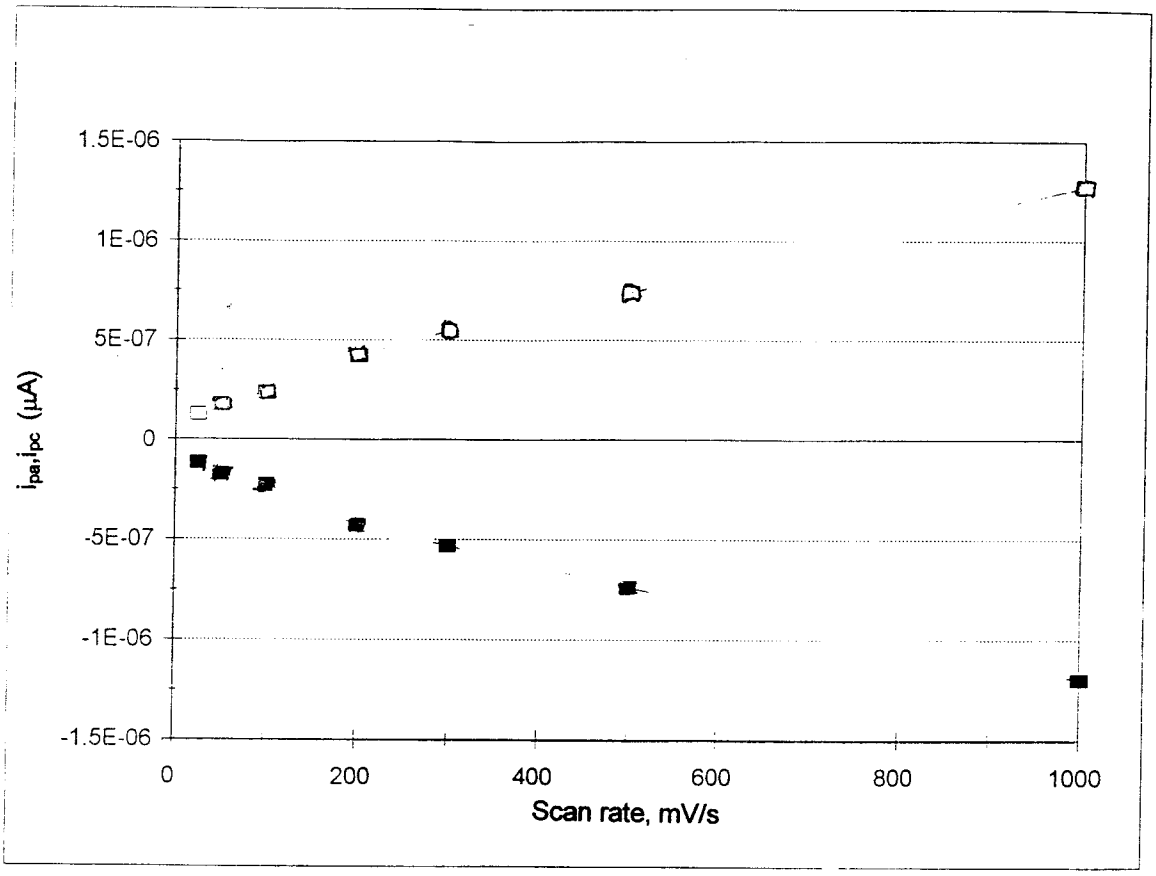

Figure 3.19 : Plot of (i_{pa}, i_{pc}) vs scan rate for the Co-F_8PC bi-layer.

the phthalocyanine. However, these peaks were difficult to analyze due to poor resolution and tailing of neighboring peaks. This species was also found to be electrochemically irreversible since the ΔE_p increased with increasing scan rate. The anodic peak was observed at + 250 mV and the cathodic peak was observed at + 90 mV at a scan rate of 100 mV/s. The peak potentials are similar to those found in the phthalocyanine bi-layer voltammetry, indicating that the monolayer is in a similar environment. The peak positions were found to slightly drift from electrode to electrode on an average of 10-20 mV. The E_{fwhm} was determined at scan rates of 50, 100 and 500 mV/s calculated to be 19.5, 20.6, and 40.9 mV for the anodic peak and 35.0, 37.2, and 44.4 mV for the cathodic peak. These values are significantly different from the cobalt phthalocyanine bi-layer voltammetry. The surface coverages based on these peaks were found to closely agree between electrodes and with previous results with an average range of 1-3 $\times$ 10^{-10} (mole/cm^2).

The cobalt octafluorophthalocyanine $2^+/3^+$ peaks were found to be chemically reversible, with an average i_{pa}/i_{pc} ratio approximately equal to one. This species was also found to be electrochemically irreversible since the ΔE_p increased with increasing scan rate. The anodic peak was observed at – 120 mV and the cathodic peak was observed at – 250 mV with an electron transfer rate constant (k_s) of 0.424 s^{-1}, at a scan rate of 100 mV/s. Since this rate constant is calculated to be the same as that of the phthalocyanine bi-layer then the octafluorophthalocyanine bi-layer is exhibiting the relatively fast electron transfer as seen in the previous layers. These results imply that the octafluorophthalocyanines are assembling onto the monolayer in much the same fashion as the unsubstituted phthalocyanines. This layer formation was very important to

establish in order to determine if the octafluorophthalocyanine would have the potential to create a molecular rectifier in the mixed multi-layer scenario, discussed below. The peak positions were found to slightly drift from electrode to electrode on an average of 30-40 mV and were found to shift to less cathodic potentials by 50 mV for the anodic wave and by 100 mV for the cathodic wave with respect to unsubstituted phthalocyanines. This is a result of the electronegative fluorines directly affecting the charge felt by the cobalt. The surface coverages, based on peak areas, were found to be fairly consistent between electrodes and comparable to the cobalt phthalocyanine layers, with an average range of 1-3 $\times$ 10^{-10} (mole/cm^2). The peak currents of these peaks were also found to be fairly linear with respect to the scan rate indicating the surface confinement of the cobalt phthalocyanines.

The cobalt octafluorophthalocyanine ring oxidation peaks were found to be much better defined than in the cobalt phthalocyanine voltammetry and were determined to be chemically reversible, with an average i_{pa}/i_{pc} ratio approximately equal to one. This species was also found to be electrochemically irreversible since the ΔE_p increased with increasing scan rate. The anodic peak was observed at + 900 mV and the cathodic peak was observed at + 450 mV at 100 mV/s. This is considered a tremendous shift to more anodic potentials when compared to the phthalocyanine case and was expected due to the strong electron withdrawing capabilities of fluorine. The electron transfer rate constant could not be calculated, by the method of Laviron,[9] as the ΔE_p in the voltammogram are too far apart. Qualitatively this separation in peak potential indicates a very slow kinetic process. The peak positions were found to slightly drift from electrode to electrode on an average of 10-20 mV. The surface coverages, based on peak areas, were found to be

fairly consistent between electrodes with an average range of 1-3 $\times$ 10^{-9} (mole/cm^2). The difference in surface coverages between the $2^+/3^+$ couple and the ring oxidation are probably due to the sloping background that the ring oxidation peak lies on. The peak currents were also found to be fairly linear with respect to the scan rate indicating the surface confinement of the cobalt octafluorophthalocyanines.

3.8.1 VOLTAMMETRY OF COBALT OCTAFLUOROPHTHALOCYANINE TRI-LAYERS

After following the outlined (see Chapter 2) soaking and rinsing procedure, the electrodes were placed into deaerated 1 M sodium acetate electrolyte solution and cyclic voltammograms were taken at scans of 25, 50, 100, 200, and 500 mV/s from +1500 mV to –1500 mV. Scans taken beyond this potential range did not provide any additional information, see Figure 3.20. The metal center's redox couple and the ring oxidation peak was found to double in surface coverage (based on the first layer) as expected. These peaks were also much broader then the first layer's, most likely due to an increased distribution of the formal potentials between the layers, and so determining the exact peak maximum is subjective to interpretation.

Plots of ΔEp versus scan rate and ip versus scan rate were taken based on the voltammograms to establish the electrochemical reversibility and the absence of diffusion of the adsorbed species, respectively, see Figures 3.21 and 3.22. The surface coverage, based on peak area, was also determined.

The 1-(10-mercaptodecyl)isonicotinate peaks were found to be chemically reversible, with an i_{pa}/i_{pc} ratio approximately equal to one. This species was also found to

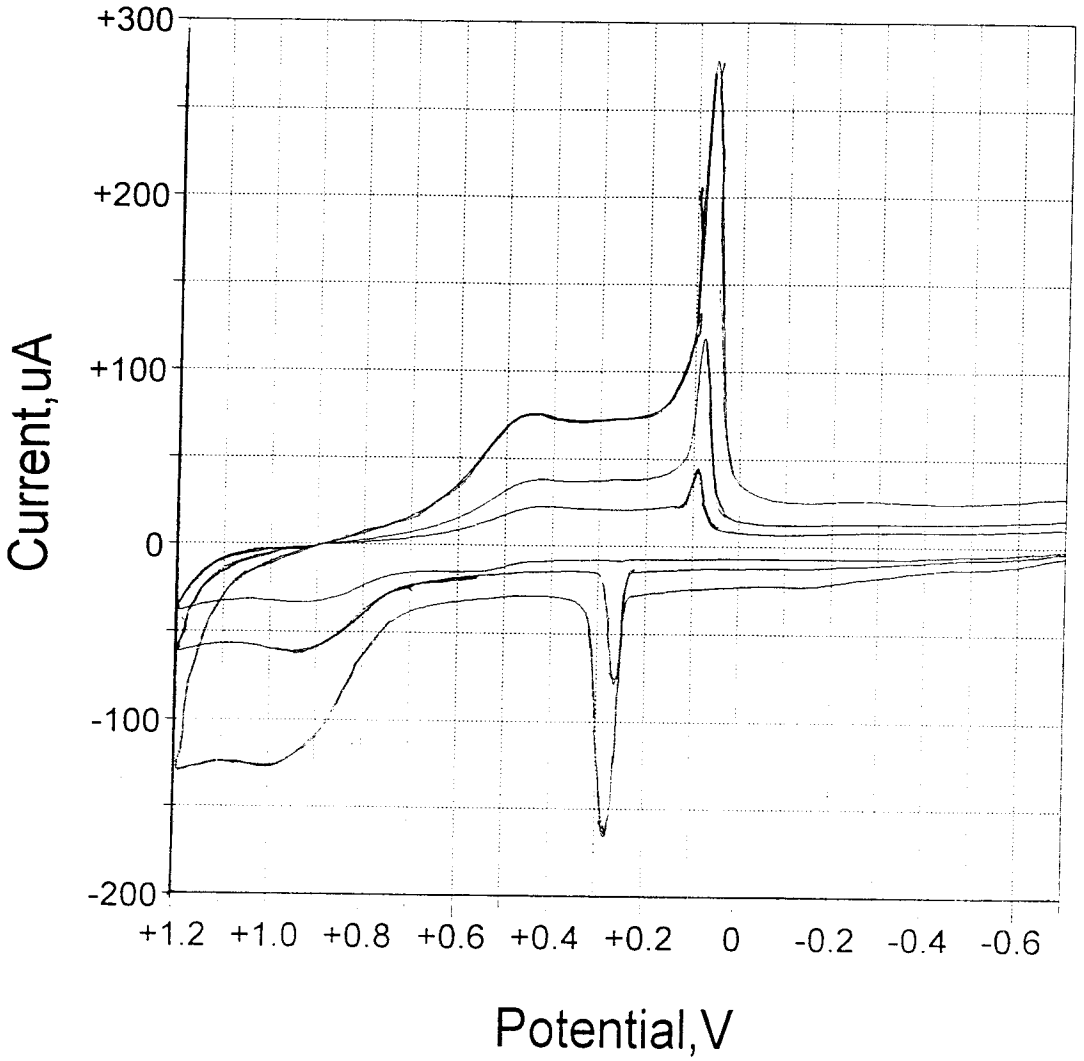

Figure 3.20 : Cyclic voltammograms of self-assembled multi-layers consisting of two layers of cobalt phthalocyanine on a monolayer of 1-(10-mercaptodecyl)isonicotinate in a 1 M solution of sodium acetate at a gold working electrode. Scan rates: 0.05, 0.1, and 0.5 V/s. Temperature: 20 °C. Reference electrode: Ag/AgCl. Counter electrode: platinum wire.

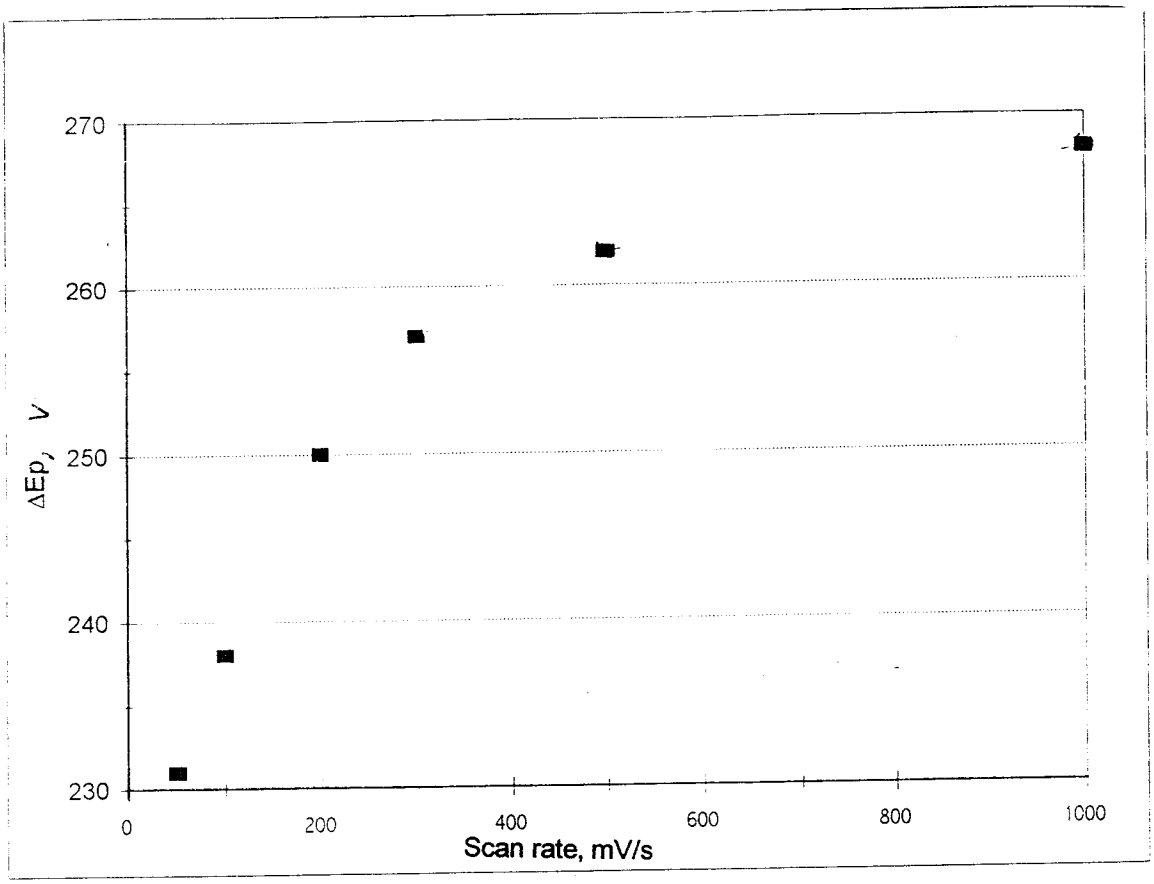

Figure 3.21 : Plot of ΔE_p vs scan rate for the Co-F_8PC tri-layer.

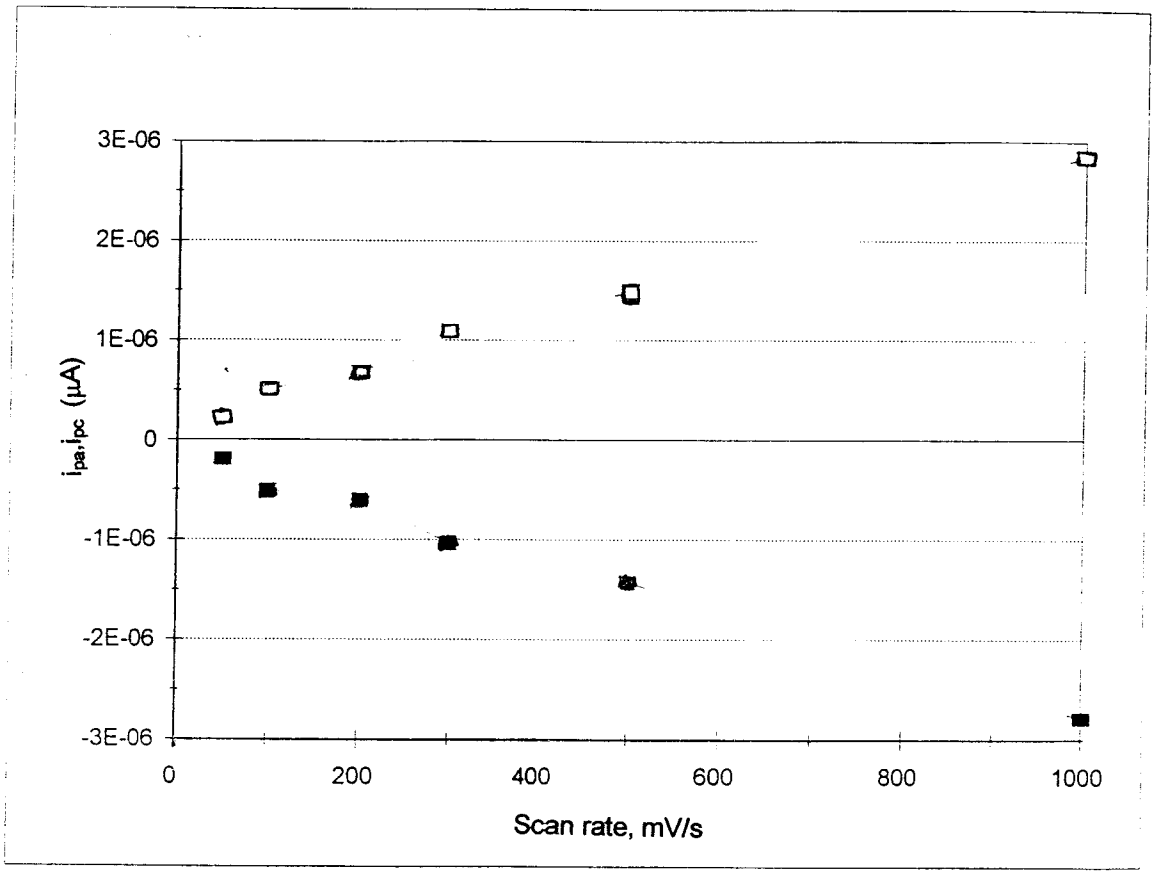

Figure 3.22 : Plot of (i_{pa}, i_{pc}) vs scan rate for the Co-F_8PC tri-layer.

be electrochemically irreversible since the ΔE_p increased with increasing scan rate. The anodic peak was observed at + 250 mV and the cathodic peak was observed at + 70 mV at a scan rate of 100 mV/s. The E_{fwhm} was determined at scan rates of 50, 100 and 500 mV/s calculated to be 19.6, 24.4, and 30.0 mV for the anodic peak and 39.1, 39.9, and 47.1 mV for the cathodic peak. These values were found to be slightly larger when compared to the phthalocyanine tri-layer and very similar to the octafluorophthalocyanine bi-layer. The greatest difference is seen in the values of the cathodic peaks, but as the octafluorophthalocyanine monolayer's cathodic peak was not well resolved from the octafluorophthalocyanine ring redox peak, this is not surprising. Since a significant difference is not observed between the octafluorophthalocyanine bi- and tri-layers, then these values indicate that the monolayer is well insulated from the electrolyte solution and the any structural rearrangement performed by the monolayer is complete. This is expected as the larger octafluorophthalocyanine can be seen to cover more of the monolayer with the bi- and tri-layers than the unsubstituted phthalocyanines were able to. The peak positions were found to slightly drift from electrode to electrode on an average of 5-10 mV. The surface coverages were found to closely agree between electrodes and at various scan rates with an average range of 1-3 $\times$ 10^{-10}(mole/cm^2).

The cobalt octafluorophthalocyanine $2^+/3^+$ redox couple was found to be chemically reversible, with an average i_{pa}/i_{pc} ratio approximately equal to one. This species was also found to be electrochemically irreversible since the ΔE_p increased with increasing scan rate. The anodic peak was observed at – 120 mV and the cathodic peak was observed at – 372 mV at a scan rate of 100 mV/s. An electron transfer rate constant was not able to be determine by the Laviron method[9] for this species, however the

dramatic increase in ΔE_p indicates that the electron transfer is being impeded. This may indicate that the tri-layer of octafluorophthalocyanines are more ordered than the tri-layers of the phthalocyanines. A slight shift to more cathodic potentials is observed in the $2^+/3^+$ couple when compared to the bi-layer. This trend was observed in the phthalocyanine voltammetry and may be a result of the broadness of the peaks and possibly to the increased number of overlapping π-clouds. The peak positions were found to slightly drift from electrode to electrode on an average of 20-30 mV. The surface coverages were found to be fairly consistent between electrodes with an average range of 3-5 $\times$ 10^{-10} (mole/cm^2). The surface coverages based on the $2^+/3^+$ couple were found to double in value from the first octafluorophthalocyanine layer, indicating the successful addition of another layer of phthalocyanines. The peak currents were also found to be fairly linear with respect to the scan rate indicating the surface confinement of the cobalt octafluorophthalocyanines.

The cobalt octafluorophthalocyanine ring oxidation peak was found to be chemically reversible, with an average i_{pa}/i_{pc} ratio approximately equal to one. This species was also found to be electrochemically irreversible since the ΔE_p increased with increasing scan rate. The anodic peak was observed at + 900 mV and the cathodic peak was observed at + 460 mV at a scan rate of 100 mV/s. Although a shift to more cathodic potentials was expected, as was observed in the phthalocyanine bi-layer, these values are fairly consistent with the octafluorophthalocyanine bi-layer potentials. This may be a result of the peaks broadening greatly when compared to both bi-layer voltammograms. The peak positions were found to slightly drift from electrode to electrode on an average of 10-20 mV. The surface coverages, based on the anodic peak area, were found to be

fairly consistent between electrodes with an average range of 4-6 $\times$ 10^{-9}(mole/cm^2). The peak currents were also found to be fairly linear with respect to the scan rate with respect to the scan rate indicating the surface confinement of the cobalt octafluorophthalocyanines.

In summary, the peak surface coverages based on the ligand oxidation were found to double in value from the first octafluorophthalocyanine layer. The cobalt $2^+/3^+$ redox couple was found to shift by 40-50 mV cathodically, compared to the octafluorophthalocyanine, and to shift anodically by 50-100 mV when compared to the phthalocyanine tri-layer. The cobalt octafluorophthalocyanine was found to greatly shift the metal's redox couple, and to enhance the ring oxidation; when compared to the phthalocyanine voltammetry.

3.9 HETEROGENEOUS MULTI-LAYER FILMS

MOLECULAR RECTIFICATION

After following the outlined (see Chapter 2) soaking and rinsing procedure, the electrodes were placed into deaerated 1 M sodium acetate electrolyte solution and cyclic voltammograms were taken at scans of 25, 50, 100, 200, and 500 mV/s from +700 mV to −1000 mV. Scans taken beyond this potential range did not provide any additional information, see Figure 3.23. The cobalt $2^+/3^+$ couple was found to be much better defined, when compared to the cobalt phthalocyanine voltammograms, with a sharp contrast between itself and the background and was found to have a surface coverage of 1-3 $\times$ 10^{-9} (mol/cm^2). This correlates into an expected increase in the surface coverage for the addition of another phthalocyanine layer. While a dramatic increase was not

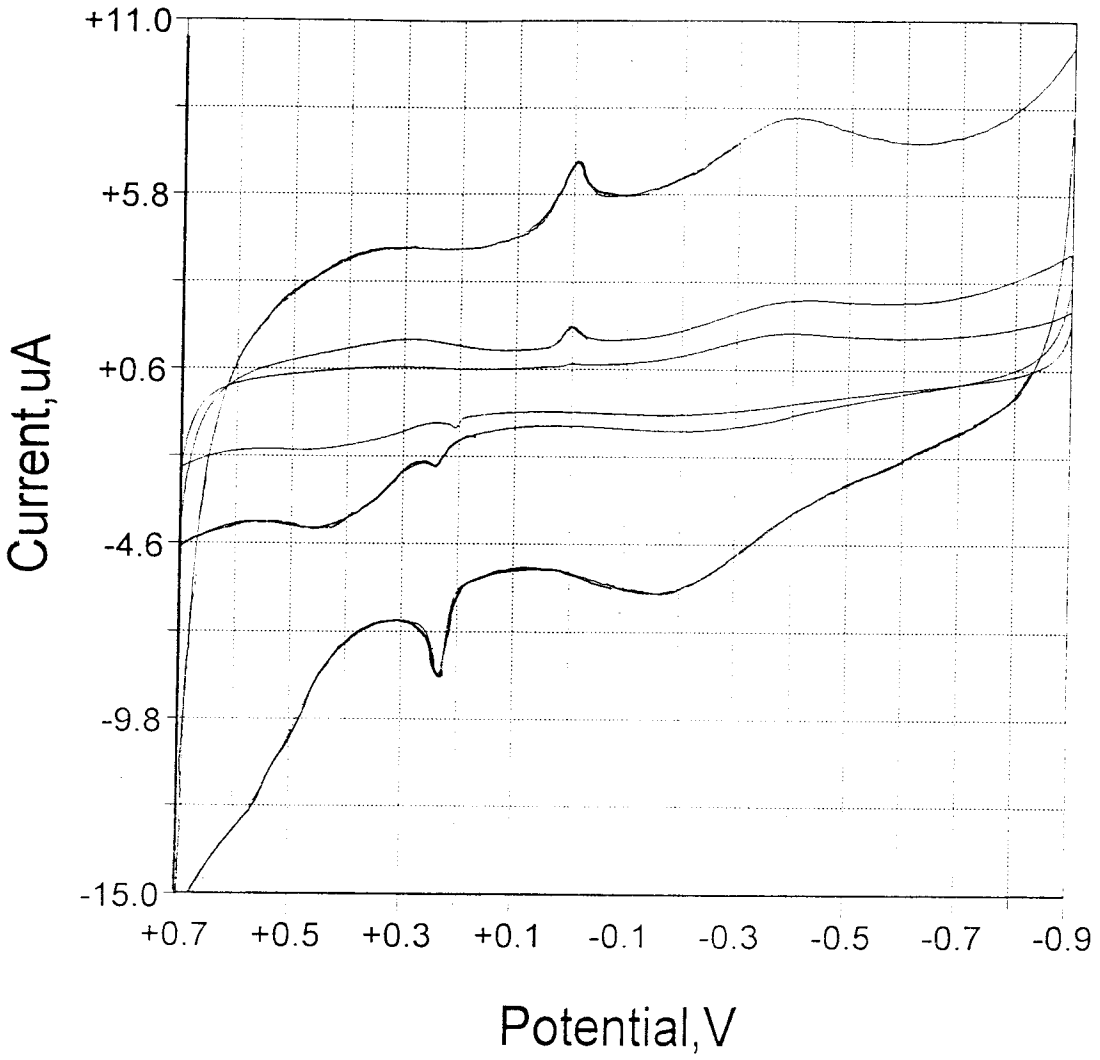

Figure 3.23 : Cyclic voltammograms of self-assembled multi-layers consisting of a layer of cobalt octafluorophthalocyanine on three layers of cobalt phthalocyanine on a monolayer of 1-(10-mercaptodecyl)isonicotinate in a 1 M solution of sodium acetate at a gold working electrode. Scan rates: 0.05, 0.1, and 0.5 V/s. Temperature: 20 °C. Reference electrode: Ag/AgCl. Counter electrode: platinum electrode.

readily observed, one indication of the formation of a molecular rectifier, other factors such as the $2^+/3^+$ couple's peak shape and large shifts in the ring oxidation potential are indicative of the formation of a molecular rectifier.

Plots of ΔEp versus scan rate and ip versus scan rate were taken based on the voltammograms to establish the electrochemical reversibility and absence of diffusion of the adsorbed species, respectively, see Figures 3.24 and 3.25.

The 1-(10-mercaptodecyl)isonicotinate peaks were found to be chemically reversible, with an i_{pa}/i_{pc} ratio approximately equal to one. This species was also found to be electrochemically irreversible since the ΔE_p increased with increasing scan rate. The anodic peak was observed at + 210 mV and the cathodic peak was observed at 0 mV at a scan rate of 100 mV/s. The peak positions were found to slightly drift from electrode to electrode on an average of 10 mV, however there was no significant difference in peak potentials between the tri-, tetra-, or this mixed multi-layer. The surface coverages were found to closely agree between electrodes and with the earlier studies, with an average range of $1\text{-}3 \times 10^{-10}$ (mole/cm^2).

The cobalt $2^+/3^+$ peaks were found to be chemical reversible, with an average i_{pa}/i_{pc} ratio approximately equal to one, however, these peaks were found to be very broad and so the assignments are not definitive. Also, this couple was expected to give a peak for the phthalocyanine layers and a separate peak for the octafluorophthalocyanine layer. However, the peak potentials of the couple for both layers were found to overlap so only one broad peak was observed. This species was also found to be electrochemically irreversible since the ΔE_p increased with increasing scan rate. The anodic peak was observed at – 240 mV and the cathodic peak was observed at – 400 mV with an electron

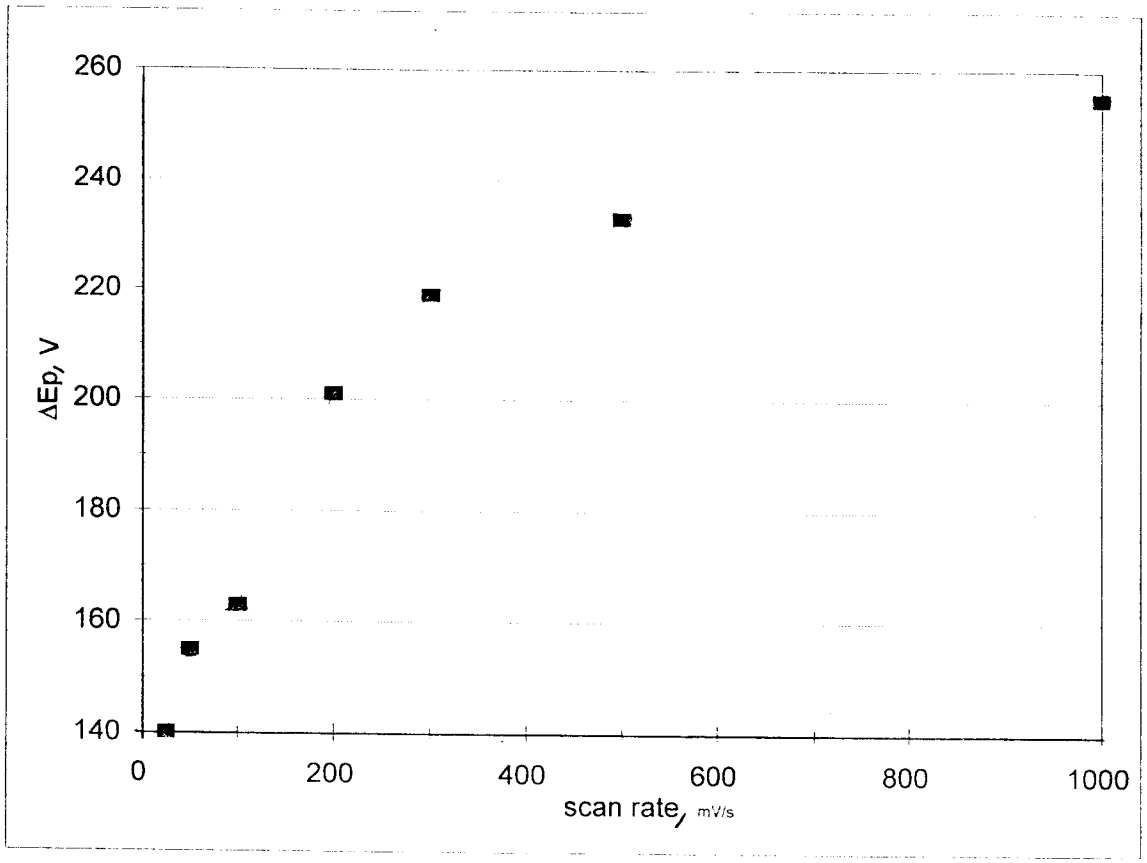

Figure 3.24 : Plot of ΔE_p vs scan rate for the mixed multi-layer.

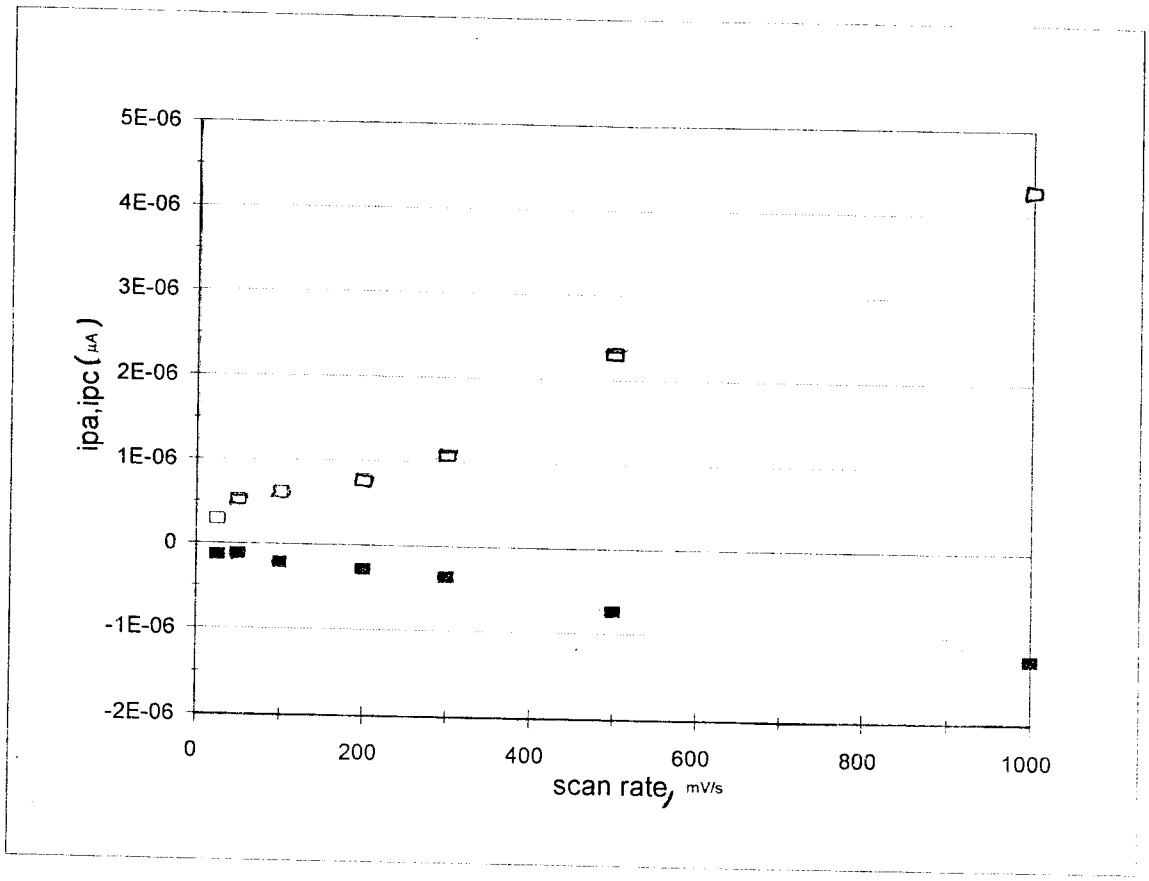

Figure 3.25 : Plot of (i_{pa}, i_{pc}) vs scan rate for the mixed multi-layer.

transfer rate constant (k_s) of 0.547 s^{-1} at a scan rate of 100 mV/s. This is a slight increase in the kinetics of the multi-layers, but it is not a great increase and probably due to the broadness of the peaks. This indicates that the rings are densely packed and that transfer is slightly enhanced by the presence of the octafluorophthalocyanine. A slight shift to more cathodic potentials is observed in the $2^+/3^+$ couple when compared to the tetra-layer of phthalocyanines and to the bi-layer of the octafluorophthalocyanines. The peak positions were found to slightly drift from electrode to electrode on an average of 10-20 mV. The surface coverages were found to be fairly consistent between electrodes and found to increase when compared to the homogeneous multi-layers of the phthalocyanines with a value range of 2-10 $\times$ 10^{-9} (mole/cm^2). While this is not a great increase, it is indicative of another layer formation. This result shows that the $2^+/3^+$ couple, while not observed independently of, is present for the cobalt phthalocyanine layers and the cobalt octafluorophthalocyanine layer. This correlation of the cobalt's redox couple of the mixed layers demonstrates that the octafluorophthalocyanine layer is not oxidized until the unfluorinated layers are oxidized. When this is compared to the separate bi- and tri-layers studies, where the cobalt's redox couple was found to occur at less cathodic potentials in octafluorophthalocyanine than in phthalocyanine, then the mixed multi-layer results indicate that the octafluorophthalocyanine is behaving as a diode. The peak currents of these peaks were also found to be fairly linear with respect to the scan rate indicating the surface confinement of the cobalt octafluorophthalocyanines.

The ring oxidation for the cobalt phthalocyanine layers were seen at approximately + 450 mV, but it was neither easily nor consistently observed and the voltammetry had similar problems to those listed above. On most scans there appeared to

be two ring oxidations, with the second potential being observed at approximately + 750 mV; this was designated as the ring oxidation for the cobalt octafluorophthalocyanine layer. This is seen as a great shift to less anodic potentials when compared to the cobalt octafluorophthalocyanine bi-layers. This process was also observed to shift to less anodic potentials when compared to the tetra-layer, indicating the rings are experiencing an further increase in π-π interactions. The most important aspect of the observation of two ring oxidations is the indication of the successful construction of a molecular rectifier. Since the rings in the phthalocyanine layer were oxidized before the octafluoro-rings and the surface coverage of the redox couple of the mixed multi-layers was calculated to be equal to that expected for a five layered system, then these results support the conclusion that molecular rectification was achieved.

3.10 CONCLUSION

The electrochemical analysis of self-assembled monolayers of cobalt phthalocyanine attached to a pyridine tagged alkanethiol, and subsequent multi-layer formation of cobalt phthalocyanines has been reported herein. These multi-layers have been shown to be stable molecular films. The molecular rectification of this multi-layer using cobalt octafluorophthalocyanine has also been presented. The measured surface coverages calculated are comparable to those found in the literature, and signify the successful construction of multi-layer films of cobalt phthalocyanine and cobalt octafluorophthalocyanine on a gold electrode. Thus, homogeneous and heterogeneous multi-layer films can be constructed via this completely general and versatile synthetic procedure. The outcome of this study is that a template now exists for the study of

phthalocyanines, and similar macrocycles, bounded to a metal electrode through an alkanethiol chain for the formation of multi-layers and for the formation of molecular electronic and optical devices.

3.11 FUTURE WORK

This project can easily be expanded to examine the effects of increasing the number of layers and of increased mixed multi-layers, to changes in electrochemical and chemical responses. The properties of these multi-layers can then be studied by spectroelectrochemical and spectrometric techniques to determine the layers optical properties and ultimately to determine if these layers can produce a molecular diode.

REFERENCES

(1) Poirier, G.; Pylant, D. *Science* **1996**, *272*, 1145-1148.

(2) Ulman, A. *Chem. Rev.* **1996**, *96*, 1533-1554.

(3) Murray, R. *Molecular Design of Electrode Surfaces*; Wiley: New York, **1992**.

(4) Bear, J.; Han, B.; Huang, S.; Kadish, K. M. *Inorg. Chem.* **1996**, *35*, 3012-3021.

(5) Rodriguez, J.; Mebrahtu, T.; Soriaga, M. *J. Electroanal. Chem.* **1987**, *233*, 283-289.

(6) Willicut, R.; McCarley, R. *J. Am. Chem. Soc.* **1994**, *116*, 10823-824.

(7) Lee, B. *Langmuir* **1990**, *6*, 709-712.

(8) Offord, D.; Sachs, S.; Ennis, M.; Eberspacher, T.; Griffin, J.; Chidsey, C.; Collman, J. *J. Am. Chem. Soc.* **1998**, *120*, 4478-4487

(9) Laviron, E. *J. Electroanal. Chem.* **1979**, *101*, 19-28

(10) Simpson, T.; Revell, D.; Cook, M.; Russell, D. *Langmuir* **1997**, *13*, 460-464.

(11) Hutchinson, J.; Postlewaithe, T.; Murray, R. *Langmuir* **1993**, *9*, 3277-3283.

Bibliography

Anderson, T.; Komplin, G.; Pietro, W. *J. Phys. Chem.* **1993**, *97*, 6577-6578.

Anson, F. *Acc. Chem. Res.* **1975**, *8*, 400-407.

Anson, F. *Anal. Chem.* **1966**, *38*, 54-57.

Anson, F.; Osteryoung, J. *J. Chem. Educ.* **1983**, *60*, 293-296.

Anson, F. *J. Chem. Educ.* **1959**, *36*, 394-395.

Bard, A.; Faulkner, L. *Electrochemical Methods*; Wiley: New York, **1980**.

Bain, C.; Evall, J.; Whitesides, G. *J. Am. Chem. Soc.* **1989**, *111*, 7155.

Bear, J.; Han, B.; Huang, S.; Kadish, K. M. *Inorg. Chem.* **1996**, *35*, 3012-3021.

Bear, J.; Han, B.; Huang, S. *J. Am. Chem. Soc.* **1993**, *115*, 1175-1177.

Bear, J.; Li, Y.; Han, B.; Van Camelbecke, E.; Kadish, K. M. *Inorg. Chem.* **1996**, *35*, 3053-3055.

Bockris, J.; Khan, S. *Surface Electrochemistry*; Plenum Press: New York, **1993**.

Brett, C. *Electrochemistry-Principles, Methods, and Applications*; Oxford University Press: New York, **1993**.

Cotton, F.; Wilkinson, G. *Advanced Inorganic Chemistry*; Wiley: NewYork, 4th Ed., **1980**.

Creager, S.; Collard, D.; Faox, M. *Langmuir* **1990**, *6*, 1617-1620.

Creuger, S.; Hockett, L.; Rowe, G. *Langmuir* **1992**, *8*, 854-861.

Curtin, L.; Peck, S.; Tender, L.; Murray, R. *Anal. Chem.* **1993**, *65*, 386-392.

Durst, H.; Gokel, G. *Experimental Organic Chemistry*; McGraw-Hill: New York, 2nd Ed., **1987**.

Evans, D. *J. Chem. Educ.* **1983**, *60*, 290-293.

Evans, D. *Acc. Chem. Res.* **1977**, *10*, 313-319.

Finklea, H.; Hanshew, D. *J. Am. Chem. Soc.* **1992**, *114*, 3173-3181.

Gale, R. *Spectroelectrochemistry- theory and practice*; Plenum Publishing: New York, **1988**.

Han, B.; Kadish, K. M.; Bear, J. *Inorg. Chem.* **1993**, *32*, 4175-4176.

Heineman, W. *J. Chem. Educ.* **1983**, *60*, 305-308.

Hutchinson, J.; Postlewaithe, T.; Murray, R. *Langmuir* **1993**, *9*, 3277-3283.

Kadish, K. M.; Adamian, V.; Van Camelbecke, E.; Tan, Z.; Tagliatesta, P.; Bianco, P.; Boschi, T.; Yi, G.; Khan, M.; Richter-Addo, G. *Inorg. Chem.* **1996**, *35*, 1343-1348.

Kissinger, P.; Heineman, W. *J. Chem. Educ.* **1983**, *60*, 702-706.

Kuwana, T.; Heineman, W. *Acc. Chem. Res.* **1976**, *9*, 241-248.

Kwan, V.; Cammarata, V.; Miller, L.; Hill, M.; Mann, K. *Langmuir* **1992**, *8*, 3003-3007.

Laviron, E. *J. Electroanal. Chem.* **1979**, *101*, 19-28.

Laviron, E. *J. Electroanal. Chem.* **1979**, *100*, 263-270.

Lee, B. *Langmuir* **1990**, *6*, 709-712.

Li, D.; Swanson, B.; Robinson, J.; Hoffbauer, M. *J. Am. Chem. Soc.* **1993**, *115*, 6975-6980.

Lingane, J. *Electroanalytical Chemistry*; Interscience: New York, 2nd ed. **1958**.

March, J. *Advanced Organic Chemistry*; Wiley: New York, 4th Ed., **1992**.

Marks, T. *Science* **1985**, 227, 881-888.

McMurry, J. *Organic Chemistry*; Brooks/Cole Publishers: California, 3rd Ed., **1992**.

Mu, X. H.; Kadish, K. M. *Inorg. Chem.* **1988**, *27*, 4720-4725.

Murray, R. *Molecular Design of Electrode Surfaces*; Wiley: New York, **1992**.

Nicholson, R; Shain, I. *Anal. Chem.* **1964**, *36*, 706-723A.

Nishimura, O.; Kitada, C.; Fukino, M.; *Chem. Pharm. Bull.* **1978**, *26*,1576-1585.

Offord, D.; Sachs, S.; Ennis, M.; Eberspacher, T.; Griffin, J.; Chidsey, C.; Collman, J. *J.*

Am. Chem. Soc. **1998**, *120*, 4478-4487.

Orihashi, Y.; Ohro, H.; Tsuchida, E. *Molecular Crystals and Liquid Crystals*, **1988,** *160*,139-149.

Pasto, D.; Johnson, C.; Miller, M. *Experiments and Techniques in Organic Chemistry*; Prentice-Hall: New Jersey, **1992**.

Peck, S.; Curtin, L.; Tender, L.; Carter, M.; Terrill, R.; Murray, R.; Collman, J.; Little, W.; Duan, H.; Hermann, A. *J. Am. Chem. Soc.* **1995**, *117*, 1121-1126.

Perrin, D.; Armarego, W.; Perrin, D. *The Purification of Laboratory Chemicals*; Pergamon: New York, 2nd Ed., **1980**.

Poirier, G.; Pylant, D. *Science* **1996**, *272*, 1145-1148.

Rodriguez, J.; Mebrahtu, T.; Soriaga, M. *J. Electroanal. Chem.* **1987**, *233*, 283-289.

Ruhlmann, L.; Nakamura, A.; Vos, J.; Fuhrhop, J. *Inorg. Chem.* **1998**, *37*, 6052-6059.

Simpson, T.; Revell, D.; Cook, M.; Russell, D. *Langmuir* **1997**, *13*, 460-64.

Tour, J.; Jores, L.; Pearson, D.; Lamba, J.; Burgin, T.; Whitesides, G.; Allara, D.; Parikh, A.; Sundar, A. *J. Am. Chem. Soc.* **1995**, *117*, 9529-9534.

Ulman, A. *Chem. Rev.* **1996**, *96*, 1533-1554.

Ulman, A. *An Introduction to Ultrathin Organic Films*; Academic Press: New York, **1994**.

Widrig, C.; Chinkap, C.; Porter, M. *J. Electroanal. Chem.* **1991**, *310*, 335-359.

Willicut, R.; McCarley, R. *J. Am. Chem. Soc.* **1994**, *116*, 10823-824.

Yamakado, H.; Yakushi, K.; Kosugi, N.; Kuroda, H.; Kawamoto, A.; Tanaka, J.; Sugano,

T.; Kinoshita, M.; Hino, S. *Bull. Chem. Soc. Jpn.* **1989**, *62*, 2267-2272.

Zak, J.; Yuan, H.; Ho, M.; Woo, L.; Porter, M. *Langmuir* **1993**, *9*, 2772-2774.